Title
THE ELECTRIC CHARGE AND SURFACE PROPERTIES OF INTACT CELLS

Author
Glaeser, Robert M.

Publication Date
1963-07-30

UCRL-10898

University of California

Ernest O. Lawrence Radiation Laboratory

THE ELECTRIC CHARGE AND SURFACE PROPERTIES OF INTACT CELLS

Berkeley, California

DISCLAIMER

Research and Development

UCRL-10898
UC-48 Biology and Medicine
TID-4500 (19th Ed.)

UNIVERSITY OF CALIFORNIA
Lawrence Radiation Laboratory
Berkeley, California

Contract No. W-7405-eng-48

THE ELECTRIC CHARGE AND SURFACE PROPERTIES OF INTACT CELLS

Robert M. Glaeser
(Thesis)

July 30, 1963

Printed in USA. Price $2.75. Available from the
Office of Technical Services
U. S. Department of Commerce
Washington 25, D.C.

THE ELECTRIC CHARGE AND SURFACE PROPERTIES OF INTACT CELLS

Contents

Abstract vi

Prologue viii

I. Introduction: Theoretical Relation of Net Charge to Electrophoretic Mobility

A. Review of Henry's Treatment 1

1. Statement of the Problem 1

2. An outline of Henry's Treatment 1

3. Comments on the Interpretation of the Electrophoresis Equation 9

B. The Charge May Exist in the Interior as Well as on the Surface of the Particle

1. Theoretical Proof of this Statement 13

2. Mechanisms by Which a Particle Can Acquire a Surface Charge 14

3. Mechanisms by Which a Particle Can Acquire an Internal Charge 15

4. Appearance of the Internal-Charge Hypothesis in the Literature 17

II. Microelectrophoresis: Procedure and Equipment

A. General Description of the Method 19

B. Detailed Description of the Apparatus Used in this Study 19

C. On the Method of Taking Data 24

III. Experimental Investigation of the Hypothesis that an Internal Net Charge Contributes Significantly to the Total Charge of Intact Cells.

A. Literature that Suggested a Net Internal Charge . . 30

1. The Phenomenon of Membrane Potentials . . 30

2. The Low Isoelectric Points of Intact Cells . . 37

3. The Effect of Low Ionic Strength Upon the Isoelectric Point of Intact Cells 40
4. Other Suggestive Evidence 42
B. Experimental Reconfirmation and Extension of the Literature that Describes the Effects of pH and Ionic Strength Upon Mobility 43
1. Motivation of This Research 43
2. Mobility-pH Curves for Various Cell Types at Two Ionic Strengths (RBC, HeLa, TA3 Ascites, Yeast, Mammary Tissue) 43
3. Mobility-Time Curves and O. D.$_{417}$-Time Curves for Rat RBC at pH≈3.1, Ionic Strength 0.145 . 58
4. Summary of Subsection III. B. 65
C. Experiments with Metabolic Inhibitors and Ion Transport (RBC, TA3 Ascites) 66
1. Motivation of this Research 66
2. Attempts at Decreasing the Mobility by Decreasing the Active Ion Transport 66
3. Attempts at Decreasing the Active Ion Transport by Decreasing the Mobility 71
IV. Rejection of the Hypothesis that an Internal Charge Contributes Significantly to the Total Charge of Intact Cells 73
V. Experimental Investigation of the Surface Charge and Other Surface Properties
A. Present Theoretical Models of Cell Surface Structure and their Expected Surface Charge Characteristics . 76
1. Davson-Danielli Model of the Cell Membrane . 76
2. Various Mosiac Structures 77
3. Bell's Modification of the Davson-Danielli Model 79
B. Combined Electrophoretic and Biochemical Studies on Intact Cells (RBC, TA3 Ascites) 80

1. Experiments Involving Hydrolytic Enzymes . . 80
2. Experiments Involving OsO_4-Fixed and $KMnO_4$-Fixed Rat RBC 104
3. Calculations Involving the Electrokinetic Charge, the Surface Area, The Amount of Sialic Acid, and the Total Carbohydrate 119

C. Electron Microscope Study of the Surface Ultrastructure (RBC) 125

D. A New Model for the Cell Membrane: Lipoprotein "Yarn" with Carbohydrate "Caps" 132

Acknowledgments 139

Notation 140

Appendices

A. The cgs System of Units 143

B. The Solution of Laplace's Equation in Henry's Electrophoresis Problem 144

C. Calculation of the Mechanical (Hydrodynamic) Force in Henry's Electrophoresis Problem . . . 148

D. Calculation of the Electrical Force (Direct Force) in Henry's Electrophoresis Problem 150

References 153

THE ELECTRIC CHARGE AND SURFACE PROPERTIES OF INTACT CELLS

Robert M. Glaeser

Lawrence Radiation Laboratory
University of California
Berkeley, California

July 30, 1963

ABSTRACT

Henry's theoretical treatment of the electrophoresis of colloidal particles is reviewed, and derivations are given for important steps omitted in his paper. The point that the charge need not be only at the outer surface is given special emphasis. Certain observations from the literature previously led me to the hypothesis that there might be a net charge in the interior of most cells (e.g., associated with membrane potentials, active ion transport) which contributed appreciably to the net charge on the cell. Measurements are reported on mobility as a function of pH and ionic strength for a number of different kinds of intact cells. Data on their isoelectric points, and the time dependence of the mobility (of erythrocytes) at pH 3.1 gave indirect support to this hypothesis. The hypothesis is, however, rejected on the basis of (a) my own negative experimental results and (b) other observations from the literature. Therefore it is concluded that the net charge on intact cells exists almost exclusively at the outer surface.

The surface properties of intact cells, primarily rat erythrocytes (RBC), are investigated by the method of microelectrophoresis in conjunction with enzymatic and chemical treatment. The discovery is reported that α-amylase (a glycosidase) releases bound sialic acid from RBC. This, together with earlier work using the receptor-destroying enzyme and proteolytic enzymes, already reported in the literature, implies that there is a protein-associated oligosaccharide at the outermost surface of the rat RBC. Fixation with OsO_4 allows us for the first time to measure both a positive mobility for RBC below the isoelectric point at pH 1.6, ionic strength 0.145, and an increase in the

absolute value of the mobility above pH 11.0. The entire mobility-pH curve from pH 0.9 to 12.3 is consistent with the hypothesis that sialic acid is chiefly responsible for the surface charge. This hypothesis is also consistent with calculations regarding the electrokinetic charge, the surface area, the amount of sialic acid, and the total carbohydrate. Preliminary electron microscope studies of rat RBC show a "pebbly" surface structure previously described for RBC of several other species, in addition to a curious "tangled rope" structure. A tentative suggestion as to the structure of the cell membrane is proposed on the basis of these studies.

PROLOGUE

At the initial stages of this research project, some theoretical-type speculations and certain experiments in the literature lead me to become quite convinced that a large fraction of the net charge on a cell could exist in the interior of the cell. In my own subsequent experiments I have been unable to find direct evidence in support of this hypothesis, and in fact, have found some against it.

The electrophoretic mobility of intact cells has usually been interpreted in terms of the dissociation of ionizable groups at the cell surface. On the other hand there are, as will be discussed later, several mechanisms by which the interior of the cell might acquire a net charge. To my knowledge, no convincing argument (theoretical or experimental) has yet been given as to why an internal charge could not contribute to the mobility of intact cells. My own failures to demonstrate such an effect—and other pertinent experiments in the literature—have caused me to believe that the vast majority of the net charge on intact cells is distributed on the surface of the cells.

Now this paper is devoted fundamentally to the surface properties of intact cells and is especially concerned with what can be inferred about the surface from electrophoretic studies on the net charge of the cell. No mistake should be made about this. Yet a considerable portion of this paper is devoted to the question of a possible internal charge. I have included these rather lengthy sections only for the purpose of logical completeness, and I hope that the reader will not be misled as to my intent in this regard.

I. INTRODUCTION: THEORETICAL RELATION OF NET CHARGE TO ELECTROPHORETIC MOBILITY

A. Review of Henry's Theoretical Treatment

1. Statement of the Problem

For the purpose of an electrophoresis experiment, intact cells are most commonly suspended in some aqueous ionic solution. Assume for the moment that the intact cell has some net charge under these conditions. If this is true, charged ions of the same sign will be repelled by the cell, while ions of opposite sign will be attracted to it. As a result there is a net charge of opposite sign accumulated about the cell. Because of thermal agitation (Brownian movement) these countercharges will be distributed in a diffuse "ionic atmosphere" throughout a volume of the aqueous solution which surrounds the cell. The question to be asked in such a situation is: What will be the velocity of this charged object when an electric field is applied to it?

A rigorous derivation of how the velocity of a particle is related to its net charge under these conditions must take into account the electrical conductivity of the particle relative to the medium, and Henry was the first person to do this.[1] Henry assumed that the viscosity and the dielectric constant of the aqueous phase were not changed by the electric field strength (which in some cases might be very large) near the surface of the charged particle. Furthermore, he assumed that the charge distribution in and around the particle was not distorted by the applied electric field. Lyklema and Overbeek[2] have considered the effect of electric-field-dependent viscosity and dielectric constants, while Booth[3] has corrected Henry's equation for the distortion of the diffuse countercharge which surrounds the particle.

2. An Outline of Henry's Treatment

The purpose of this section will be to outline the procedure by which Henry derived the equation relating electrophoretic velocity to the charge of a particle. In general, the mathematics is too long and tedious to reproduce completely here. On the other hand, there are some instances in which statements are made without mathematical

justification. The validity of these statements will be mathematically derived here when it is deemed necessary or useful. References will be made throughout the following text either to specific equations when they were numbered in Henry's original paper, or to specific pages when a numbered equation is not involved.

The general approach adopted by Henry was as follows. First he calculated the equation of motion of the fluid surrounding the particle. From this he was able to calculate the force exerted upon the particle due to the motion of the viscous fluid past the particle. In addition to this "hydrodynamic" or "mechanical" force, the particle is acted upon directly by the electric field. When these two forces are equal, the particle will no longer accelerate and will have reached a terminal velocity. The ratio of this velocity to the applied electric field is known as the mobility of the particle.

To simplify the problem these calculations were performed in the frame of reference in which the particle was at rest. That is to say, an externally applied pressure was assumed, such that the velocity of the fluid infinitely far away from the particle was equal in magnitude to the velocity which the particle itself would have had in the absence of such an applied pressure gradient.

The differential equations which govern the motion of viscous incompressible fluids are given in Joos (p.217).[4]

$$g\frac{\partial \vec{v}}{\partial t} + g\vec{v}\cdot\vec{\nabla}\vec{v} + \vec{\nabla}p + \eta\vec{\nabla}\times\vec{\nabla}\times\vec{v} = \vec{G} \quad , \qquad \vec{\nabla}\cdot\vec{v} = 0 \, , \tag{1}$$

where

g = mass per unit volume of the fluid,

$\vec{v}$ = linear velocity of the fluid at a point,

$\vec{\nabla} = \hat{x}\frac{\partial}{\partial x} + \hat{y}\frac{\partial}{\partial y} + \hat{z}\frac{\partial}{\partial z}$; $\hat{x}$, $\hat{y}$, $\hat{z}$ are the unit vectors along the x, y, and z axes,

p = pressure at a point in the fluid,

η = viscosity,

$\vec{G}$ = (externally applied) force per unit volume exerted on the fluid.

The scalar product between vectors is indicated with a dot while the vector product is indicated with a cross.

After a brief initial acceleration, the fluid velocity will reach a constant steady-state value. Therefore, the term $\partial \vec{v}/\partial t$ will vanish. Furthermore, the term $\vec{v} \cdot \vec{\nabla} \vec{v}$ is small and can be neglected when considering a spherical particle and small fluid velocities (Joos, p. 218).[4]

The (externally applied) force per unit volume exerted upon the fluid is given by*

$$\vec{G} = \rho \vec{E} \quad , \tag{2}$$

where ρ = (net) charge per unit volume at a point in the fluid, and $\vec{E}$ = the electric field at a point in the fluid. This volume force may be expressed in terms of the potential Ψ (the value of Ψ at the surface will later be identified as the zeta potential), associated with the charge on the particle, and the potential Φ, associated with the applied electric field, according to the following relationships:

$$\rho = -\frac{\vec{\nabla}}{4\pi} \cdot K\vec{\nabla}(\Phi + \Psi) = -\frac{K}{4\pi} \vec{\nabla} \cdot \vec{\nabla} \Psi \, ,$$

$$\vec{E} = -\vec{\nabla}(\Phi + \Psi), \tag{3}$$

where K is the dielectric constant (see Appendix A) at a point, assumed to be everywhere the same in the following equations, and $\vec{\nabla} \cdot \vec{\nabla}\Phi = 0$ by definition (see Appendix B).

If Eqs. (2) and (3) are substituted into Eq. (1) and the inertia terms $g(\partial \vec{v}/\partial t)$ and $g\vec{v} \cdot \vec{\nabla} \vec{v}$ are assumed to vanish, the equations of motion for the fluid flow are (Henry, p. 109)

$$\eta \vec{\nabla} \times \vec{\nabla} \times \vec{v} + \vec{\nabla} p = \left(\frac{K}{4\pi} \vec{\nabla} \cdot \vec{\nabla} \Psi\right) \vec{\nabla}(\Phi + \Psi), \quad \vec{\nabla} \cdot \vec{\nabla} = 0 \, . \tag{4}$$

---

* This is the expression used by Henry. The complete expression for the volume force in a dielectric medium can be found in Panofsky and Phillips, p. 95.[5]

$$\vec{F} = \rho \vec{E} - \frac{1}{8\pi} E^2 \vec{\nabla} K + \frac{1}{8\pi} \vec{\nabla} \left(E^2 \frac{dK}{dg} g\right) \tag{2'}$$

where

g = mass per unit volume of the dielectric

K = dielectric constant

One cannot proceed beyond this point without a further definition of the problem. We shall in the future assume that the particle is a smooth sphere of radius "a" and uniform conductivity σ'. In general intact cells will not satisfy these conditions. In particular the conductivity of a cell will not be uniform. Therefore one must emagine that σ' is an appropriate average value of the conductivities of the various components of the cell. The conductivity of the fluid phase will be assumed to be everywhere the same and will be denoted by σ. The potential associated with the applied electric field will then be (Henry, p. 109; see also Appendix B)

$$\begin{aligned} \Phi_{\text{outside}} &= -E_0\left(r + \frac{\lambda a^3}{r^2}\right)\cos\theta, \\ \Phi_{\text{inside}} &= -E_0(1+\lambda)r\cos\theta, \end{aligned} \tag{5}$$

where

E_0 = the magnitude of the applied field infinitely far away from the particle,

θ = the angle that the radius makes with the direction of the applied field (infinitely far away),

$$\lambda = \frac{\sigma - \sigma'}{2\sigma + \sigma'}.$$

It is therefore evident that the applied field is distorted in the vicinity of the particle, unless $\sigma' = \sigma$.

If the first of Eqs. (5) is employed, Eqs. (4) can be solved for $\vec{v}$ and for p. Keeping in mind the boundary conditions

$$\text{at } r = \infty \quad \begin{cases} v_r = -U\cos\theta \\ v_\theta = U\sin\theta \\ \Psi = 0, \end{cases} \qquad U \equiv \text{electrophoretic velocity} \tag{6a}$$

$$\text{at } r = a \quad \begin{cases} v_r = 0 \\ v_\theta = 0 \\ \Psi = \Psi_a. \end{cases} \tag{6b}$$

Henry obtained the result,* (Henry, p. 114) that

$$p = \int_{\infty}^{r} \left(-\frac{K}{4\pi} \vec{\nabla} \cdot \vec{\nabla} \Psi\right) \frac{\partial \Psi}{\partial r} \, dr$$

$$+ \cos\theta \left[\frac{3\eta a}{2r^2} U - \frac{a}{r^2} \frac{KE_0}{4\pi} \int_{\infty}^{a} \xi \, dr \right.$$

$$\left. - \frac{KE_0}{4\pi} \left(3 \frac{\partial \Psi}{\partial r} - 2\xi\right)\right],$$

$$v_r = - \cos\theta \left[\left(1 - \frac{3a}{2r} + \frac{a^3}{2r^3}\right) U + \left(\frac{a}{r} - \frac{a^3}{3r^3}\right) \frac{KE_0}{4\pi\eta} \int_{\infty}^{a} \xi \, dr \right.$$

$$\left. - \frac{KE_0}{6\pi\eta} \left(\int_{\infty}^{r} \xi \, dr - \frac{1}{r^3} \int_{a}^{r} r^3 \xi \, dr\right)\right],$$

$$v_\theta = \sin\theta \left[\left(1 - \frac{3a}{4r} - \frac{a^3}{4r^3}\right) U + \left(\frac{a}{2r} + \frac{a^3}{6r^3}\right) \frac{KE_0}{4\pi\eta} \int_{\infty}^{a} \xi \, dr \right.$$

$$\left. - \frac{KE_0}{6\pi\eta} \left(\int_{\infty}^{r} \xi \, dr + \frac{1}{2r^3} \int_{a}^{r} r^3 \xi \, dr\right)\right],$$

$$v_\phi = 0,$$

$$\xi = \frac{\partial \Psi}{\partial r} + \lambda a^3 r \int_{\infty}^{r} \frac{1}{r^4} \vec{\nabla} \cdot \vec{\nabla} \Psi \, dr. \qquad (7)$$

---

* In Henry's paper there is an error in the sign of the third term in the expression for v_r. This error has been corrected in Eq. (7).

The pressure and fluid velocity define a mechanical stress tensor (Joos, pp. 217, 221) which is given by

$$\underset{\sim}{T}_{mech} = \underset{\sim}{P} - \underset{\sim}{1}\, p\,,$$

$$P_{ij} = \eta(\nabla_i v_j + \nabla_j v_i), \tag{8}$$

where $\underset{\sim}{1}$ is the unit tensor (i.e., $\underset{\sim}{1} \cdot \vec{A} = \vec{A}$ for any vector $\vec{A}$). The net mechanical force exerted on a body is then the integral over the surface of the body (Joos, p. 169). of the mechanical stress tensor

$$\vec{F}_{mech} = \oint \underset{\sim}{T}_{mech} \cdot \overrightarrow{dS}, \tag{9}$$

which I have found from Eqs. (7), (8), and (9) to be (see Appendix C)

$$\vec{F}_{mech} = \hat{z}\left[-6\pi\eta\, aU + KE_0\, a \int_{\infty}^{a} \xi\, dr \right.$$

$$\left. + KE_0\, a^2 \left(\frac{\partial \Psi}{\partial r}\right)_a \right], \tag{10}$$

where $\hat{z}$ is the unit vector in the direction of the applied electric field (infinitely far away).

In his paper, Henry (p. 115) gave the following equations for the mechanical (hydrodynamic) force:*

$$\vec{F}_{mech} = \hat{z}\, 2\pi\, a^2 \int_0^{\pi} P_{rz} \sin\theta\, d\theta$$

where

$$P_{rz} \equiv \left(-p + 2\eta \frac{\partial v_r}{\partial r}\right)_{r=a} \cos\theta$$

$$- \eta\left(\frac{\partial v_\theta}{\partial r} + \frac{1}{r}\frac{\partial v_r}{\partial \theta} - \frac{v_\theta}{r}\right)_{r=a} \sin\theta\,. \tag{11}$$

---

* These equations were derived from equations (8), expressed in cartesian coordinates. The z component of the stress is found from the expression (Joos, p. 170)[4]

$$P_{rz} = P_{xz}\, \hat{x}\cdot\hat{r} + P_{yz}\, \hat{y}\cdot\hat{r} + P_{zz}\, \hat{z}\cdot\hat{r}\,. \tag{11'}$$

From Eqs. (11) and (7) Henry obtained the result that

$$\vec{F}_{mech} = \hat{z}\left[-6\pi\eta\, a U + KE_0\, a \int_{\infty}^{a} \xi\, dr + KE_0\, a^2 \left(\frac{\partial \Psi}{\partial r}\right)_a\right], \tag{12}$$

which is the same as Eq. (10). Finally it is convenient to make the substitution

$$\left.\frac{\partial \Psi}{\partial r}\right|_a = -\frac{Q}{K a^2},$$

where Q is the net charge on the cell, to obtain the result

$$\vec{F}_{mech} = \hat{z}\left(-6\pi\eta\, aU + KE_0\, a \int_{\infty}^{a} \xi\, dr - QE_0\right) \tag{13}$$

Having computed the force exerted upon the charged sphere by the mechanical stress, it is now necessary to compute the direct force exerted upon the charged sphere by the applied electric field. Henry found the result

$$\vec{F}_{direct} = \hat{z}\, QE_0, \tag{14}$$

which he apparently obtained by assuming that the charge existed only on the surface. It is possible to demonstrate the validity of Eq. (14) with no assumptions (other than spherical symmetry–also used by Henry) regarding the distribution of charge.

Just as the mechanical force was calculated by integrating a mechanical stress tensor over the surface of the sphere [cf. Eqs. (8) and (9)], so too the electrical force can be calculated by integrating the so-called Maxwell stress tensor over the surface of the sphere. The Maxwell stress tensor is given in Panofsky and Phillips, (p. 97)[5] as

$$\underset{\sim}{T}_{elec} = \frac{K}{4\pi}\left[\vec{E}\vec{E} - \underset{\sim}{1}\left(\frac{1-b}{2}\right)\vec{E}\cdot\vec{E}\right],$$

where

$$b = \frac{g}{K}\frac{dK}{dg},$$

$$\vec{E} = \vec{E}_Q + \vec{E}_{applied}. \tag{15}$$

The electric field is the vector sum of the applied field and the field associated with the charge Q on the sphere. The so-called electrostriction term b was not included in the hydrodynamic equations [see Eq. (2)] and to be consistent in this rederivation of Henry's result it will also be disregarded in the following. I have, however, included it throughout the calculations in Appendix D. If spherical symmetry is assumed, the electric field at the surface of the sphere, due to the charge on the sphere, is

$$\vec{E}_Q(a) = \frac{Q}{Ka^2}\,\hat{r}\ , \tag{16}$$

where $\hat{r}$ = unit vector along the radical direction,

a = radius of the sphere,

Q = total net charge within the radius of the sphere regardless of the radial distribution of charge.

Furthermore, the applied electric field is found from Eq. (5) by evaluating $-\vec{\nabla}\Phi$ at $r = a$. In this way it is found that

$$\vec{E}_{\text{applied}}(a) = \hat{r}\,(1 - 2\lambda)\,E_0 \cos\theta - \hat{\theta}(1 + \lambda)\,E_0 \sin\theta. \tag{17}$$

The direct electrical force,

$$\vec{F}_{\text{direct}} = \oint_{\substack{\text{surface}\\ \text{of sphere}}} \underset{\sim}{T}_{\text{elect}} \cdot \vec{dS} = \hat{z}\,QE_0\ , \tag{18}$$

has been calculated from Eqs. (15), (16), and (17). These calculations may be found in Appendix D.

It remains yet to combine Eqs. (13) and (18), and thus relate the velocity of the particle in an applied field to the net charge on the particle. When the applied field is first turned on, the particle will accelerate until the viscous mechanical force is just equal and opposite to the direct electrical force. It then follows that

$$\vec{F}_{\text{mech}} + \vec{F}_{\text{direct}} = 0. \tag{19}$$

But from Eqs. (13) and (18) it follows that the two terms $-QE_0$ and $+QE_0$ cancel, and as a result (Henry, p. 115)

$$U = \frac{KE_0}{6\pi\eta} \int_{\infty}^{a} \xi \, dr$$

$$= \frac{KE_0}{6\pi\eta} \left[\Psi(a)(1+\lambda) + 3\lambda a^3 \left(5a^2 \int_{\infty}^{a} \frac{\Psi}{r^6} \, dr - 2 \int_{\infty}^{a} \frac{\Psi}{r^4} \, dr \right) \right] . \tag{20}$$

Henry (p. 116) has further shown by several partial integrations in the last expression that Eq. (20) may be reduced to

$$U = \frac{KE_0}{6\pi\eta} \Psi(a)(1+\lambda) \tag{21}$$

when the thickness of the countercharge distribution is very small compared with the radius of curvature of the sphere.

The small Greek letter zeta is commonly used to denote the value of the potential (which is associated with the charge on the sphere) at the "surface", relative to the potential at a point in the fluid infinitely far from the surface. This potential difference is known as the electrokinetic potential, or more commonly the zeta potential.

When the conductivity of the sphere is much smaller than that of the surrounding fluid, λ approaches a value of 1/2. In this case Eq. (21) becomes

$$U = \frac{K\zeta}{4\pi\eta} E_0 , \tag{22}$$

where ζ = electrokinetic potential, which is the usual equation of electrophoresis.

3. Comments on the Interpretation of the Electrophoresis Equation

An attempt will be made at this time to explain with words the significance of Henry's result, which is given in Eq. (20). One must first recall the picture of a charged particle suspended in an aqueous ionic solution. Ions of like sign are repelled while ions of opposite sign are attracted. Thermal agitation prevents the counterions from packing tightly around the particle, and so a diffuse "ionic atmosphere"

is formed. The electrical potential associated with the charge on the particle (and its countercharges in solution) is denoted by the symbol Ψ.

Henry's equation, Eq. (20), tells us that the velocity of a charged particle in an electric field is only indirectly related to the net charge on the particle. The force exerted directly upon the particle by the electric field is QE_0 as we expect. This force is exactly canceled, however, by a term which arises from the hydrodynamic resistance that the particle experiences as it moves through the fluid. The velocity is therefore determined solely by "second order" terms involving the potential generated by the charged particle in the ionic solution.

A reasonably good "physical" argument can be given as to why the QE_0 term cancels out of the final equation. It has already been shown that if the sphere has charge $+Q$ on it, the electric field will exert a force on the sphere which is QE_0. The sphere is, on the other hand, surrounded by a total charge $-Q$. One can estimate crudely what force would be exerted on the sphere due to this countercharge by imagining what would happen to an uncharged sphere that was surrounded in exactly the same manner by a charge $-Q$. This particle exists within a spherical volume of fluid containing the charge $-Q$. Consequently it may be calculated (by means of the Maxwell stress tensor, for example) that the force exerted on the volume of fluid and, hence, the force exerted on the particle itself will be $-QE_0$. The two forces acting on the sphere are equal and opposite, so that cancellation of these forces would occur.

This argument is not absolutely correct, of course, because the sphere and the surrounding fluid, which bears a charge $-Q$, are not rigidly connected to one another. Forces are transmitted between the sphere and the surrounding fluid only by viscous shear in the fluid. Consequently the force exerted upon the sphere due to the surrounding charge will be less than $-QE_0$, by an amount $KE_0 a \int_\infty^a \xi \, dr$ as was rigorously derived in Eq. (13).

The remaining term in Eq. (13) is $-6\pi\eta aU$, and it represents the viscous resistance experienced by a sphere as it moves with a velocity U through a fluid with viscosity coefficient η. This viscous-

resistance term will be the same regardless of whether or not the particle and the surrounding fluid are electrically charged. The reason for this is that the force term $-6\pi\eta aU$ arises from the general solution of the differential equations which describe the fluid motion (i.e., the solution of the homogeneous differential equations). Therefore, this term will always be present in any given problem, provided that the boundary conditions are the same.

Henry has shown, for the case of spheres and cylindrical rods at least, that under certain conditions the electrophoretic velocity is independent of the size and shape of the particle. These conditions are that the particle be nonconducting (relative to the surrounding fluid) and that the distance over which the countercharge is distributed should be very small relative to the dimensions of the particle. Under these conditions Eq. (22) is valid, and the electrophoretic velocity is directly proportional to the value of the potential at the surface of the particle (the potential at infinity is taken to be zero).

A special word must be said about the meaning of "surface" in this context. It is not too difficult, perhaps, to consider an imaginary closed surface, within which there is nothing but "particle" and outside of which there is nothing but aqueous solution. This mathematical fiction is especially easy to conceive of in the case of a completely smooth nonporous particle. It is this surface which would on first thought be considered as the surface of the particle.

How nice it would be if the matter were this simple! In reality it is quite possible that there are one or more "layers" of water which are (to varying degrees) firmly attached to the particle. It therefore becomes necessary for one to think of a new surface -- the so-called "surface of shear." By definition everything which lies within the surface of shear moves with the particle as a single hydrodynamic unit, while everything outside of the surface of shear is free to move independently, except for the viscous interaction between the particle and the surrounding fluid. It does not seem likely to me that such a surface exists in anything but a statistical sense. If in fact there are one or more layers of water firmly bound to the particle, then before one gets

to the point where the water is no longer bound, one must pass through a transition region in which the water may be considered to be sometimes bound and sometimes free. Nevertheless, the surface of shear is a commonly accepted notion which, even as stated, improves our description of the problem.

In the theory given above, it was necessary to define a surface for two reasons. First of all, it was necessary to specify the radius of the particle. For particles as large as intact cells, the addition of a few angstroms, to account for bound water at the surface, will not cause a measurable change in the radius. Secondly, it was necessary to state certain boundary conditions with regard to the velocity and the electric potential at the surface [Eq. (6b)]. In this instance it must be understood that one is speaking of the surface of shear when one talks about the surface of the particle. This fact has very important implications regarding the net charge of the particle. It should be recognized that water is not the only thing which will be bound within the surface of shear. There will be, in addition, a certain number of counterions, depending upon how thick the layer of bound water is. As a result the net charge within the surface of shear will be somewhat less than the net charge within what would ordinarily be called the surface of the particle.

Since we do not know how thick the layer of bound water might be, nor what percent of the countercharge is contained there, there must necessarily be some uncertainty associated with the interpretation of the zeta potential in terms of the charge on the particle itself. Strictly speaking, the zeta potential is the value of the electric potential at the surface of shear and, as such, it reflects only the net charge within the surface of shear. For the purpose of a quantitative estimation of the net charge on the particle one usually ignores the possibility that some of the countercharge may lie within the surface of shear. This is all that can be done because of the lack of further information.

B. The Charge May Exist in the Interior as Well as on the Surface of the Particle

1. Theoretical Proof of this Statement

When Henry presented his theoretical treatment of the electrophoresis of particles, he commented in a footnote (p. 108)[4] that "it is not essential that the fixed charge should be a surface distribution, but merely that it should have central symmetry." Nevertheless, electrophoresis experiments on intact cells are consistently interpreted only in terms of a surface distribution of charge. Brinton and Lauffer (p. 486)[6] have, in fact stated that the hypothesis of a volume charge contributing to the mobility is "... incompatible with electrophoretic theory and experiment which show that only the surface charge density determines mobility." I am unaware of any valid basis for this restriction in interpretation.

It is sometimes said that an internal charge cannot contribute appreciably to the mobility of an intact cell because the high electrical resistance of the cell membrane causes the electric current to flow around, rather than through, the cell. While it is indeed true that the electric current will "avoid" an insulating particle (see Appendix B), this in itself proves nothing, for what we are most interested in is the electric field, which is given by

$$\vec{E} = \frac{1}{\sigma}\vec{j} \,,$$

where

$\vec{E}$ = electric field,

$\vec{j}$ = electric current per unit area,

σ = electrical conductivity. (23)

An exact statement as to how extensively an internal charge might contribute requires, in this type of analysis, a complete knowledge of the current and the conductivity throughout the body of the cell.

In view of the prevalent opinion that the electrophoretic mobility of a particle is a measure of the surface charge only, it has seemed worthwhile to correct this misconception in a rigorous and completely general manner. It has already been stated (Subsec. I. A. 2) that the

"direct" force exerted on a charged particle (cell) by an applied field is given by the integral of the Maxwell stress tensor over the surface of the particle. The Maxwell stress tensor, however, involves only the value of the electric field at the surface of the particle, as has been stated in Eq. (15):

$$\underset{\sim}{T} = \frac{K}{4\pi}\left[\vec{E}\vec{E} - \underset{\sim}{1}\,\frac{(1-b)}{2}\,\vec{E}\cdot\vec{E}\right] ,$$

$$\vec{E} = \vec{E}_{Q} + \vec{E}_{\text{applied}},$$

where the electric field is the vector sum of the electric field associated with the charge on the particle and the applied electric field.

Now the electric field associated with the charge on the particle is the same regardless of whether the charge is in the interior or on the surface. (Gauss' law states that

$$\oint_{\substack{\text{closed}\\ \text{surface}}} \vec{E}\cdot d\vec{S} = \frac{4\pi Q}{K} ; \tag{24}$$

i.e., the surface integral of the electric field is proportional to the total charge within the closed surface, regardless of the way in which the charge is distributed). Consequently, the force exerted upon the particle will be the same, regardless of whether the charge is in the interior or on the surface.

2. Mechanisms by Which a Particle Can Acquire a Surface Charge

There are two fundamentally different ways in which a colloidal particle can acquire a net surface charge when suspended in an aqueous solution. First of all, ionizable molecules which are an intrinsic part of the colloid surface can dissociate. When this occurs there will be ions of one sign permanently attached to the surface of the colloid while the counterions will be free to move independently. For example, this is undoubtedly the primary mechanism by which the many amphoteric colloids of biological origin acquire a surface charge.

Alternatively, it is possible that ions from the aqueous solution could be adsorbed on the surface of the colloid. This is different from

the first mechanism in that the charged ions, which are now bound to the surface of the colloid, are not an intrinsic part of the colloid. This, most likely, is the mechanism by which "inert" colloids such as metallic sols, glass particles, gas bubbles, etc. acquire a surface charge.

While the dissociation of surface groups and the adsorption of ions are conceptually independent mechanisms, it should not be inferred that if one mechanism prevails the other cannot. In most situations, it is probable that both mechanisms are involved.

3. Mechanisms by Which a Particle Can Acquire an Internal Charge

There is, perhaps, a word or two of caution which must be said at the beginning of this section. The previous paragraphs, which treated mechanisms of surface-charge formation, presented commonly accepted ideas which may be found in any text on electrokinetics. The following paragraphs contain ideas which represent a somewhat original synthesis of available information, and which must not be considered as proven concepts. While I believe that these ideas are very elementary and logically sound, I must confess a profound respect for the facility with which nature can disprove what we so often believe to be elementary and logical.

The arguments to be presented below rest upon two simple principles. First of all, if an electrical potential can be measured across the surface between two phases, then there must be a charge separation occurring at this surface. [There are two types of charge separation that are not of interest at this point. The first is the surface charge (with a countercharge in the surrounding phase), which has already been discussed. The second is the orientation of dipoles.* A surface of oriented dipoles will indeed produce a potential difference across the surface of a particle, but will not confer a net charge on the particle.] The second principle is this: if a potential difference exists across the surface of a particle, and it is known that this potential difference is

---

* Or higher multipoles. A dipole is defined as a charge of one sign separated a given distance from a charge of the same magnitude but opposite sign.

not caused by a surface charge or by the orientation of dipoles, then it must be true that the interior of the particle has a net charge.

If the two principles above are accepted, the following line of argument will show that it is possible for a colloidal particle to acquire an internal charge. There are certain situations in physical chemistry and biology in which a potential difference can be measured across the interface between two phases. In the instances cited below, good arguments can be presented which discount the possibility that the potential difference is caused by a surface charge or the orientation of dipoles. It then follows that the interior of the two phases must bear a net charge. Three such mechanisms by which a colloidal particle might acquire a net internal charge will be described below.

Consider, first of all, a particle composed of a homogeneous liquid that is immiscible with the aqueous phase in which it is suspended. If ions of one sigh from the aqueous phase are more soluble in the particle phase than are ions of the opposite sign, then a preponderance of the first will exist in the particle, and an internal charge will occur. This is the mechanism that is responsible for the potential difference across an oil-water interface (distribution potential).[7]

A second possibility exists when the particle is bounded by a semipermeable membrane. In this case ions of one sign are constrained to stay within the boundaries of the particle, while ions of the opposite sign are free to diffuse out. As they do so, they leave behind a net charge in the interior of the particle. This is the mechanism that gives rise to the so called Donnan potential.[7]

A final, third, possible mechanism exists in the case of intact living cells. By virtue of their "energy" metabolism, living cells are able to perform various kinds of useful work. It is widely believed that the cell is capable of using part of its available energy to selectively "pump" charged ions across its surface. Such an "active transport" of ions across the cell surface opens up the possibility that the interior of the cell contains an excess of charges of one sign. The Bernstein theory of membrane potentials specifically proposes that the interior of the cell has a net negative charge, while the medium surrounding the cell is positively charged (Heilbrunn, p. 462).[8] I only wish to touch

lightly on the question of membrane potentials at this time. I will return in Sec. III to consider, first of all, the extent to which active ion transport is involved, and secondly, to the question of whether membrane potentials are produced by an internal charge or by a surface of oriented dipoles. (A surface-charge mechanism has never been seriously considered as being responsible for the biological membrane potentials.)

A very special word of caution must be said in regard to the concept of an interior charge. The question is often asked whether the charged colloids and membranous systems within the cell might not contribute to the net charge of the cell. One thinks especially of the endoplasmic reticulum and the nucleic acids, not to mention the many soluble proteins, etc. In considering this question, one must be careful to realize that all of these charged systems are surrounded by counterions. As a result, electrical neutrality will be achieved over distances that are extremely small compared with the size of the cell. If, therefore, these counterions move as a hydrodynamic unit with the whole of the cell, then the cellular constituents, together with their counterions, will not contribute to the net charge of the cell.

The real question to be asked then is: To what extent do the counterions that are associated with the cellular constituents move as a unit with the whole cell? I know of no definitive way in which to answer this question. It seems certain to me, however, that in the normal situation these "interior" counterions will move with the cell, for the cell membrane will restrain them from doing otherwise. It may be safely concluded, therefore, that the cytoplasmic colloids and the cytoplasmic structures will not contribute to the net charge of the cell nor to its electrophoretic mobility.

4. Appearance of the Internal-Charge Hypothesis in the Literature

In the microelectrophoresis literature, one rarely sees a discussion of the possible involvement of interior charges. Heilbrunn was one of the very few persons to caution against the interpretation of cellular electrophoresis experiments strictly in terms of a surface

charge (pp. 99FF, 120).[8] More recently Philpot and Stanier have observed that freshly prepared rat-liver nuclei remain stationary in an applied electric field, while the nuclear contents move rapidly to one side. They have interpreted this to mean that the nuclear contents are negatively charged while the surface of the nucleus bears an equal positive charge. As a result, the nucleus as a whole bears no net charge and cannot move in an applied field.[9]

II. MICROELECTROPHORESIS: PROCEDURE AND EQUIPMENT

A. General Description of the Method

Electrophoresis is the word used to refer to the movement of a charged particle (which is dissolved or suspended in a fluid medium) due to the force exerted on it by an electric field. It is possible to quantitatively measure the velocity of such a particle and thus infer something about the magnitude (as well as the sign) of the charge on the particle. If the particle has dimensions of the order of a micron or larger, it is possible to see the object in a microscope. Microelectrophoresis refers to the technique in which a microscope is employed in order to observe the particle and the rate at which it moves in an electric field.

In the microelectrophoretic technique the suspension of particles is contained in what amounts to a hollow microscope slide–which I have chosen to call the microelectrophoresis chamber rather than cell, in order to avoid confusion with the use of the word cell in a biological context. A microscope is brought to focus upon a particle somewhere within the chamber. After the electric field has been applied, the velocity of the particle is determined by measuring the time that it takes for it to move a given distance. This distance is most easily determined by counting the number of lines crossed on a calibrated reticule inserted in the eyepiece of the microscope.

B. Detailed Description of the Apparatus Used in This Study

Figure 1 gives an overall view of the microelectrophoresis apparatus. A microscope equipped with bright-field and phase-contrast optics was mounted on a pivoting base such that the microelectrophoresis chamber could be used in either the horizontal, vertical, or lateral orientation (see Brinton and Lauffer[6] for a description of the advantages and disadvantages associated with each orientation). All work described in this report was performed with the chamber in the lateral position, as pictured. The microscope (and pivots), the light source, and ring-stand bars were attached to a common base and placed on the surface of a shock-mounted table.

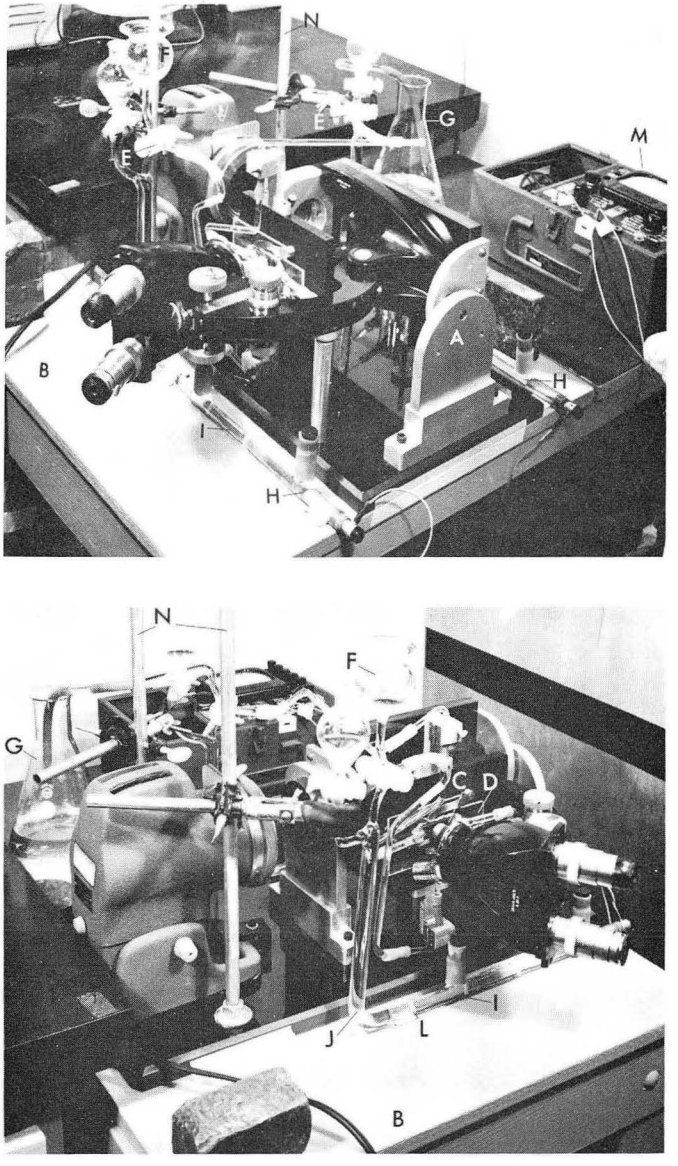

ZN-3877

Fig. 1. Overall view, from two angles, of the microelectrophoresis apparatus: (A) pivoting base upon which the microscope is mounted, (B) surface of the shock-mounted table, (C) microelectrophoresis chamber, (D) Lucite plate, (E) three-way stopcocks, (F) thistle tube, (G) waste bottle, (H) Zn-$ZnSO_4$ electrodes, (I) saturated-Na_2SO_4 chamber, (J) Standard Buffer chamber, (L) sintered-glass disks, (M) ammeter, (N) ring-stand rods.

The microelectrophoresis chamber itself was mounted in a thin Lucite plate with the aid of "liquid rubber" (Flex-O-Fix, Pyroil Co., Inc., La Crosse, Wis.) to facilitate clamping it to the microscope stage, as shown in Fig. 2. The chamber is of the rectangular-Northrup-Kunitz type (Arthur H. Thomas Co., Philadelphia), the width (≈ 12 mm) being greater than 20 times the depth (≈ 0.5 mm). The chamber is connected via suitable glass and rubber tubing to three-way stopcocks. Originally, greased glass stopcocks were used, but Teflon stopcocks which do not require grease have subsequently been found to be more desirable. These stopcocks may be turned so as to connect the microelectrophoresis chamber either to the thistle tube and wash bottle (for rinsing and for introduction of sample) or to the $Zn\text{-}ZnSO_4$ electrodes. The electrodes are isolated from the stopcocks by the following sequence of barriers: an 11-in.-long glass tube filled with Standard Buffer* (with glucose added to prevent convective exchange of specimen and buffer at the stopcock); fine sintered glass disk; 5-in.-long glass tube filled with saturated $NaSO_4$; fine sintered glass disk; and finally $Zn\text{-}ZnSO_4$ electrode chamber. The purpose of these barriers is to keep the Zn^{++} ions in the electrode chamber from mixing with the biological material in the microelectrophoresis chamber.

A 325-V (maximum) voltage-regulated power supply (Lambda Electronics, College Point, N. Y.), equipped with a reversing switch, was connected to the electrodes, and the current passing through the circuit was measured with an ammeter which could read 0 to 10 mA, 0 to 1 mA, and 0 to 50 μA full-scale deflection (Supreme Instrument Corp., Philadelphia). The electrical circuit is shown schematically in Fig. 3.

Three microelectrophoresis chambers were used during the period of this research. It was necessary in each case to measure the cross-sectional area of the chamber. The width of the chamber was measured with the aid of a seven-power eyepiece equipped with a calibrated reticule. The depth of the chamber was determined by successively focusing on the two inner walls of the chamber and recording the distance by means of the fine-focus micrometer scale.

* See notation page for definition.

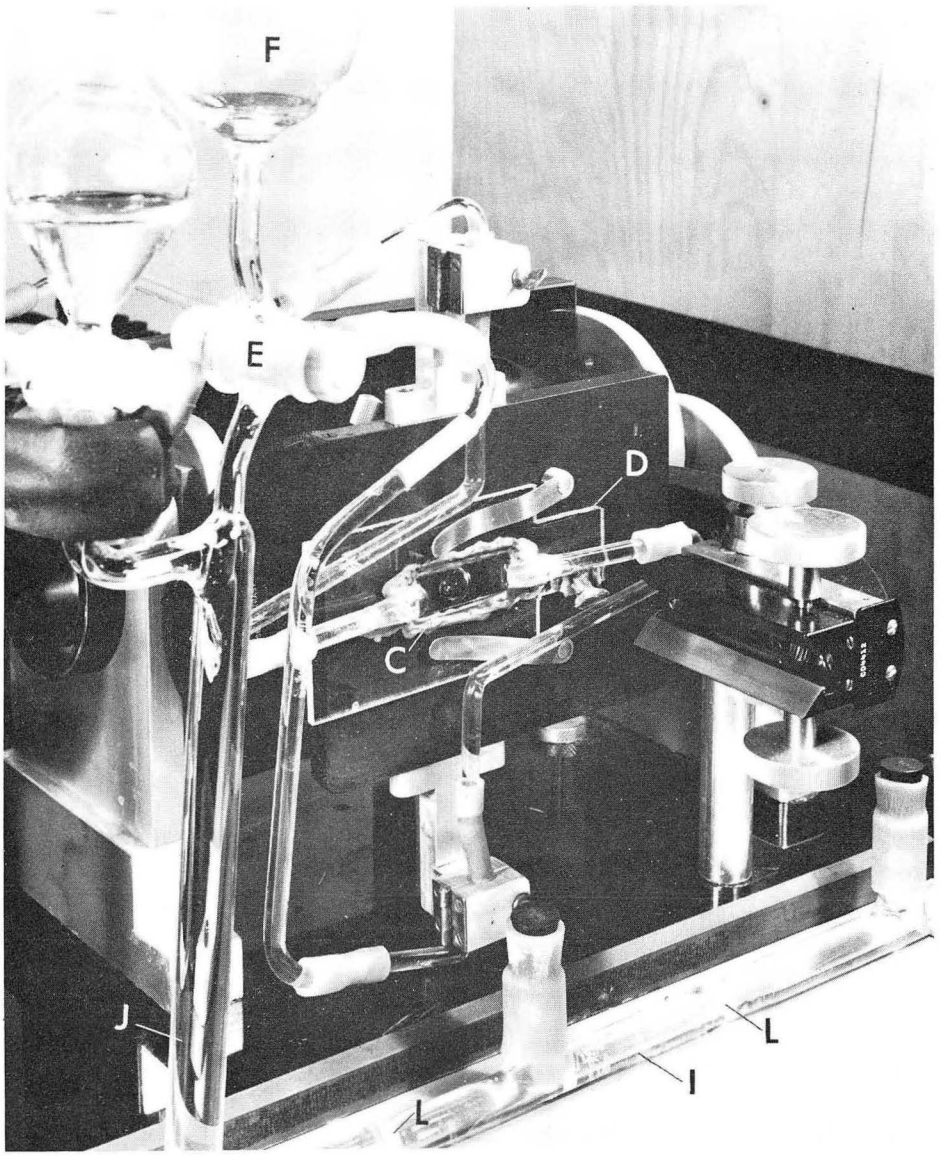

ZN-3871

Fig. 2. Close-up view of the microelectrophoresis apparatus: (C) microelectrophoresis chamber, (D) Lucite plate, (E) three-way stopcocks, (F) thistle tube, (I) saturated-Na_2SO_4 chamber, (J) Standard Buffer chamber, (L) sintered-glass disks.

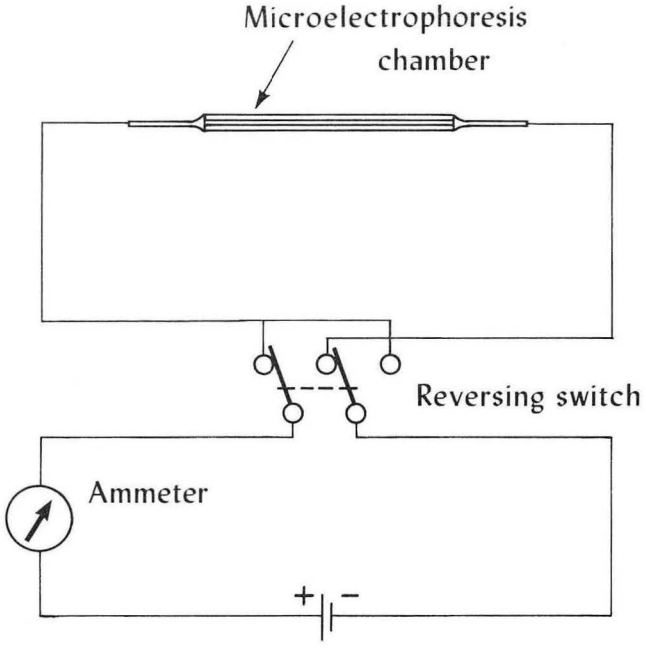

MU-31373

Fig. 3. Schematic diagram of the electrical circuit used in the microelectrophoresis apparatus. See text for further details.

The scale had previously been calibrated by measuring the distance (through air) from the top of one glass slide to the top of a second slide, upon which the first was lying at right angles. These measurements cannot be made through the glass, as the apparent thickness will be reduced by a value equal to the index of refraction of the glass. The actual thickness of the glass slide was determined by measurement with a micrometer caliper.

The specific resistances of the various experimental solutions were measured with the Leeds and Northrup model 4960 conductivity cell and bridge shown in Fig. 4. The sample was poured into the thistle tube and allowed to run through the cell until a constant reading was obtained. The temperature was controlled by adding hot water or ice cubes to the water bath in which the conductivity cell was immersed. The absolute resistance in ohms of the solution within the cell was determined with the Wheatstone bridge. The conductivity cell constant had been determine to be 1.46 cm^{-1} as shown in Fig. 5, so that the absolute resistance in ohms divided by this factor gives the value of the specific resistance in ohm-cm.

C. On the Method of Taking Data

Because of electroosmosis there will be fluid flow in one direction along both walls of the microelectrophoresis chamber while the electric field is on, and fluid flow in the opposite direction down the center of the chamber. Evidently there must be two positions at which the fluid flows in neither direction. The positions of zero fluid flow are referred to as the stationary levels. The exact position of the stationary levels depends somewhat upon the relative dimensions of the microelectrophoresis chamber. In the apparatus used the stationary levels existed at a fractional depth 0.204 away from the walls of the chamber, which is very near to the fractional depth (0.211) at which the stationary levels exist in the limit of an infinitely thin chamber. The theory relating to this subject is reviewed in Brinton and Lauffer.[6]

Because of the fluid flow the apparent velocity, which is the vector sum of the fluid velocity and the electrophoretic velocity, will vary in

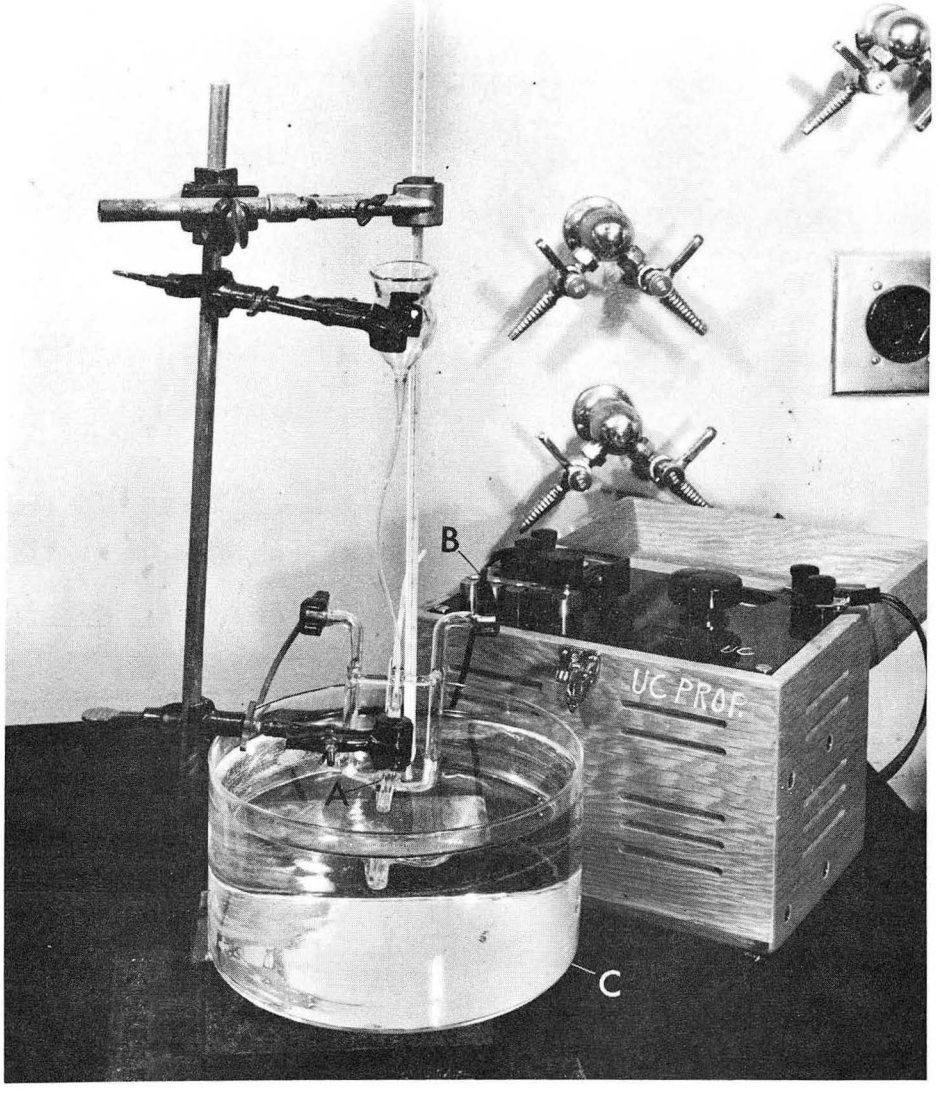

ZN-3870

Fig. 4. Photograph of the conductivity bridge and cell: (A) glass conductivity cell, (B) Wheatstone bridge, (C) water bath.

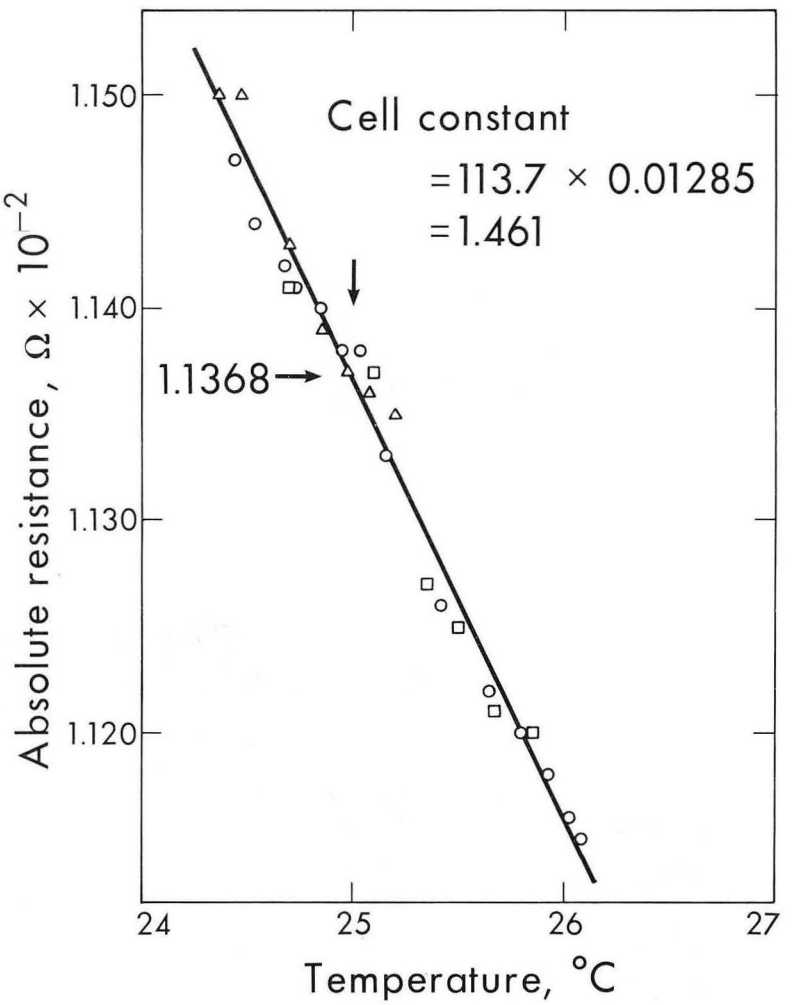

Fig. 5. Calibration of the conductivity cell. A standard KCl solution (7.4191 g KCl per 1000 g of solution) was run through the cell until a constant reading was obtained. The absolute resistance across the leads of the conductivity cell was measured with the Wheatstone bridge. The specific conductivity of the standard solution at 25° C is 0.012856 ohm^{-1} cm^{-1} (Leeds and Northrup Co. No. 4960 Portable Electrolytic Resistance Indicator manual, Std. 10899, Issue 3). Therefore the cell constant can be determined by multiplying the measured resistance by the known specific conductivity. Data from three separate experiments are shown on the graph.

a parabolic manner from the center of the coordinate system, which is located at the center of the chamber.[6] An example of such a parabolic velocity profile is shown in Fig. 6. The apparent velocity (in divisions of the eyepiece reticule per hundredth of a minute) of rat erythrocytes suspended in $NaHCO_3$ (3×10^{-4} M) buffered NaCl (0.145 M) is plotted vs the depth of the chamber (measured in divisions of the microscope's fine-focus micrometer scale). A parabola is fitted to the experimental data by choosing a base line (by eye) which best fits the data at the center of the chamber, plotting the data as they appear in this coordinate system on log-log paper, and fitting the data with a straight line having a slope of two. (The equation of a parabola is $y = Kx^2$; therefore, the plot of log y vs log x should have a slope of two. I have found this method much more convenient than plotting $\sqrt{y}$ vs x, which is the common way of fitting a parabola to the data.) After the data have been fitted with a parabola, the velocity at the stationary level is read from the graph, and the mobility is calculated according to the equation

$$\text{Mobility} = \frac{\text{distance}}{\text{time}} \times \frac{\text{cross-sectional area} \times \text{conductivity-cell constant.}}{\text{current} \times \text{absolute resistance}}$$

The conventional units of mobility, used throughout this report, are (micron)(sec^{-1})($volt^{-1}$)(cm).

To insure that the apparatus was working properly a complete velocity profile was measured in almost all cases. Between ten and twenty points were taken for each such parabola. With some experience, this amount of data can be taken in a period of 15 to 20 min. The observed velocity at a given level was obtained by averaging the velocities for cells first in one direction, and then (with the field reversed) in the other direction. This averaging process serves to cancel out the effect of any fluid drift which may arise from leakage in the system, or from other factors such as thermal gradients.

Under certain conditions, especially when the mobilities of the cells in a given medium are not constant over short periods of time, it is not possible to obtain a complete velocity profile. In those instances, all measurements were made at a single stationary level.

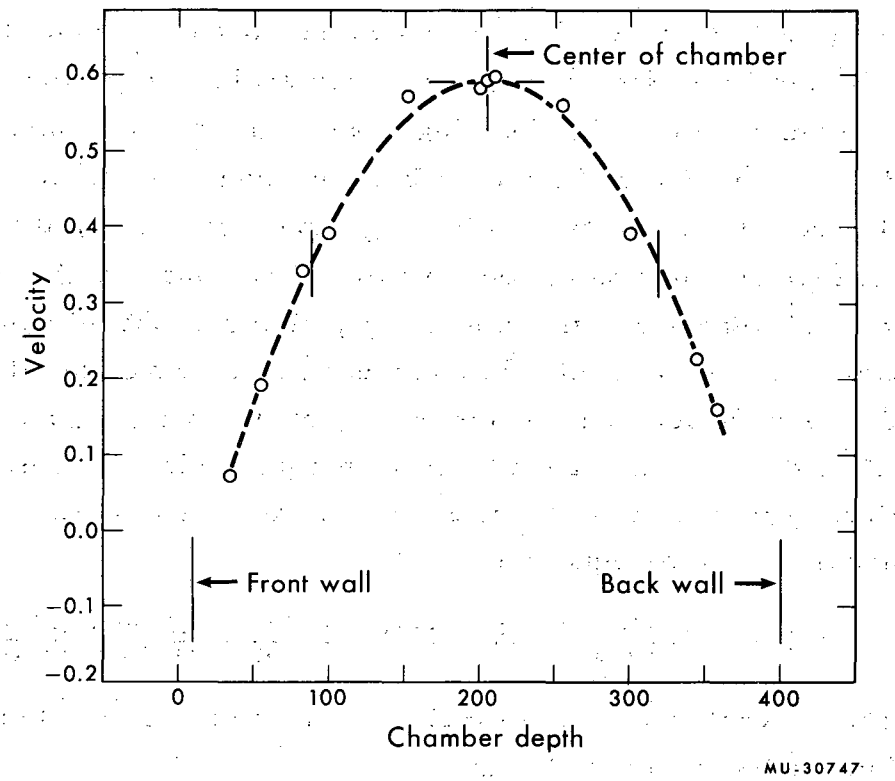

Fig. 6. Parabolic velocity profile. The observed velocities of rat RBC are plotted vs the depth in the chamber at which the measurements were made. A true parabola is fitted to the data. The two stationary levels are indicated by the marker on each leg of the parabola. See the text for the dimensions used in this plot and for the method by which the parabola was fitted to the data.

Data were again recorded with the field first in one direction and then with the field reversed, and the velocities averaged in order to cancel out the effect of any possible fluid drift.

If the technique of measuring a complete velocity parabola is employed, it is possible to work with samples having a much lower cell concentration than otherwise. The reason for this is that one may focus on a cell, regardless of at what level it is in the chamber, record the position, and measure the apparent velocity at that level. In the other technique, it is necessary to work with a sufficiently high cell concentration that there will always be a few cells in focus at the stationary level.

All electrophoretic velocity measurements were made at room temperature (23 to 26° C). The electrophoretic velocity at constant electric current is essentially constant over such a small temperature range, since the temperature coefficients of the viscosity and the conductivity (which are about 2% per degree) tend to cancel each other.[6] The value of the mobility at 25° C can therefore be obtained by using the value of the conductivity at 25° C in the mobility calculations. For this reason, all conductivity measurements were made in a water bath thermostated at 25° C; as described in Subsec. B.

The pH of all solutions was measured with a Beckman model G pH meter with a standard glass electrode and a calomel reference electrode. All pH measurements were recorded after the addition of the cells. This was especially necessary when salt solutions of low buffering capacity were being used, for the pH of such solutions sometimes changed as much as one unit after addition of the cells. When solutions of low buffering capacity were being used, it was also found necessary to rinse the electrodes of the pH meter repeatedly with the cell suspension being measured, before constant readings could be obtained.

This concludes the description of apparatus and general methods. The special techniques of cell-sample preparations, handling, etc. will be described at the appropriate time in the remainder of the text.

III. EXPERIMENTAL INVESTIGATION OF THE HYPOTHESIS THAT AN INTERNAL NET CHARGE CONTRIBUTES SIGNIFICANTLY TO THE TOTAL CHARGE OF INTACT CELLS

A. Literature that Suggested a Net Internal Charge

1. The Phenomenon of Membrane Potentials

The phenomenon of membrane potentials was touched upon lightly in Sec. I, when mechanisms for producing an internal net charge distribution were being discussed. (The reader must keep in mind, during the following discussion, that electroneutrality holds over a sufficiently large volume about the cell.) The subject will be further developed at this point. Potential differences across many cellular membranes can be measured directly by inserting a microelectrode into the cytoplasm of the cell. This sort of experiment is of course limited to cells that can accommodate a microelectrode. When such experiments are performed upon cells in the resting state it is found that the potential of the cell interior is negative with respect to the surrounding medium in amoebae,[10] animal nerve axon and muscle,[11] and fresh-water algae.[11] The magnitude of such membrane potentials is in all cases on the order of 10 to 100 millivolts. The only known instances in which the cell interior is positive with respect to the exterior (in the resting state) are in cases of certain marine plant cells.[11]

There have been many theories proposed throughout the years to explain the phenomenon of biological membrane potentials. In general these theories have centered about the behavior of physico-chemical models that can be studied in the laboratory.[12,13] These proposals have included both the Donnan potential (the Bernstein theory[8] was a special case of this type of mechanism) and the "distribution" potential (especially as studied by Beutner and by Bauer).[7,11] It is the diffusion potential, however, that has enjoyed the most recent popularity in explaining biological membrane potentials (Scheer, p. 274 ff).[11] The so-called diffusion potential arises when two aqueous phases are separated by a permeable interface. The concentration of salt must be initially greater in one phase than in the other. If then the

ions of one sign are able to diffuse across the interface more rapidly than the ions of opposite sign, a net charge separation will occur, and a potential difference will result. Osterhout and Blinks have been primarily responsible for developing the diffusion-potential theory for fresh-water algae and marine plants, respectively, while Hodgkin and Huxley have done much of the fundamental work on nerve and muscle systems in animals.[11]

It is clear that the diffusion potential can be maintained only under special circumstances. As diffusion proceeds, the ionic concentrations in the two aqueous phases will become equal. At this point diffusion will cease, and the potential will fall to zero. The only way in which this can be prevented is for the ionic concentrations in the two aqueous phases to be continually replenished. In the case of a living cell, this means that salts must be transported $\begin{matrix}\text{into}\\ \text{out of}\end{matrix}$ the cytoplasm as rapidly as they are $\begin{matrix}\text{out of}\\ \text{into}\end{matrix}$ the cytoplasm. It should be clear that energy will be required to transport ions in a direction opposite to that of free diffusion. Therefore the active transport of ions will likely be required for the permanent maintenance of diffusion potentials in biological systems.

The diffusion-potential theory is very good in explaining bioelectric potentials. On the other hand, I know of no compelling reason to exclude the possibility that a surface charge or a surface of oriented dipoles might be partially responsible for the membrane potential. As yet, it has been unnecessary to postulate their existence for the sake of explaining experiments, and so one tends to believe that they are not important. Furthermore, it is known that bioelectric potentials require metabolic energy for maintenance of their normal values,[11] as the diffusion-potential theory would require. On the other hand it is difficult to understand why the surface charge or dipole layer theories would, a priori, require metabolic energy for the maintenance of the membrane potential. Thus at least the metabolically controlled component should not have a fixed dipole origin.

To summarize what has been said so far, my interpretation of the evidence to date suggests that the charge separation across the membrane associated with the ubiquitous biological membrane potentials

results in some net charge in the cell interior. In all cases yet measured, except for certain marine plants, this net interior charge must be a negative charge. It is well documented that metabolic energy participates in the maintenance of this charge separation, and it seems most probable that this energy is utilized in the active transport of ions.

If the statements above regarding internal charge are correct, it then becomes very important to inquire to what extent these internal charges can contribute to the net charge on the cell. If we assume that the internal charge is solely responsible for the (resting) membrane potential, we can calculate an upper limit on the magnitude of the internal charge. The equation which is required for such a calculation is

$$Q = C \cdot V \cdot A,$$

where

C = membrane capacitance per unit area,

V = membrane potential,

A = cell area. (25)

As an example, consider the human red blood cell (RBC). In this case, the membrane capacitance[14] is about 1 $\mu F/cm^2$, the membrane potential may be expected to be in the range from 10 to 100 mV, and the cell area[15] is about 160 μ^2. The net charge then calculates out to be

$$Q = 1\times10^{-6}\ \frac{\text{farad}}{\text{cm}^2} \times (0.1 \text{ to } 0.01) \text{ volts} \times 1.6\times10^{-6}\ \text{cm}^2$$

$$= 1.6\times10^{-13} \text{ to } 1.6\times10^{-14} \text{ coulomb.} \quad (26)$$

Since there are 1.6×10^{-19} coulomb per electron, the total number of elementary charges lies in the range from 10^5 to 10^6 charges per cell.

To determine whether or not this is a significant amount of charge compared with the net charge, one must use the equations of electrophoresis to calculate the charge from the measured electrophoretic mobility. In order that this may be accomplished, some assumptions must be made regarding the relationship between the net charge and the electrokinetic potential. Many possibilities exist here, but the most commonly used relationships suppose that the Debye-Hückel approximation (Brinton and Lauffer, p. 436)[6] holds. In this case,

$$\nabla^2 \Psi = \kappa^2 \Psi ,$$

$$\kappa^2 = \frac{4\pi e^2 \Sigma c_i Z_i^2}{KkT} , \qquad (27)$$

where

e = electron charge,
c_i = concentration of the ith ion,
Z_i = valence of the ith ion,
K = dielectric constant,
k = Boltzman's constant,
T = temperature.

Here the zeta potential is related to the charge on a sphere by the equation[6]

$$\zeta = \frac{Q}{\kappa a} \frac{1}{1+\kappa a} . \qquad (28)$$

This equation may be used directly to find the net charge from the mobility. More commonly, Gorin's equation correcting for the finite size of the counterions (Brinton and Lauffer, p. 482)[6] is used. When this is substituted into Eq. (22) one obtains the following relationship between charge and mobility:

$$Q = \frac{4\pi a^2 \mu \eta}{(a_i + 1/\kappa)} ,$$

where

a = radius of the sphere,
μ = mobility,
η = viscosity,
a_i = radius of the counterions,
κ = the Debye-Hückel constant, defined in Eq. (27). (29)

The net charge on a (human) RBC can be calculated from Eq. (29) by inserting the following numerical values:

$$4\pi a^2 = 1.6\times10^{-10}\ m^2 = \text{surface area of human RBC,}^{15}$$

$$\mu = 1.08\times10^{-8}\ m^2/\text{sec-volt} = \text{mobility of human RBC in } 0.145\ \underline{M}\ \text{NaCl, pH} = 7.4 \text{ (from reference 16),}$$

$$\eta = 10^{-3}\ \text{Newton-sec}/m^2 = \text{viscosity of water at 25° C,}$$

$$a_i = 1.85\times10^{-10}\ m = \text{extrapolated value of Furchgott and Ponder,}^{17}$$

$$\kappa = 0.327\times10^{8}\ (\Gamma/2)^{1/2}\ cm^{-1},\ (\Gamma/2 = \text{ionic strength}) \text{ at } 25°C$$

$$1/\kappa = 8.05\times10^{-10}\ m \text{ at } 25°\ C \text{ in } 0.145\ \underline{M}\ \text{NaCl.} \qquad (30)$$

When this caluclation is performed it is found that

$$Q = 1.75\times10^{-12}\ \text{coulomb per cell}$$

$$= 1.1\times10^{7}\ \text{charges per cell,} \qquad (31)$$

which is between 10 and 100 times as large as the (maximum) assumed internal charge.

If these numbers could be taken with complete confidence, it would seem that the charge associated with membrane potentials contributes but a very small portion to the net charge on a cell. Before such a conclusion is drawn, however, attention should be drawn to various uncertainties in these calculations. First of all, the quoted value of the membrane capacitance was calculated from ac impedance measurements on RBC suspensions. The nature of the equation used for such calculations, and consequently the value of the quoted capacitance, depends upon the model that is assumed to describe the cell.[14] Secondly, the quoted value was the value of the membrane's capacitance at high frequencies.[14] The dc capacitance ought to be used in calculations such as in Eq. (26), but the membrane capacitance can only be measured at high frequencies.[14] Finally, the use of the Debye-Hückel equation to relate the zeta potential to net charge may result in a large overestimation of the net charge, as has been shown by the computer calculations of Loeb et. al.[17a]

Consequently, it would not be safe to discount the possibility of a contribution from a net internal charge solely on the basis of these

calculations. The answers obtained in the caluclations above are sufficiently close to each other in value that were the uncertainties mentioned above to be corrected somehow, it might turn out that the internal charge could compose a sizable percentage of the total charge. With this in mind, it would seem worthwile to attack the problem experimentally.

The calculations in this section bring up another interesting point. The question might be asked: How can it be, even in principle, that the net charge on a cell exceeds the charge that is associated with the membrane potential? One would on first thought be of the opinion that all of the net charge should contribute to the membrane potential, in which case the calculated values in Eqs. (26) and (31) should agree. This need not necessarily be true, as can be seen by assuming that the majority of the net charge exists on the surface of the cell and originates from the dissociation of ionizable groups. Just as there is a surface charge with its counterions on the outside of the cell, so will there be a similar surface charge and associated counterions on the inside (assuming a reasonable symmetry of the cell membrane). The two potentials generated by the charge-countercharge distributions have the opposite sign, and so they cancel (or at least tend to cancel) each other. This proposed cancellation of surface-charge-associated potentials is shown schematically in Fig. 7. A great deal more could be said about the expected behavior of the total potential difference in such a system when the pH or ionic strength is varied on only one side of the membrane, for under these conditions the two potentials would no longer cancel one another. This discussion has already gotten too far from the main line of discussion, though, and no more will be said.

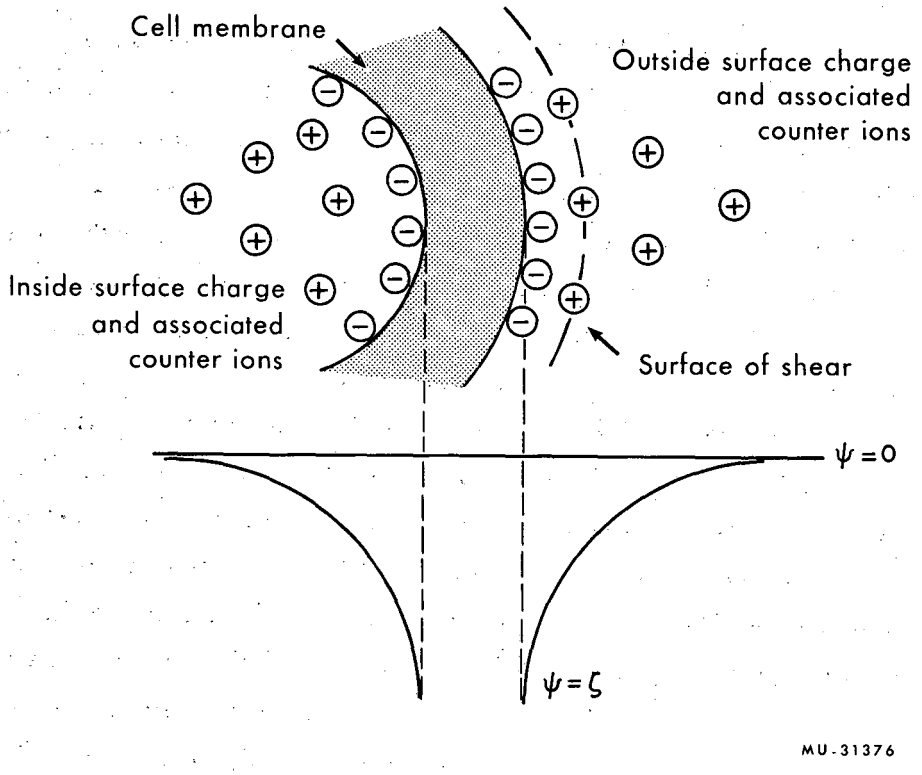

Fig. 7. Proposed cancellation of surface-charge-associated potentials. Both the inner and the outer surfaces of the cell membrane have an excess of negatively charged dissociable groups (at normal pH), and a diffuse distribution of countercharge. The charge distribution on the inside has, however, the opposite orientation of that on the outside. Therefore the potentials generated by the two charge distributions cancel, or at least tend to cancel.

2. The Low Isoelectric Points of Intact Cells

The somewhat equivocal results of the above charge calculations were not the only thing that suggested it would be worthwile to design experiments to test the internal-charge hypothesis. At the time when this research began there were several phenomena reported in the literature which suggested that an internal charge might be involved. Perhaps foremost among these was the extremely low isoelectric point of human RBC in isotonic saline. Furchgott and Ponder[17] found that if mobility measurements were made within two minutes after exposing the cells to low pH, then the cells remained negatively charged down to pH 1.7, as may be seen in Fig. 8. Below pH 4.0 the RBC suffered an irreversible decrease in mobility after a length of time that became progressively shorter at progressively lower pH. At pH approximately 2.0, it was observed that the RBC hemolyzed within 2 min and that the cells which previously were negatively charged suddenly acquired a positive charge. Heard and Seaman[16,18] have also worked extensively with human RBC. Figure 8 shows that while the shape of their curve is quite different from that found by Furchgott and Ponder, it appears as though the RBC would be isoelectric in the vicinity of pH 2.0.

The existence of such a low isoelectric point for intact RBC seemed, at least at first thought, inconsistent with the common belief that the exterior of the cell was coated with protein (see Sec. III), since proteins which have an isoelectric point below pH 3.0 to 4.0 are extremely rare. The low isoelectric point of RBC was, in fact, tentatively ascribed for many years to the phosphate groups of the membrane's phospholipids, rather than to groups from the membrane's protein component.[19]

Furthermore, RBC are not alone in having a very low isoelectric point. Bangham et al.[19] have found that sheep lymphocytes were isoelectric at pH 2.6. These authors, as well as Wilkins et. al.,[20] have found that sheep polymorphonuclear leukocytes were still negatively charged at pH 2.0. The ascites tumor cells studied by Cook et. al.[21] showed an isoelectric point of 3.8. Bangham and Pethica[22] have reported that mouse lymphocytes are isoelectric at pH 2.2,

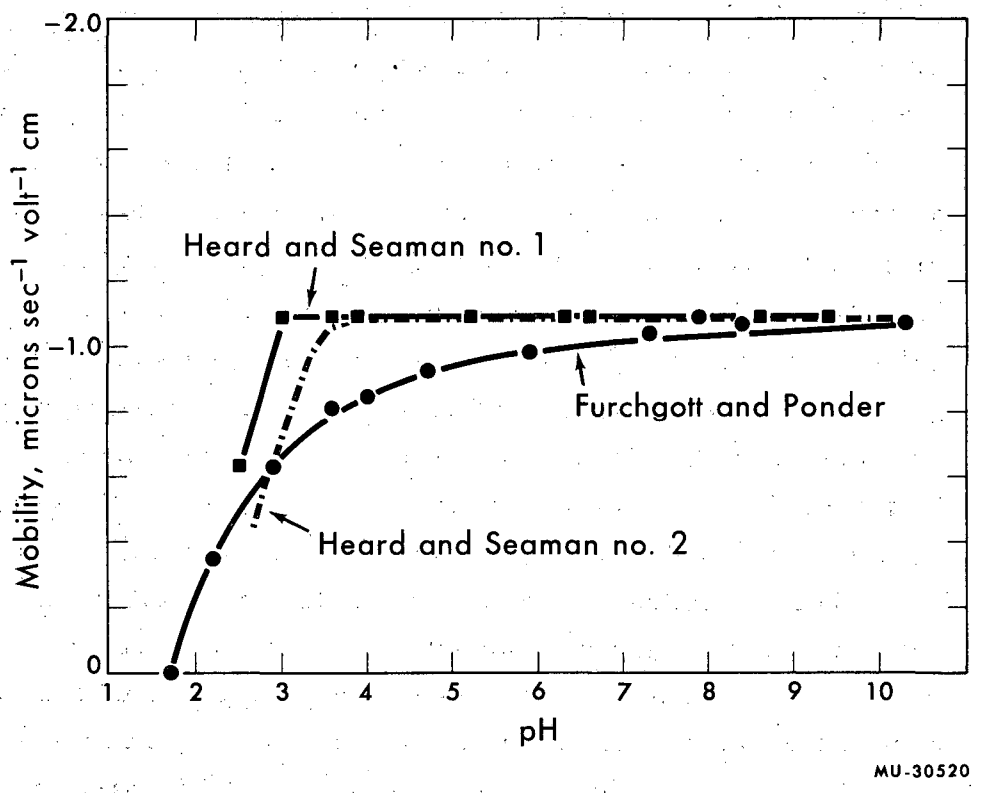

Fig. 8. A comparison of mobility-pH curves for human RBC obtained by Furchgott and Ponder[17] (using the buffered saline solution described in Subsec. III. B. 2. b) and by Heard and Seaman's group (using the Standard Buffer described in Subsec. II. B. 2. a). Heard and Seaman No. 1 is from ref. 16, Heard and Seaman No. 2 is from ref. 18.

Ehrlich ascites cells at 2.8, and normal mouse liver cells at 3.9. One of the notable virtues of the interior-charge hypothesis is that it suggests a natural explanation for the low isoelectric point of intact cells, which does not conflict with the common belief that the cell exterior is a layer of protein. In order to achieve such an explanation it is necessary to suppose that the cell membrane is relatively impermeable to hydrogen ions. I know of no experimental evidence in this regard with respect to mammalian cells, but Gilby and Few have described such a membrane barrier to hydrogen ions in bacteria.[23] They have also found that this barrier will break down after prolonged exposure to high hydrogen-ion concentrations.

If such a permeability barrier to hydrogen ions exists in the cell membrane, then one would expect that the internal charge would not be altered by variations in the external pH. (It is assumed here that the concentrations of freely diffusible ions are held constant.) The surface charge, on the other hand, would be dependent upon the external pH. The effect of the interior charge will consequently be the same as the effect of strongly acidic surface charges whose pK's are well below the range of pH over which the experiments are being performed.

If we can further suppose that the membrane barrier to hydrogen ions eventually breaks down at low pH, we might predict the following behavior. As the membrane becomes more permeable, hydrogen ions (or possibly other cations) will be attracted to the negatively charged interior by simple electrostatic forces and so will tend to neutralize the interior charge. But this is not all that can happen. This permeability barrier is imagined to break down at external hydrogen-ion concentrations in the vicinity of 10^{-1} to 10^{-4} molar. The initial hydrogen-ion concentration of the cell interior may reasonably be assumed to be in the range 10^{-6} to 10^{-8} molar. Consequently, we might expect to see a diffusion potential established during the time over which the pH of the cell interior is being made equal to the pH of the surrounding medium. The effect of such a diffusion potential would be to produce a positive charge in the cell interior. At equilibrium this internal charge would, however, vanish. This behavior is strictly analogous to the present

interpretation of the action potential in animal and plant cells, except that here we are talking about hydrogen ions, and in the action potentials it appears that sodium ions are primarily involved.

It is possible that this mechanism might explain the time behavior of the mobility of RBC at low pH (see Subsec. III. B), which has already been described qualitatively by Furchgott and Ponder.[17] Similar time variations in the mobility do not appear to exist in other mammalian cells, however, and this tends to cast some doubt on the validity of this hypothesis.

3. The Effect of Low Ionic Strength upon the Isoelectric Point of Intact Cells

The isoelectric point (extrapolated) of human RBC increases very rapidly with decreasing ionic strength, especially at very low ionic strengths.[24] A similar behavior was found for sheep polymorphonuclear leukocytes by Wilkins et al.,[20] but the isoelectric point of the ascites tumor cells studied by Cook, et al.[21] showed no noticeable dependence upon the ionic strength. My own observations on ascites tumor cells (see Subsec. III. B) do not agree with those of Cook et al. in this regard. In general it appears that the increase in the isoelectric point of any given cell is much greater than that found for proteins,[25, 26, 27] as may be seen in Fig. 9.

It is conceivable that this extreme behavior of the intact cells might be associated with a net interior charge. Bolinbroke and Maizels have reported that the RBC membrane becomes leaky to positive ions at low ionic strengths.[28] One would therefore tend to believe that positive ions from the medium would pass through the membrane and neutralize the internal charge. Since an internal charge might be responsible for an artificially low isoelectric point (as has been discussed in Subsec. III. A. 2), it follows that the progressive removal of this internal charge at lower and lower ionic strengths would be responsible for an unusually rapid increase in the isoelectric point.

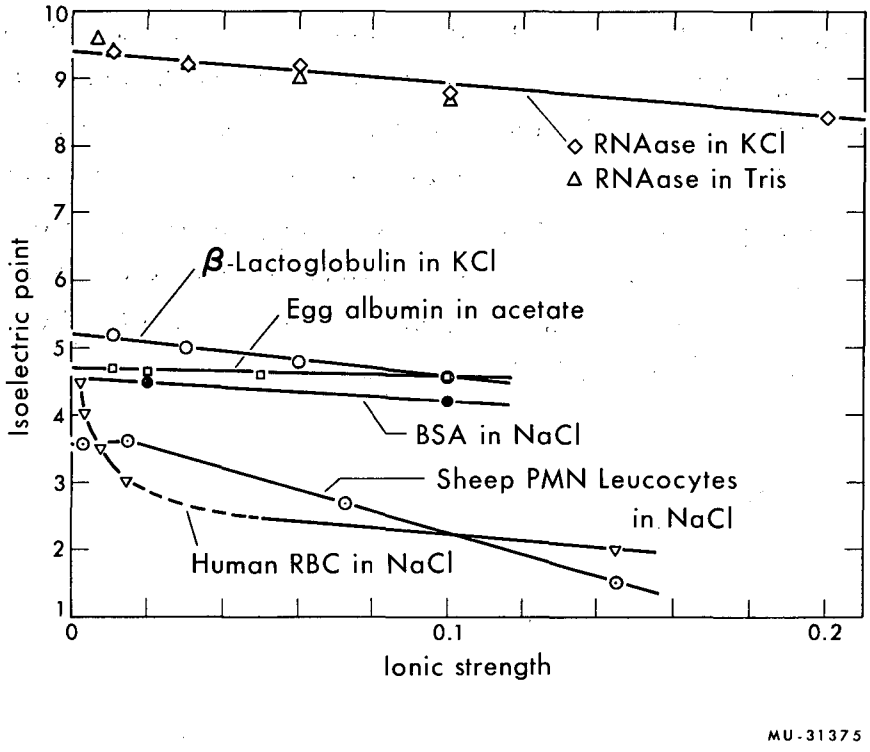

Fig. 9. A comparison of the variation in the isoelectric points of selected proteins with those of intact cells. Egg albumin, ref. 25; Ribonuclease and β-Lactoglobulin, ref. 26; BSA, ref. 27; Human RBC, ref 24; Sheep PMN Leucocytes, ref. 20.

4. Other Suggestive Evidence

Further circumstantial evidence that is consistent with the existence of an internal charge is the observation that spermatazoa are oriented in an electric field with their tails toward the positive electrode. Nevo[29] among others has first of all observed that when the electric field is reversed, both the head and tail move toward the anode. The tail is seen to move more rapidly, however, and soon the sperm is reoriented with the tail in the forward direction. This observation suggests that the orientation of spermatozoa may result from a greater net negative charge on the tail compared with that on the head, rather than from the tail being negatively charged while the head bears a positive charge. Secondly Masaki and Hartree[30] have found that the tails of spermatazoa are more metabolically active than the heads. Following the previous assumption that internal charge requires metabolic energy, their results would be consistent with the hypothesis that the greater tail charge is an internal charge.

B. Experimental Reconfirmation and Extension of the Literature that Describes the Effects of pH and Ionic Strength upon Mobility

1. Motivation of This Research

The experiments to be described in this section were undertaken with three goals in mind. First of all, there was something of a discrepancy between the mobility-pH curves that had been found for RBC by two different groups, as indicated in Fig. 8. Consequently, experiments were designed to determine if this descrepancy was caused by the different buffer salts used by the two groups or if other factors were responsible. Secondly, it seemed desirable to determine if the isoelectric points of cells which had not previously been studied were in every case very low, and if there was in every case a large increase in isoelectric point with decreasing ionic strength. The results of such experiments would have important implications for the rather elaborate arguments about internal charge which were made in Subsecs. III. A. 2 and 3. Finally the time-dependent decrease in the mobility of RBC at low pH's had been described qualitatively for many years. No quantitative studies had been reported, however. In view of the possibility that this phenomenon might be explained in terms of an internal charge (as described in Subsec. III. A. 2), experiments were undertaken to quantitate this phenomenon.

2. Mobility-pH Curves for Various Cell Types at Two Ionic Strengths (RBC, HeLa, TA3 Ascites, Yeast, Mammary Tissue)

a. Special experimental methods. Fresh cells were obtained from experimental animals prior to each experiment and used within 10 hours. The exact method of cell-sample preparation will be described in each case. The cells were centrifuged and washed at least twice, each time in no less than 10 volumes of Standard Buffer at pH 7.3 to 7.5. The final pellet was then made up into a 10 to 20% volume/volume cell suspension. The cells were stored in this form until use.

Only one experiment was performed with Furchgott and Ponder's buffered saline solutions.[17] These solutions will be described in Part b.

In all other cases the Standard Buffer was 0.145 M NaCl in 3×10^{-4} M $NaHCO_3$. Solutions of various pH's but of the same ionic strength were obtained by the addition of 0.145 M HCl or 0.145 M NaOH. Experimental solutions of different ionic strength were kept approximately isotonic by the addition of 0.25 M glucose in 3×10^{-4} M $NaHCO_3$.

Immediately prior to making a mobility measurement, an aliquot of the stock cell suspension was mixed with the experimental solution. This was usually done in the ratio of one part of stock suspension to 100 parts of experimental solution. The pH and conductivity were always recorded after the addition of cells.

b. Mobility-pH curves for RBC. Fresh blood was taken from the vena cava of ether-anesthetized Long Evans rats. The blood was drawn into plastic syringes through a No. 20 hypodermic needle. No anticoagulants were used. The blood was delivered immediately into at least 10 volumes of Standard Buffer and centrifuged to remove the plasma proteins. Rats weighing 150 to 200 g were employed since they are quite easy to handle, and 5 cc of whole blood can be obtained from one rat with no difficulty. The human blood was obtained by venipuncture from a normal human undergoing a routine medical examination. A tourniquet was used only for the insertion of the needle. Other details were as described above.

The buffered NaCl solutions of Furchgott and Ponder were used in one experiment. These solutions are composed of 9 volumes 1% NaCl and 1 volume buffer. The nature of the buffer used depended upon what pH range was desired. The buffer solutions used were: 0.1 M NaOH-glycine-NaCl, $\frac{1}{15}$ M Na_2HPO_4-KH_2PO_4, 0.1 M NaAc-HAc, 0.1 M HCl-glycine, and 0.13 M HCl as described by these authors.[17]

A special word should be said about the difficulty of obtaining mobility measurements at very low pH. As has already been mentioned, RBC are unstable at a very low pH: the lower the pH, the shorter the period of stability. Measurements must be made within one or two minutes after mixing the cells into experimental solutions of pH 2.0 or less. A finite time is required to introduce the specimen into the microelectrophoresis chamber. Furthermore, this operation usually produces

time-varying pressure gradients in the system which persist for at least a minute and often more. Fluid flow is necessarily associated with such pressure gradients, so it is not possible to obtain reliable data until these pressure gradients have died away. I can say from experience that it is only with considerable patience that reliable measurements can be obtained below pH 2.0.

The results of experiments performed in normal saline are presented in Fig. 10, and they show that the same mobility-pH curve is obtained for rat RBC and human RBC.* The curve is independent of the type of buffered saline employed. The curve is the same whether the cells have been washed only twice or washed as often as four times. The shape of the curve is also identical to that reported by Furchgott and Ponder.[17] It seems quite probable that the unique curve shape reported by Heard and Seaman may very well be due to errors in their measurement of the pH. (see Sec. II).

The experiments depicted in Fig. 10 also serve to reconfirm the value of 1.7 as the apparent isoelectric point of intact RBC.

Experiments were also performed with rat RBC at ionic strength 0.029. The curve in Fig. 11 shows that the isoelectric point of rat RBC is greatly increased at this ionic strength. The increase to a value of 3.6 is in fact considerably more than what would be expected from the data of Heard and Seaman (Fig. 9). The striking difference between the shape of the curves shown in Figs. 10 and 11 implies that the charge-determining characteristics of the RBC are grossly altered at the lower ionic strength. Perhaps the most interesting feature is the fact that at this ionic strength there is very little change in the mobility over the

---

* It seems that there is a strain difference in the mobility of rat RBC. In this phase of the work only Long-Evans rats were used, and the mobilities were in the range 1.00 to 1.10 (micron)(sec^{-1})(volt^{-1})(cm) at pH 7.4. In the work reported in Sec. V, however, Sprague-Dawley rats were used, and the mobilities consistently fell in the range 1.15 to 1.25 (micron)(sec^{-1})(volt^{-1})(cm) at pH 7.4. Species differences of a much greater magnitude have been reported by Abramson.[31]

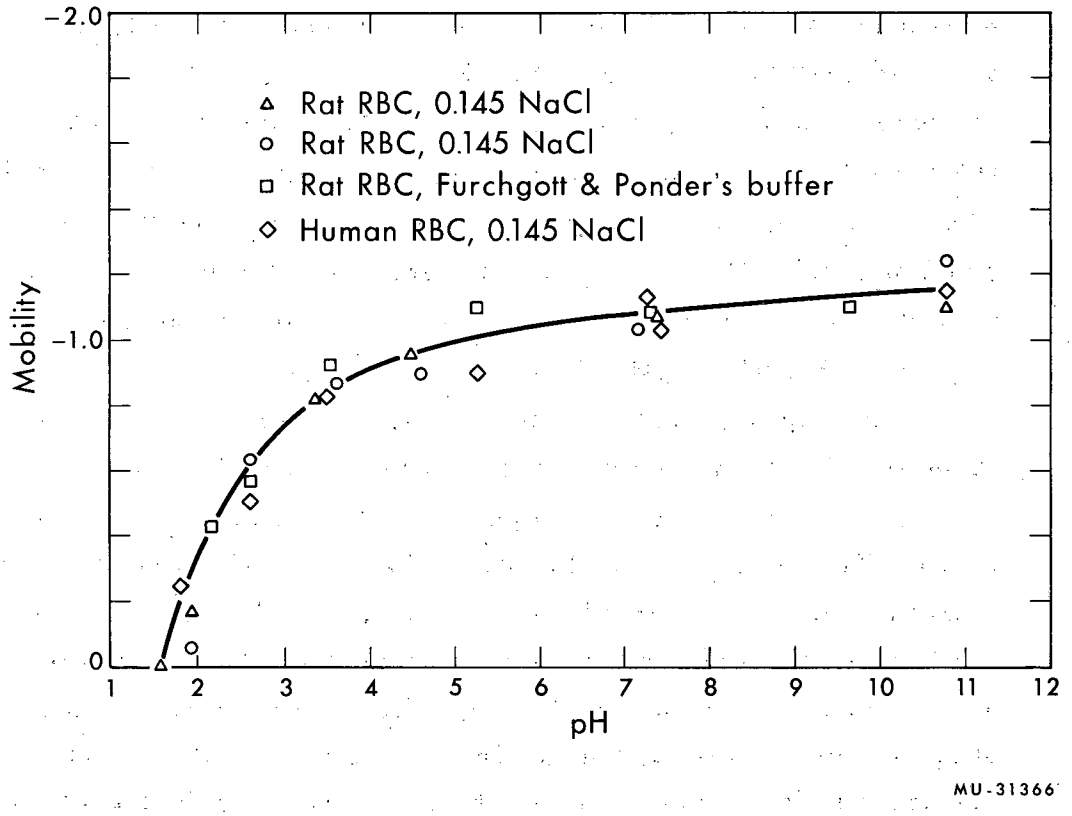

Fig. 10. Mobility-pH data obtained with Long-Evans rat RBC and with human RBC. The two experiments with rat RBC in 0.145 M NaCl differed, in that in one instance the RBC were washed twice prior to use, and in the other they were washed four times prior to use. The shape of the curve is qualitatively identical to that reported by Furchgott and Ponder:[17] the peculiar shape at low pH reported by Heard and Seaman[16] was not observed in this study, even with human RBC and with the same buffer system used by them (see Fig. 8 for a comparison).

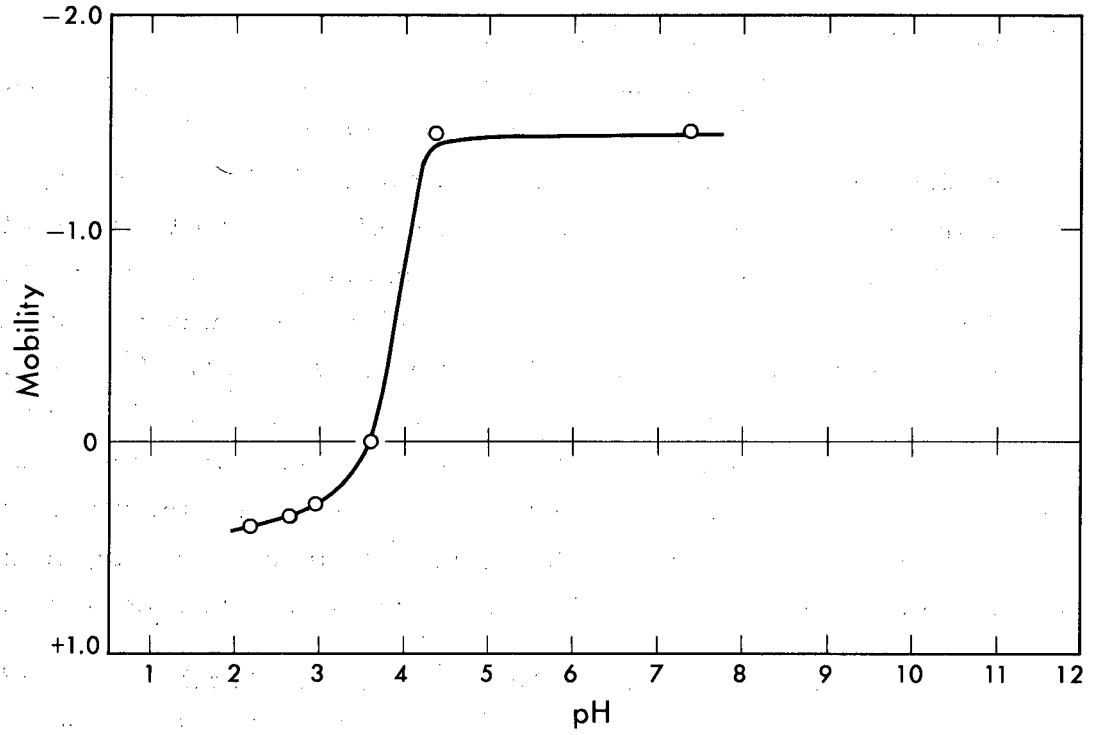

Fig. 11. Mobility-pH curve obtained for Long-Evans rat RBC at ionic strength 0.029.

range pH 2.0 to 3.0, whereas at ionic strength 0.145 the majority of the change occurs in this range.

c. Mobility-pH curves for HeLa cells. Mr. Paul Todd kindly provided the HeLa cells, which were cultured in glass bottles under standard conditions. The cells were freed from the glass by trypsinization and washed in Standard Buffer. The mobility-pH curve of these cells was determined at ionic strength 0.145 in two experiments. At this point the HeLa cell cultures were lost: no further experiments could be carried out with these samples.

The results of these experiments, shown in Fig. 12, indicate that the HeLa cells are isoelectric at approximately pH 2.2. The shape of the curve is generally similar to that of RBC. It must be noted that trypsin will reduce the absolute value of the mobility of RBC by about 30%[32] at pH 7.4. (Its effect on the isoelectric point has not been carefully measured.) This decrease is almost certainly a result of the proteolytic action of enzyme, as simple adsorption of this protein onto the cell surface probably does not occur.[16] It would be reasonable to assume that trypsin has had a similar action upon HeLa cells. Therefore the data in Fig. 12 probably do not represent the "true" mobility-pH curve for HeLa cells. Nevertheless, it is interesting to find that in spite of trypsinization they have such a low isoelectric point.

d. Mobility-pH curves for TA3 ascites cells. The TA3 ascites tumor has been maintained locally, for the purpose of radiobiological studies, in white laboratory mice. Extra mice not needed for those studies were obtained as they were available. No attempts were made to control the age of these tumors or any other possibly relevant factors. The animals were sacrificed either with ether or by neck fracture. The ascites fluid was withdrawn into a hypodermic syringe and immediately delivered into at least 10 volumes of standard buffer, since the more bloody tumors had a tendency to clot. The tumor cells were washed free of the fluid proteins and RBC by repeated gentle differential centrifugation at about 100× gravity for 5 min. In some of the experiments the final 10 or 20% stock suspension was stored in an ice

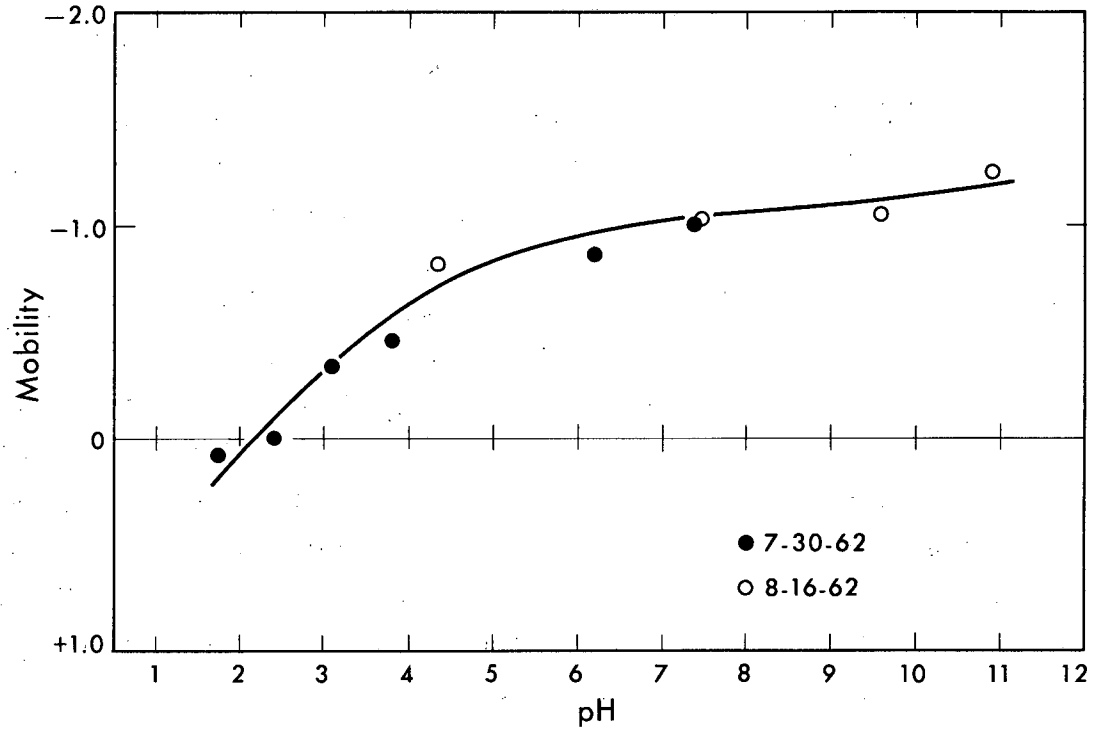

Fig. 12. Mobility-pH curve obtained for HeLa cells at ionic strength 0.145. The curve is a composite of data obtained in two separate experiments.

bath. This procedure had no noticeable effect on the ascites cells. In all experiments reported in this section, the ascites fluid from a single animal was used each time.

Three complete experiments were performed to measure the mobility-pH curve at ionic strength 0.145. As is seen in Fig. 13, these data are not so reproducible as those for RBC. Nevertheless, the isoelectric point seems always to fall in the range 2.5 to 3.5, again very low. Two experiments were performed at ionic strength 0.0145; these data are shown in Fig. 14. As at the higher ionic strengths, the curves show considerable variation. In spite of the variability, it can be said with certainty that the isoelectric point has been increased by nearly two pH units to a value in the range 4.0 to 5.5.

It was noticed throughout the course of these experiments that the population of ascites cells obtained according to the procedure above was always very heterogeneous with respect to electrophoretic mobility. This heterogeneity necessarily leads to a certain statistical error when one attempts to assign an "average" mobility to the cell population. It did not appear experimentally that this was limiting the reproducibility of the mobility-pH curves. There are some other factors which can be thought of to explain the lack of reproducibility. For one thing a process of selection is involved in the growth of each tumor, and the outcome is likely to be different each time. Also, tumor age was not controlled and that too allows for variability.

A few pertinent comments with regard to cell appearance should be made at this time. When first obtained, the TA3 cells appeared very nearly spherical, with smooth surface contours. With bright field optics, the cell interior appeared generally homogeneous. After storage for several hours–as a 10 to 20% cell suspension in the standard saline buffer–the surface contours became irregular and many vacuoles were formed in the cytoplasm. As is shown in the figures, however, the mobility at pH 7.4 was no different at the end of an experiment from the mobility at the beginning. These cells also reacted very rapidly to the extremely low pH's in the vicinity of their isoelectric point (and below). The most striking change was an apparent "clarification" of

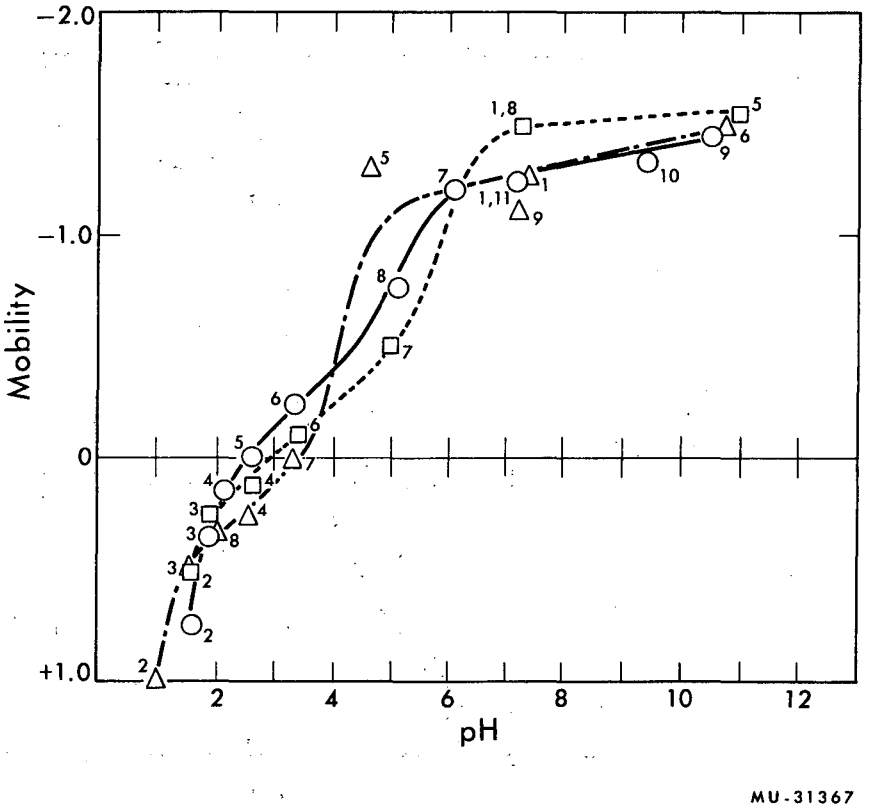

Fig. 13. Mobility-pH curves obtained for TA3 ascites tumor cells at ionic strength 0.145. Three separate experiments were performed on different days, as indicated by the circles, squares, and triangles. The accompanying numbers indicate the sequence in which the data were obtained in each experiment.

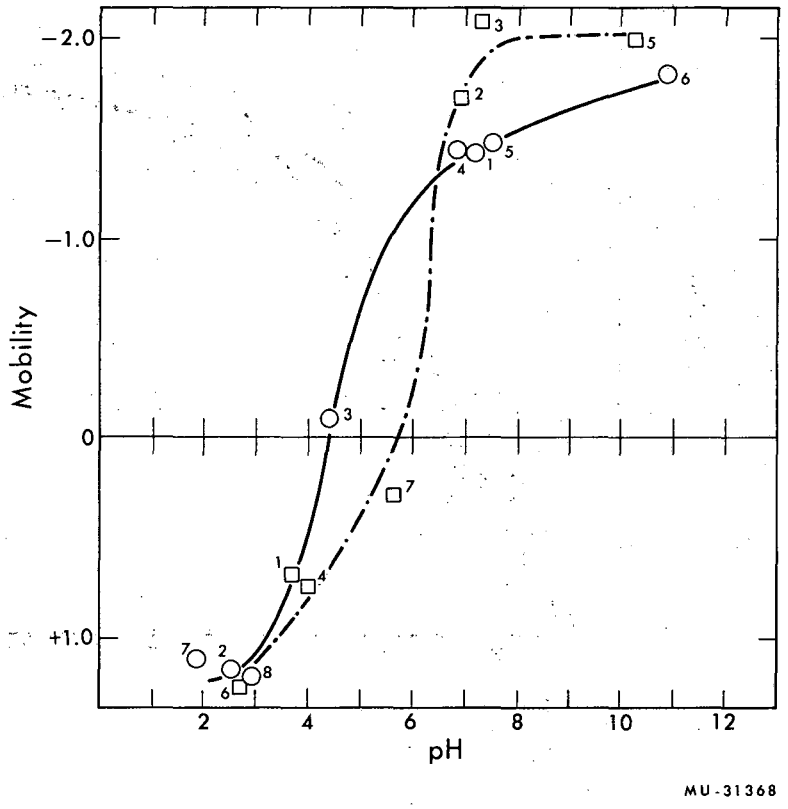

Fig. 14. Mobility-pH curves obtained for TA3 ascites cells at ionic strength 0.0145. The squares and the circles represent two experiments performed on separate days.

the cytoplasm. Under these conditions the cell membrane and the nucleus of these cells become very easy to visualize even with ordinary optics. It is not known if this cytoplasmic "clearing" was due to lysis or to a transformation of the cell contents due to the low pH. These changes always occurred before mobility measurements could be started. The mobility of these cells when measured was always constant with time (as best as could be determined in view of the natural heterogeneity of the cell populations), even at the most extreme pH's. Mobility measurements could not be performed at a pH much above 11.0 because rapid lysis occurred and the suspension turned into a soapy gel.

e. Mobility-pH curves for yeast and yeast protoplasts. It seems worthwhile to explain for a moment the reasoning that went into the design of the following experiments. It should be remembered that this series of experiments was designed to demonstrate that the isoelectric point of intact cells was lower than would be expected if (a) the surface of the cells were composed of protein, and (b) all the charge on the cells existed at the surface. Now it must be remembered that the surface of the intact yeast is a cell wall that is composed primarily of carbohydrate. On the other hand, it was expected that the surface of the yeast protoplast would be a plasma membrane with characteristics similar to the plasma membrane of mammalian cells. Consequently, it seemed that the yeast protoplast would be a suitable test object for continuing this investigation.

A diploid strain of Saccharomyces cerevisae was used in these studies (Prof. Robert Mortimer's strain X 901, revertant). About 40 ml of YEPD medium (1% yeast extract, 2% peptone, 2% dextrose in distilled water) in a 250-ml flask was innoculated with a loopful of yeast and incubated at 30° C on a shaker for 7-1/2 h. The cells were in the logarithmic stage of growth at this time and the cell concentration was of the order of 5×10^{5} cells/ml. The cells were then harvested by centrifugation and resuspended in NaCl solutions of the desired ionic strength, made 3×10^{-4} M with respect to $NaHCO_3$. The solutions at

ionic strength 0.0145 were also made 1.2 M with respect to sorbitol. At ionic strength 0.145, no sorbitol was added to the suspensions of intact yeast, whereas the solutions used for yeast protoplasts were made 0.90 M with respect to sorbitol.

Fresh "snail enzyme" was used in the preparation of yeast protoplasts. The enzyme was prepared by dissection of ordinary garden snails. The enzyme is contained in the red fluid of the "crop" after the snails have been starved for several days. The fluid was clarified by filtration through a very fine sintered glass disk. Approximately equal volumes of water were added during the preparation procedure.

Yeast protoplasts were made according to the method of Roman:[33] 0.5 ml of the enzyme preparation was added to 25 ml of the yeast suspended in the buffered saline-sorbitol solution. The sorbitol was added for osmotic protection of the protoplasts. These suspensions were allowed to stand overnight in a refrigerator. The cells were washed once in the NaCl-sorbitol-$NaHCO_3$ solutions. The snail enzyme is most effective in forming protoplasts when the yeast have been grown to a concentration of about 5×10^5 per ml. I found that about 90% of the cells would lyse in distilled water after this treatment.

The mobilities of both these intact yeast and yeast protoplasts were found to be very close to zero throughout the entire pH range at ionic strength 0.145, as shown in Fig. 15. Similarly Fig. 16 shows that even at ionic strength 0.0145 these objects still have a very small mobility. There is, however, an indication that the protoplasts might be isoelectric near pH 3.0, while the intact cells remain negatively charged even at pH 2.4. The similarity in the mobility-pH curves found for intact yeast and the yeast protoplasts throws serious doubt on the prior belief that the surface of the protoplast would be a plasma membrane similar to that found in mammalian cells. Instead it would appear that the surface of the protoplast must be more similar in character to the original cell wall.

The small values of the mobilities found in this yeast study might be attributed to the particular strain that was used. Eddy and Rudin[34] found that the value of the mobility (at pH 7.0) of intact yeast at ionic strength 0.005 (sodium acetate buffer) ranged between 0.2 and 1.6

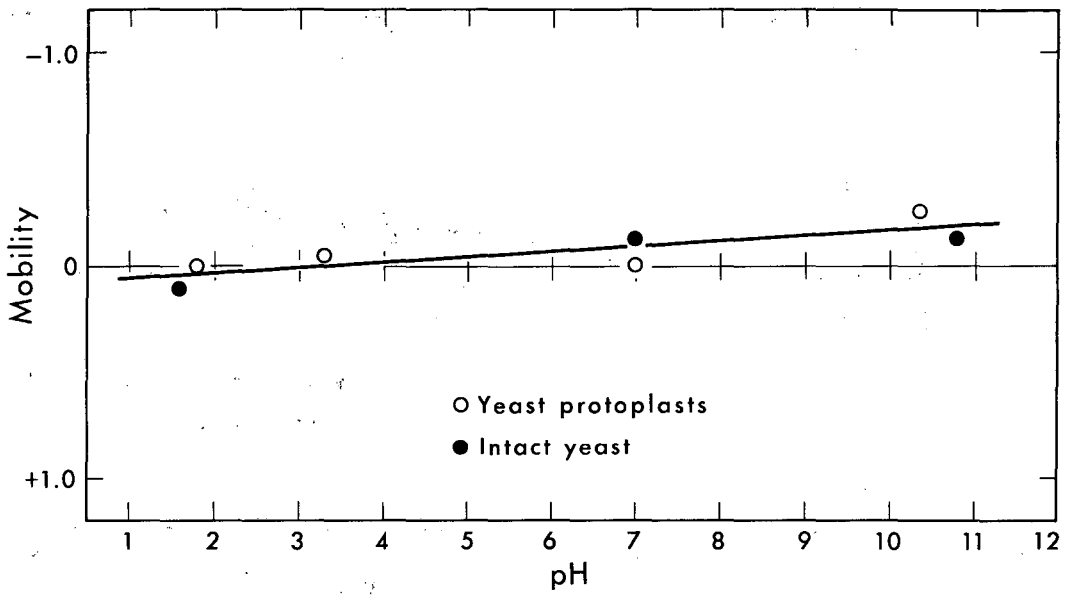

Fig. 15. Mobility-pH data at ionic strength 0.145 obtained for intact yeast (X 901 revertant) and yeast protoplasts.

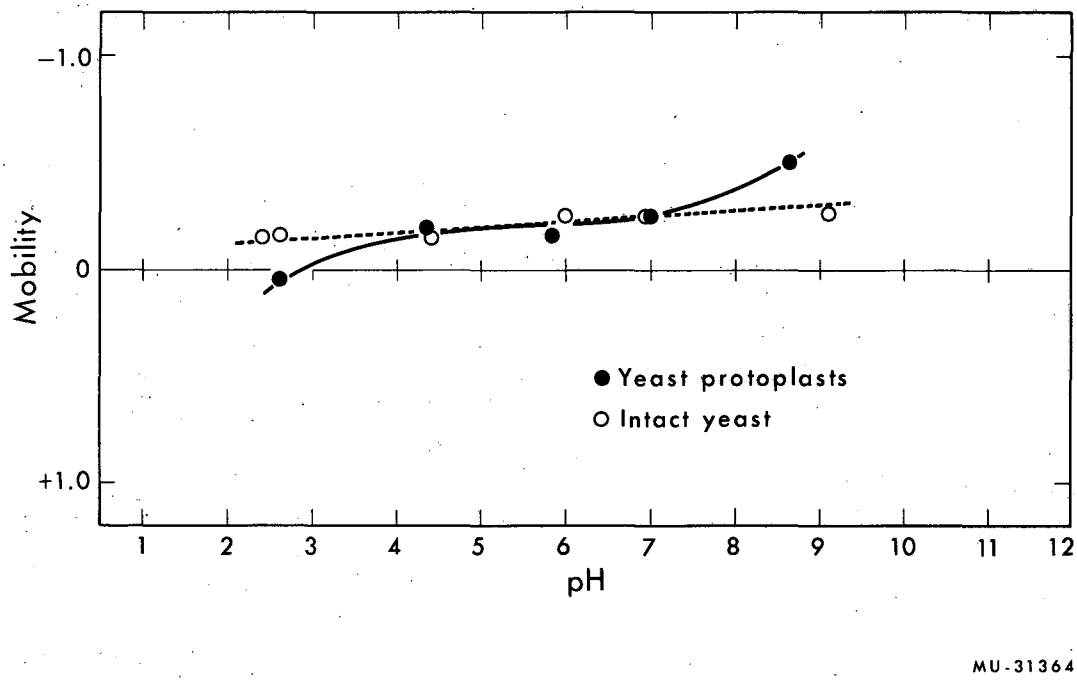

Fig. 16. Mobility-pH data at ionic strength 0.0145 obtained for intact yeast (X 901 revertant) and yeast protoplasts. The cells were suspended in 1.2 M sorbitol. The data have not been corrected to the viscosity of water.

(micron)($\overline{\text{sec}}^{-1}$)(volt^{-1})(cm) depending upon the yeast strain used. Presumably, higher mobilities could have been obtained in this study if solutions of lower ionic strength had been used, but use of such a low ionic strength would have invalidated a comparison with the studies on the mammalian cells.

Since it was impossible to be certain that the surface of the yeast protoplast was indeed the plasma membrane of this cell, and since the low values of the mobility made it impossible to see small percentage changes in the mobility, it was decided to abandon further work on this system at this time. Nevertheless the yeast-yeast protoplast system merits further investigation with regard to the internal-charge hypothesis.

f. Mobility-pH curves for tumorous tissue cells from mouse mammary glands. Cell suspensions were obtained from the mammary tissue of female C3H mice as follows. The animals were sacrificed by neck fracture and the desired tissue was removed. Normal tissue was obtained from pregnant prelactating mice, while the tumor tissue was obtained from single spontaneous tumors which had grown to a size of several millimeters in diameter. This tissue was chopped with a razor blade until a fairly smooth slurry was obtained. The slurry was then suspended in a few milliliters of 0.145 M NaCl buffered with 3×10^{-4} M $NaHCO_3$ and agitated by a magnetic stirrer for about one hour at room temperature. In most of these experiments, collagenase [Worthington, Freehold, New Jersey; 40% $(NH_4)_2SO_4$ fraction of Cl. histolyticum cultures] was added in an amount of 1.5 mg/ml. The collagenase was necessary for the complete disruption of tissue in all cases except for the more diffuse tumors. Even in that case the collagenase gave a better cell preparation than did simple mechanical disruption.

At the end of this treatment, most of the cells existed in multiple clumps, both with themselves and with minute fat droplets. These clumps could be dispersed by passing the suspension through a No. 25 hypodermic needle. Repeated passage through such a needle was also required to resuspend the pellet whenever these cells were centrifuged. This treatment undoubtedly ruptures many of the cells.

Table I is a list of the values of the mobilities measured in three separate experiments at pH 7.4 and ionic strength 0.145. Because the cell populations were all rather heterogeneous with respect to mobility, it is not clear whether the differences shown in the table are significant or not. Entire mobility-pH curves, at ionic strength 0.145, were measured for tumor cells that had been obtained both with and without collagenase. Figure 17 shows that these cells are isoelectric at anomalously high pH's lying in the range 4.0 to 5.0. It seems quite likely that the high isoelectric points reflect adsorption onto the cell surface of proteins from cells ruptured during the preparative process. Although these data cannot be considered as being very reliable, they are presented at this time so that a comparison may be made with cells eventually prepared by more gentle methods.

3. Mobility-Time Curves and O. D.$_{417}$-Time Curves for Rat RBC at pH ≈ 3.1 Ionic Strength 0.145

It was mentioned in Subsec. III. A. 2 that the time-dependent behavior of the mobility of RBC at low pH had already been described in a qualitative manner by Furchgott and Ponder.[17] I have found that it is possible to investigate this phenomenon quantitatively in the vicinity of pH 3.1. In such experiments it was necessary to obtain all the data at a single stationary level. Measurements were made at various time intervals by recording the velocity of a single cell, once with the electric field in one direction and once with the field reversed. No effort was made to use the same cell for subsequent measurements. The length of time required to make a single measurement was of the order of 20 sec.

Figures 18(a), 18(b), and 19(a) show some typical curves of mobility vs the length of time exposed to low pH. The mobility remains constant for the first few minutes. Then the cells rapidly lose their negative charge and actually become positively charged. This rapid reversal is followed by a slower decrease in the (positive) mobility. While the qualitative aspects of this behavior were always reproducible the curves obtained on different days, with different specimens, always

Table I. Mobility values* from three experiments with mouse mammary tissue cells in Standard Buffer.

Date of experiment	Tumor cells (collagenase-treated)	Tumor cells (no collagenase)	Normal cells (collagenase-treated)
7-3-62	-0.64 (small tumor) -0.70 (metastasizing tumor)		-0.72
7-27-62 (same tumor)	-0.67	-0.92	
8-3-62 (four tumors, pooled)	-0.94	-0.80 -0.76	

* (micron)(sec^{-1})(volt^{-1})(cm).

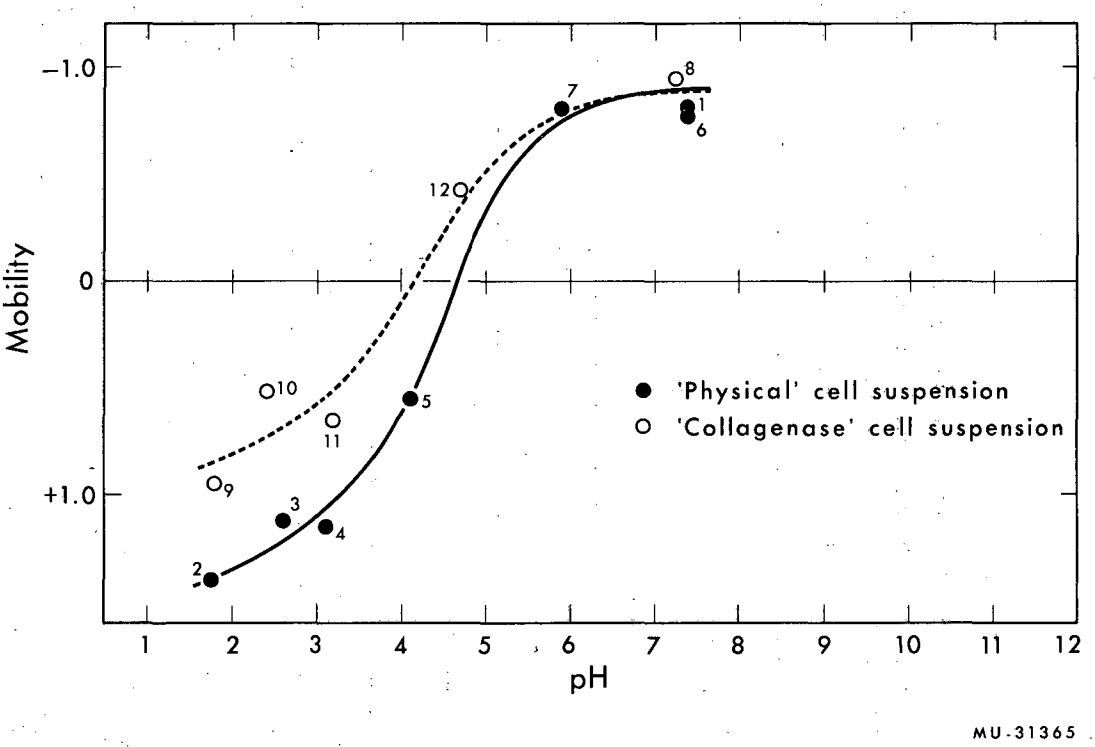

Fig. 17. Mobility-pH curves for mouse mammary gland tumor cells at ionic strength 0.145. The cell suspensions were obtained by mechanical agitation and by incubation with collagenase. In order to obtain enough cells for the two complete curves it was necessary to pool several tumors. Each tumor was cut in half prior to pooling, and one half was run through the "collagenase" procedure while the other was used in the "mechanical" procedure.

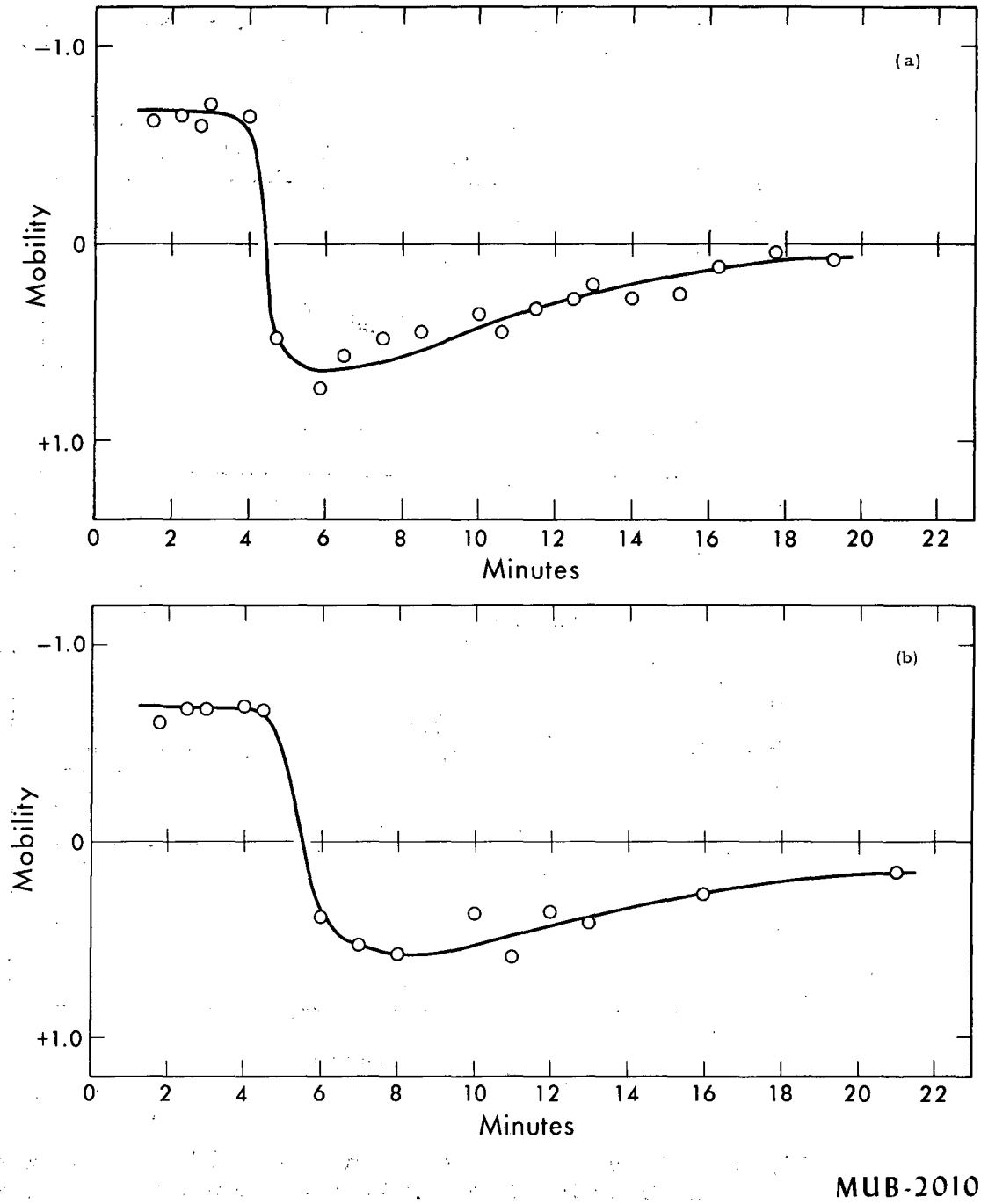

Fig. 18. Two typical examples of the mobility-time curves that have been obtained for rat RBC near pH 3.1.

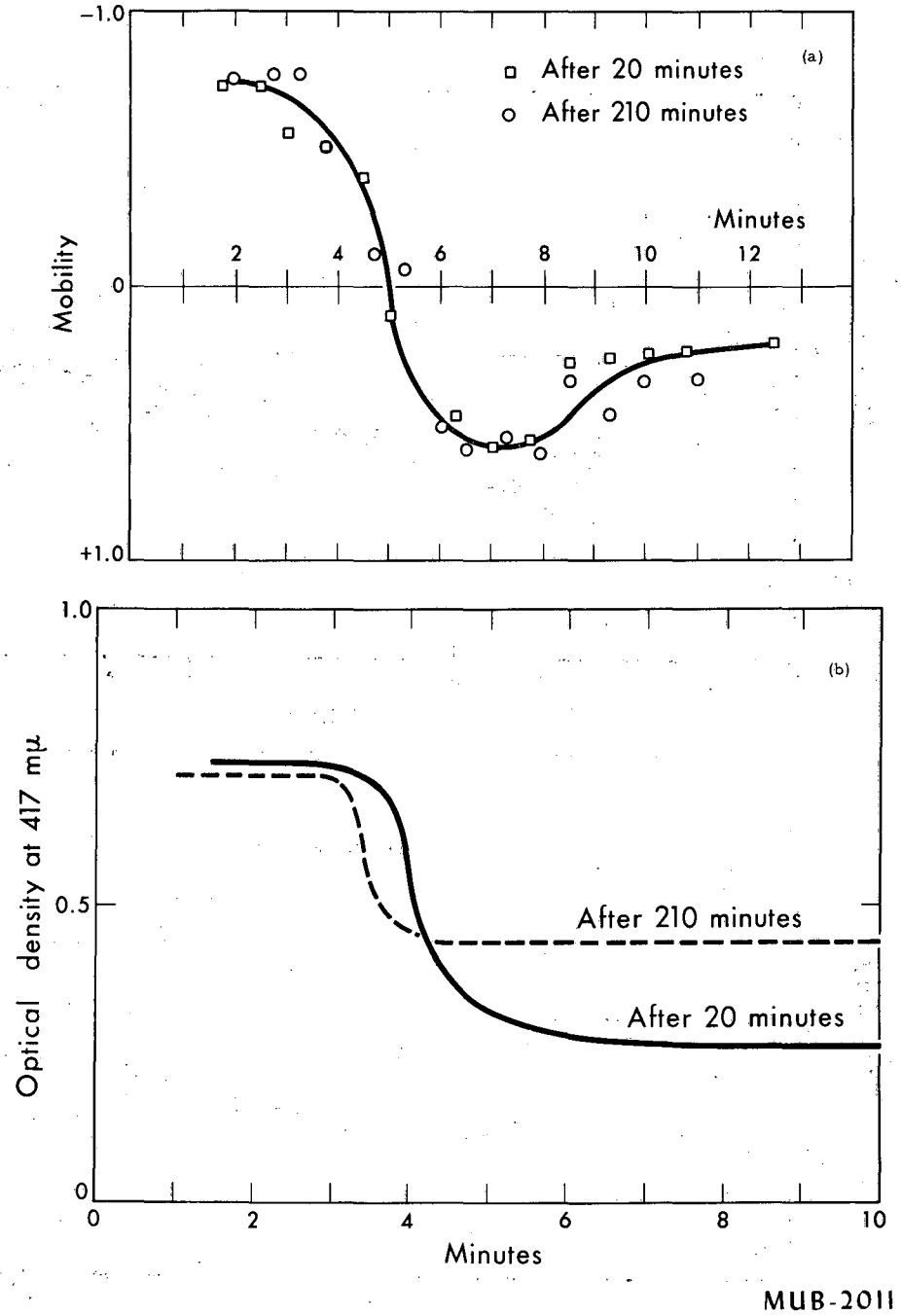

Fig. 19. Simultaneous measurements of the time changes in the mobility of rat RBC and in the optical density at 417 mμ of the RBC suspension. The pH at which these measurements were made was 3.1 ± 0.1. Figure 19(a) shows the mobility-time data for an aliquot of RBC suspended in the low-pH solution 20 min after the blood was drawn (squares), and for a second aliquot suspended in the low-pH solution 210 min after the blood was drawn. Figure 19(b) shows the corresponding (continuous) recordings of the optical density of these two cell suspensions.

showed some quantitative difference with regard to time required to reach neutrality and with regard to the detailed shape of the overshoot and recovery. Nevertheless the general behavior is in accord with the theoretical speculation of Subsec. III. A. 2, and consequently these observations were tentatively considered to support the internal-charge hypothesis.

When these experiments were first done it was noticed that the RBC suspensions changed color at the same time that the sign of the charge on the RBC was reversing. The normal reddish color of the suspensions turned to a straw color identical to that of RBC hemolysate at the same pH. Although a certain fraction of the cells can be seen to hemolyze at this time, if the cell suspension is centrifuged, it is seen that hemolysis is not extensive as judged by the intensity of color in the supernatant. The majority of the color sediments with the cells, implying that there is a spectral change in the intracellular hemoglobin associated with the change in mobility.

This spectral change in the intracellular hemoglobin can also be explained by the theoretical speculations of Subsec. III. A. 2: Initially the RBC is imagined to be impermeable to hydrogen ions; with the pH of the interior remaining constant there will be no spectral change in the hemoglobin. The subsequent change in mobility, imagined to result from a breakdown of the cell's barrier to hydrogen ions, would cause the pH of the cell's interior to decrease to that of the external medium. Thus one would expect to see a change in the color of the hemoglobin.

In order to explore these possibilities more thoroughly, quantitative measurements were made simultaneously of the mobility and the optical density at 417 mμ ($O.D._{417}$), the maximum adsorption for RBC hemolyzed in distilled water. The O. D. measurements were made in a Beckman recording spectrophotometer, model DK-1. Since the O. D. measurements were made without the use of a wide-angle photoreceptor[35] they are of questionable significance. Light-scattering by the cells and light-absorption by the hemoglobin both contribute to the optical density; the relative contribution of each has not been quantitatively measured.

It was repeatedly observed, however, that the $O.D._{417}$ was very nearly the same for whole RBC and for hemolyzed RBC–at the same concentration. This suggests that the absorption of light at 417 mμ by the intracellular hemoglobin somehow compensates for the known light-scattering at that wavelength. That is to say, light-scattering changes at 417 mμ do not appear to lead to changes in the total O.D. at that wavelength. Thus we are considering $O.D._{417}$ to be a measure of the amount of normal hemoglobin. Consequently it seems likely that the time changes in the O.D. at 417 mμ are due to spectral changes in the hemoglobin itself, rather than to changes in light-scattering.

Figures 19(a) and 19(b) show the results of an experiment in which the mobility measurements and the O.D. measurements were made simultaneously on the same specimen. It can be seen that the O.D. - time curves are dependent upon the freshness of the RBC sample. This pertains both to the magnitude of the O.D. change and to the time (after mixing with the low-pH solution) at which the change occurs. These observations have been borne out in separate experiments designed to verify this behavior. The O.D. changes and the mobility changes are seen to begin at very nearly the same time, as would be predicted from the internal-charge hypothesis. However, the subsequent rate of change of mobility may be somewhat slower than that of the O.D.

In summary, it has been assumed that the $O.D._{417}$-time curves represent a quantitative measurement of the time course of the cell's color change, which was first observed qualitatively by eye. This color change is interpreted to mean that the pH of the RBC interior changes from some initially constant value (about 6.8?) to a pH $\approx$ 3.1 (the pH of the external medium). Since there is not an exact one-to-one correspondence between the mobility changes and the color changes, it seems unlikely that both of these phenomena can be explained in exactly the same way, as was originally hoped. While these experiments do not constitute strong evidence in support of the internal-charge hypothesis they nevertheless are not inconsistent with that hypothesis.

It might be argued that the mobility changes occur because of adsorption of the hemoglobin from cells which undergo lysis. This

possibility cannot be ruled out for the initial changes, but additional factors must be involved to explain the subsequent recovery phase of the mobility curve.

It is possible that the O. D. -time curves and the mobility-time curves are measurements of somewhat independent phenomena. The mobility curves may represent a rather complex sequence of changes in the surface structure (rather than in the internal charge) during which different surface cationogenic groups sequentially dissociate, with a concomitant change in the sign of the net charge. The color change on the other hand probably reflects a change in the cell membrane's permeability to hydrogen ions. This permeability change would involve a change in the total structure of the cell membrane and not just in the surface structure.

4. Summary of Subsection III. B

(a) The shape of the mobility-pH curves for RBC as found by Furchgott and Ponder has been confirmed.[17] The unusual shape of the curves at low pH as found by Heard and Seaman[16] appears to be in error.

(b) The previously reported large increase in the RBC isoelectric point has been confirmed for a particular low ionic strength, 0.029.

(c) New mobility-pH data and ionic-strength data have been obtained for HeLa cells, TA3 ascites cells, intact yeast and yeast protoplasts, and mouse mammary tissue cells.

(d) The time changes in RBC mobility after exposure to low pH have been confirmed and quantitated. In addition simultaneous measurements were made of the change in the optical density of these RBC suspensions at 417 mμ.

(e) All these data are consistent with the internal-charge hypothesis, but they cannot be considered to be a proof of the hypothesis. They are instead an extended confirmation of the literature that originally suggested the hypothesis.

C. Experiments with Metabolic Inhibitors and Ion Transport (RBC, TA3 Ascites)

1. Motivation of this Research

It should be recalled that the theoretical speculations of Subsec. III.A interpreted membrane potentials in living cells in terms of a corresponding net charge in the interior of the cell. Furthermore, these membrane potentials require metabolic energy for maintenance of their normal values, and one is lead to believe that the active transport of ions is involved in the production of these potentials.

At the time when the following experiments were first being considered, I felt quite confident that active ion transport was responsible for the production of an internal charge and that this charge was responsible for the cellular membrane potentials. Furthermore, I believed that this (supposed) internal charge made a significant contribution to the total charge on a cell. As a result, it seemed that an obvious next step would be to show that active ion transport was associated with the electrophoretic mobility of cells.

As a first step toward such a proof, I hoped to show that when active ion transport was decreased, the mobility would decrease. As the second step, I hoped to show that when the mobility was decreased by appropriate external stress, the active ion transport would decrease. In this way I was hoping to show an "if and only if" relationship, in the tradition of a mathematical proof.

The experiments to be described below were designed primarily to give a rapid confirmation of my theoretical speculations. These preliminary experiments were to have been followed up with more careful work if positive results were obtained. As it turned out, the experiments all gave negative results.

2. Attempts at Decreasing the Mobility by Decreasing the Active Ion Transport

In the first of these experiments, rat RBC were incubated with well-known metabolic inhibitors in an attempt to inhibit their capacity for active ion transport. (No experiments were performed to determine whether or not inhibition was actually accomplished.) As mentioned

before, what was actually being sought in these experiments was a qualitative confirmation of my predictions; more careful work would follow if the results indicated that it would be worthwhile to do so.

There has, in fact, been rather little work done on the effects of metabolic inhibitors upon ion transport in the particular case of RBC. The best general references that I have found on the subject are contained in monographs by Ponder[36] and by Prankerd.[37] It is well established that mature RBC can utilize glucose by the glycolytic pathway. RBC glycolysis is inhibited by both fluoride ion and by iodoacetic acid (Prankerd, p. 66; Ponder, p. 365). While glycolysis is the major factor in energy metabolism, mature RBC also utilize very small amounts of O_2 in the consumption of glucose (Prankerd, p. 59). What small respiratory activity does exist in RBC can be further reduced by the addition of trace amounts of cyanide (Ponder, p. 360). In addition to inhibiting glycolysis, fluoride ion and iodoacetic acid produce a large potassium ion loss from RBC (Ponder, p. 367). Washing the RBC with saline apparently delays this effect of fluoride ion and iodoacetic acid. Further evidence regarding the effect of metabolic inhibitors on RBC ion transport comes from studies on RBC which have been stored at 4° C. These cells lose a considerable amount of their potassium ions, which are replaced by sodium ions from the medium. If incubated at 37° C with glucose, these RBC are able to regain their potassium, and sodium is expelled at the same time. This restoration of ionic gradients is inhibited by fluoride (Prankerd, p. 48).

In an attempt to discover a relationship between active transport and mobility, several experiments were performed in which RBC were incubated at room temperature with separate solutions of KCN (3×10^{-4} M), NaF (1×10^{-2} M), or iodoacetic acid (1 to 5×10^{-3} M) in Standard Buffer. Dinitrophenol (1 to 5×10^{-4} M) was also tried as it is known to inhibit oxidative metabolism in nerve and muscle, though little is known about its action in RBC. The hope was that one or more of these inhibitors would reduce the energy metabolism of the RBC, and therefore decrease the absolute value of the mobility. On the basis of the information given

in the previous paragraphs particularly fluoride and iodoacetic and should have accomplished this goal.

When these experiments were carried out, it was found that the metabolic inhibitors produced no change in the mobility (within a 10% experimental error). It was essential to be sure that the pH of these solutions was well controlled. Early experiments with dinitrophenol gave the result that the mobility of RBC was greatly decreased in the presence of this reagent. Subsequently it was discovered that the entire effect resulted from a decrease in the pH which occurred when this reagent was added to the weakly buffered saline solutions being used.

In most of these experiments, the mobility of the RBC was measured during a three- to four-hour period after addition of the metabolic inhibitors to the cell suspensions. In one experiment, however, the mobility was also measured on the seventh day after exposure to these four reagents. The RBC were stored at room temperature during all this time. By the seventh day, the control cells had been completely destroyed. The KCN-treated RBC appeared quite normal and had the same mobility as they—and the control RBC—had had at the beginning of the experiment. The IAA-treated cells had also survived quite well, though not so well as those treated with KCN, and the cells that remained also had the same mobility. The RBC which had been stored in NaF and dinitrophenol were mostly destroyed; the mobility of the cells that remained was somewhat lower than it was initially.

In view of the rather special character of the RBC, it seemed wise to repeat the same experiments with a more "typical" mammalian cell, so similar experiments were also performed with TA3 ascites tumor cells (see Subsec. III. B. 2). The mice were sacrificed only by neck fracture. The ascitic fluid was withdrawn into a plastic syringe, and the cells were washed by repeated centrifugation. The washed cells were suspended in the various experimental solutions (see above) at a concentration of 0.2% volume/volume. The cell suspensions were incubated at 25 or at 37° C. At various time intervals an aliquot of the cell suspension was removed and used for the mobility measurements

without further washing or dilution. In each of these experiments, the ascites cells from two mice were pooled in order to obtain enough material.

The results of these experiments are shown in Fig. 20, where mobility is plotted vs the length of time that the ascites cells were incubated in the experimental solutions. In most of these experiments it was found that the mobility of the control cells–as well as those incubated with NaF and with iodoacetic acid–decreased with time to a limiting value of about 0.8 (micron)(sec^{-1})(volt^{-1})(cm). In one instance there was no variation; the mobility of all cells remained remarkably constant at a value of 0.85 (micron)(sec^{-1})(volt^{-1})(cm). The addition of dextrose to the control cells had no apparent effect upon this mobility decrease. It is not clear why no such time-dependent decrease in mobility was seen in earlier experiments, when the mobility-pH curves were obtained. The most significant difference between the experiments was that for the mobility-pH experiments the cells were stored in a 10 to 20% stock suspension, whereas in these experiments the cells were stored as a 0.2% volume/volume cell suspension.

The decrease in mobility that was seen in the control cells could be delayed by KCN and possibly also by dinitrophenol. Such a delay was <u>not</u> achieved, however, if the cells were preincubated with KCN for 1/2 h, washed once, and then incubated in the Standard Buffer. This "protective" action of KCN is reminiscent of the result mentioned for the seven-day experiment, when RBC were incubated with KCN. It hardly seems likely that this "protective" action is being brought about by inhibition of the energy metabolism. It is possible that the cyanide ion, which is very reactive with many substances,[38] acts in some way to stabilize the structure of the cell surface.

In summary, the metabolic inhibitors used in this study failed to cause a decrease in the electrophoretic mobility. Consequently these experiments do not support the hypothesis that an internal charge, associated with the membrane potential and maintained by the active transport of ions (if such a charge exists in the first place), contributes

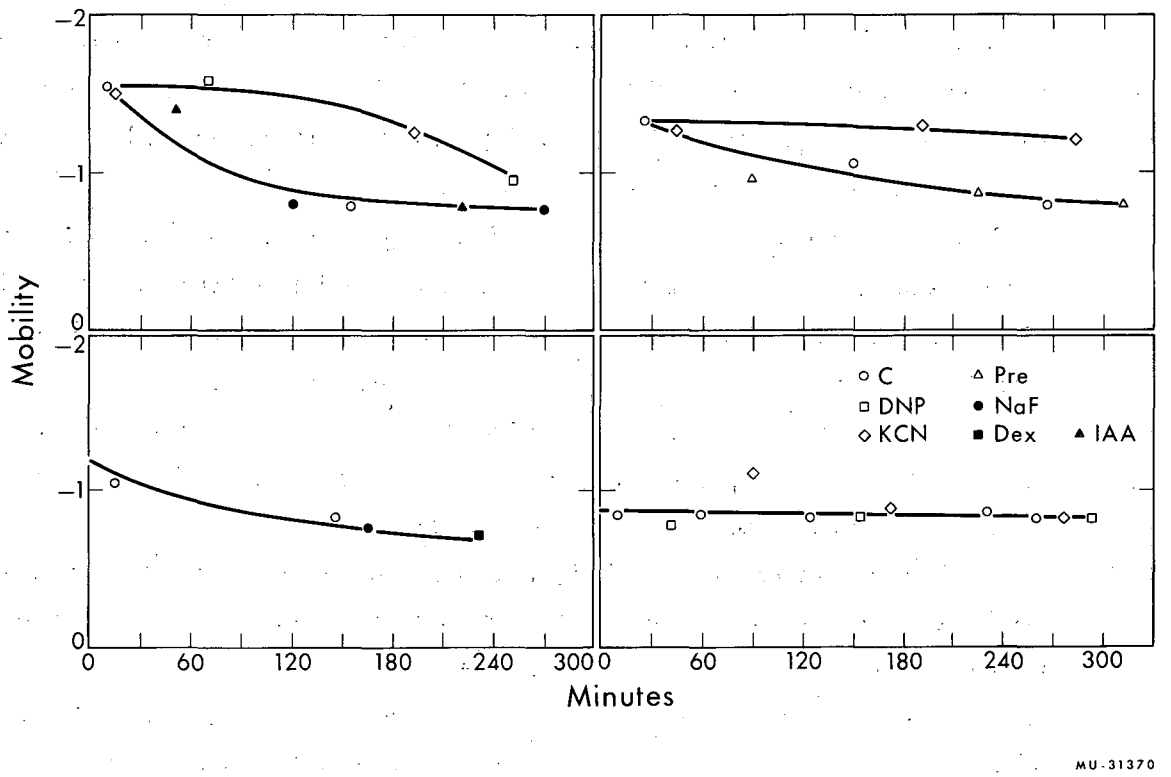

Fig. 20. Four mobility-time curves obtained with TA3 ascites cells at pH 7.4, ionic strength 0.145. Zero minutes corresponds to the time at which cells were made into an 0.2% vol/vol cell suspension. The legend shown in the lower right-hand corner applies to all four curves. The following abreviations have been used: C for untreated control; DNP for dinitrophenol; KCN for potassium cyanide; Pre for cells incubated 1/2 h in potassium cyanide, then washed and resuspended in Standard Buffer; NaF for sodium fluoride; Dex for dextrose; IAA for iodoacetic acid. The concentration of dextrose was 0.1% wt/vol; the compositions of the remaining solutions are given in the text.

significantly to the total charge on the cell.

An attempt was made to interfere with the active transport of ions by a second method. Bolingbroke and Maizels[28] have shown that exposure to low ionic strength causes human RBC to become leaky to sodium ions and potassium ions. This leakiness could be prevented by the addition of small amounts of calcium ion. It has already been suggested in Subsec. III.A that the large increase in the RBC isoelectric point might possibly be attributed to such a cation permeability, induced by exposure to low ionic strength. This explanation of course presupposes the existence of a net internal charge. If this speculation is correct then one would expect that the addition of calcium ion would produce a decrease in the isoelectric point, since the leakiness to cations would be prevented.

The following experiment was performed to test this point. The mobility of rat RBC was measured as a function of pH at ionic strength 0.029, with 0.25 M glucose added to maintain osmolarity. The control cells were suspended in 0.029 M NaCl with 3×10^{-4} M $NaHCO_3$, whereas the experimental cells were suspended in 0.014 M NaCl, 5×10^{-3} M $CaCl_2$ with 3×10^{-4} M $NaHCO_3$. It was found that the isoelectric point of the RBC was no different in the solution containing calcium ion. Consequently, this experiment failed to support the hypothesis that the breakdown in ion transport (i.e., leakiness to sodium and potassium) was responsible for the large increase in the RBC isoelectric point at low ionic strength.

3. Attempts at Decreasing the Active Ion Transport by Decreasing the Mobility

In a final attempt to obtain evidence in support of the active-transport—internal-charge hypothesis, the following experiments were performed. The mobility of rat RBC was decreased by an external stress and a breakdown in the active ion transport was looked for. Leakage of potassium from the RBC into the suspension medium was used as the criterion for the breakdown of active ion transport. Aliquots of the RBC suspension were withdrawn at different time intervals.

The mobility of these cells was measured. Some of the RBC were centrifuged and the supernatant withdrawn for potassium determination (by flame photometry). The mobility of these cells was also determined.

Two kinds of external stress were used. In the first instance the RBC were subjected to extremely low ionic strength (2.0×10^{-4} M phosphate, 0.28 M glucose, pH = 7.3). In the second instance the RBC were incubated at 37°C in Standard Buffer to which had been added the receptor-destroying enzyme (RDE). (The action of this enzyme is thoroughly discussed in Sec. V.) In both cases there was an appreciable decrease in the mobility with time, but in neither case was it possible to demonstrate a loss of potassium that was correlated with the decrease in mobility. So once again the preliminary experiments in search of a relationship between active ion transport and electrophoretic mobility ended with negative results.

IV. REJECTION OF THE HYPOTHESIS THAT AN INTERNAL CHARGE CONTRIBUTES SIGNIFICANTLY TO THE TOTAL CHARGE OF INTACT CELLS

It had been theorized at the initial stages of this research project that there might well be a net charge on the interior of intact cells which was of comparable magnitude to the total net charge on the cell (the important quantity from the electrophoretic standpoint). Several experiments were described in Subsec. III. C which were designed to demonstrate directly an internal charge, particularly related to cell metabolism. These experiments all gave negative results. It might be recalled that some evidence of an indirect nature, which was consistent with the internal-charge hypothesis, was also described. However, more compelling arguments against the internal-charge hypothesis can now be made on the basis of additional experiments described below. Therefore I wish at this point to reject the internal-charge hypothesis, subject to certain qualifications given below.

Ponder has shown that the mobility of human RBC ghosts is not significantly different from that of the intact RBC.[39] I have observed the same thing in my experiments with intact rat RBC and ghosts. This observation is not what one might expect if there were an appreciable net internal charge on RBC. Rather, one would expect that the internal charge would be lost due to free flow of ions during hemolysis, and consequently the mobility should decrease. The negative result of the hemolysis experiments does not constitute an air-tight case against the internal-charge hypothesis, however, for the movement of small ions is not so free as one might expect, as may be deduced from Teorell's experiments on ion retention during hemolysis.[40]

A second argument comes from the work with chemically fixed RBC. Heard and Seaman have fixed human RBC with formaldehyde and acetaldehyde.[41] This fixation procedure requires three weeks to complete. I have also reported experiments with OsO_4-fixed and

$KMnO_4$-fixed rat RBC (see Subsec. V.B). If the net charge of the cell were to depend significantly upon energy metabolism, one should surely see a decrease in the mobility after such treatments. The fact is that no such change in the mobility occurs at pH 7.4. Furthermore these fixed RBC no longer show the unstable behavior (with regard to their mobility) that is exhibited by the unfixed RBC at low pH and low ionic strength. It should be recalled that the internal-charge hypothesis had been invoked earlier to explain this unstable behavior.

A third objection comes from the combined enzymatic and microelectrophoretic studies currently being reported in the literature. It was reported in 1950 that the receptor-destroying enzyme (RDE) is capable of reducing the mobility of human RBC.[42] RDE is a glycosidase specific for the removal of terminal sialic acid[43] (see Subsec. V.B). Eylar et al. subsequently have shown that the percent decrease in the mobility of RBC (various species) produced by exposure to RDE is proportional to the percent of the sialic acid removed from the RBC.[44] A maximum reduction in the mobility of 94% was obtained for human RBC. This result constitutes convincing evidence that the carboxyl group of sialic acid is responsible for the vast majority of the negative charge on RBC. This matter is discussed in greater detail in Subsec. V.B.

The fact that the internal-charge hypothesis is being rejected ought not be construed to mean that there is no internal charge. What is implied by this rejection is that an internal charge, if it is present, appears not to be comparable in magnitude with the total amount of charge on the cell. Mobility differences as large as 10% can be detected without too much difficulty if different experiments are performed on the same sample, on the same day, and if the sample itself is fairly homogeneous with respect to mobility. It is a more difficult matter to be absolutely certain that differences of less than 5% are indeed significant. To be more precise we can say that the net internal charge is apparently less than 5% of the total net charge

at pH 7.4. By definition the only other possible source of charge is at the outer surface of the cell; the mechanisms of such charge formation have already been discussed in Subsec. I.B.

V. EXPERIMENTAL INVESTIGATION OF THE SURFACE CHARGE AND OTHER SURFACE PROPERTIES

A. Present Theoretical Models of Cell Surface Structure, and Their Expected Surface Charge Characteristics

1. Davson-Danielli Model of the Cell Membrane

The Davson-Danielli model of the cell membrane supposes that the lipid component of the membrane is arranged in a bimolecular sheet with the nonpolar groups on the inside and the polar groups at the two surfaces. Protein is imagined to be "spread" or "unrolled" at the lipid surfaces with its hydrophobic groups penetrating the lipid layer and its polar groups approximately in the same plane as those of the lipids. In addition there is the possibility that globular proteins may be attached to the two extreme surfaces of this structure.

Davson has recently reviewed the historical development of this theory,[45] which is based primarily upon the experiments of Gorter and Grendel.[46] The latter authors calculated that there is just enough lipid in the human RBC ghost to make a layer two-lipid-molecules thick around the RBC surface. The theory in addition is based upon studies of the "surface tension" of cells as related to the effects of protein at a water-oil interface.[47] Davson has also indicated how subsequent ac impedance, optical reflectance, and polarization optical measurements have been interpreted in terms of this model. At the same time he has indicated some of the ambiguities inherent in these indirect studies of the membrane structure. Furthermore, the original calculation by Gorter and Grendel has been found to be erroneous, as has been indicated in Davson's review and, more explicitly, in the discussion which follows on page 1073.[45] In spite of the uncertainty in this basic observation and the ambiguity of the subsequent supporting evidence, this picture remains by far the most widely quoted and accepted molecular model of the cell membrane.

According to this model, the surface charge of intact cells would be expected, at least upon first consideration, to show the characteristics of a protein. Consequently it would be expected that the

isoelectric point of intact cells would lie roughly in the pH region from 3.0 to 10.0. While some types of cells are isoelectric above pH 3.0, the majority exhibit an isoelectric point below pH 3.0 at normal ionic strength. Certain cells, e.g., polymorphonuclear leukocytes and erythrocytes, appear to be isoelectric below pH 2.0 (see Subsec. III. A for references). In addition the mobility of most cells remains virtually constant over the pH range from 5.0 to 11.0. This implies that charged groups that have a pK in this region—such as the ϵ amino group of lysine, the imidazolyl group of histidine, the sulphydryl group of cysteine, and the hydroxy group of tyrosine—are virtually absent from the surface of these cells.

In order to reconcile these data with the Davson-Danielli model it becomes necessary to imagine the attached protein at the outer surface of the cell membrane to be oriented or structured in such a way that a large number of negatively charged groups with very low pK are exposed at the surface, while most of the positively charged groups and those with intermediate pK are not exposed. Alternatively, it may be imagined that only "unrolled" protein exists at the outer surface. In such a situation, the phosphate groups from the phospholipids could penetrate through the thin layer of protein and dominate the charge characteristics of the cell surface. It remains difficult, in such a picture, to imagine why the positively charged groups (choline, ethanol amine, serine) from the same phospholipids are not also exposed at the surface. The low isoelectric point (especially of RBC) and the absence of a change in mobility between pH 9.0 and 11.0 would argue that these particular cationic groups cannot be present at the outer surface of intact cells.

2. Various Mosaic Structures

Two basically similar mosaic theories regarding the molecular structure of the RBC surface have been put forward by Ponder[36] and by Parpart and associates.[48] In these theoretical structures, it is imagined that the lipid and the protein components of the membrane are arranged in separate "micro-phases" having the dimensions of approximately 50 Å. In Parpart's model these separate phases are

continuous throughout the thickness of the membrane, whereas Ponder's model suggests that the protein is composed of fibers that are woven about the lipid aggregates in three dimensions.* Both models have apparently originated from the authors' belief that the large number of lipid molecules available for binding onto a given protein molecule requires that the lipid and protein must be arranged together in three dimensions rather than in the lamellar arrangement of the Davson-Danielli model. The model of Ponder also seems to have been motivated by a knowledge of the extremely low isoelectric point exhibited by human RBC. He observed that if the lipid were arranged in "palisades" (as opposed to sheets) it would be possible for polar groups of the various phospholipids to stick out into the external medium and thus to dominate the surface from an electrophoretic standpoint. This same hypothesis would apply to the structure proposed by Parpart, although he did not speculate on this possibility.

Just recently the mosaic theory of the cell membrane appeared to receive dramatic support. It was reported that electron micrographs of "saponin"-treated (and phosphotungstic-acid-stained) cell membranes showed a hexagonal array of "pits" 140 to 160 Å in diameter.[50] It has since been reported that cholesterol and lecithin-cholesterol films show the same hexagonal pattern after saponin treatment;[51] that x-ray diffraction patterns of saponin-treated RBC ghosts show the existence of a hexagonal phase (whereas untreated ghosts fail to give evidence for any hexagonal structure);[52] and that nerve myelin separates into "residual lipoprotein," cholesterol, and "residual mixed lipid" phases upon being air-dried with sodium phosphotungstate as the only fixative.[53] In view of the latter reports it appears that the structures seen in the saponin-treated cell membranes consist entirely of artifacts produced by the method of sample preparation.

---

*Kavanau has recently proposed a "dynamic" model of the membrane, based upon the lamellar theory of the lipid and protein phases, but in which lipid "palisades" can fluctuate as to height and diameter.[49] In my opinion the information contained in his paper does not justify a discussion of his model at this time.

The mosaic models of the cell membrane differ from the Davson-Danielli model with regard to their expected surface charge characteristics. In the mosaic model, it no longer is necessary to conceive of a protein with all of its groups of intermediate pK tucked out of sight. If the surface charge were dominated by the strongly acidic phosphate groups of the phospholipids, as suggested by Ponder, this would account for the extremely low isoelectric point of cells in general, and the RBC in particular. On the other hand, it still remains a mystery to this author why the amino groups of serine and ethanolamine fail to be neutralizable—as evidenced by an absence of any increase in the mobility in the range of pH 9.0 to 11.0, where one would expect the pK of these groups to lie.

3. Bell's Modification of the Davson-Danielli Model

Bell has recently proposed a modification of the Davson-Danielli model of the cell membrane to include a layer of carbohydrate attached to the outermost protein layer.[54] The major evidence he cited in support of this proposal was that: (a) polysaccharide is a ubiquitous component of cell surfaces, (b) certain polysaccharides are highly reactive with proteins and lipoproteins, and (c) various polysaccharides can cause a stabilization of protein so that it no longer spreads on a Langmuir trough. This latter observation would appear to make the carbohydrate-protein hypothesis inconsistent with the Davson-Danielli model, for one of the fundamental hypotheses of that theory was that the protein was spread at the lipid surface.

The main point of Bell's proposal is not affected by this argument, however. It is entirely possible that the outer surface of the cell might consist largely of polysaccharide, regardless of whether or not the inner lipid and protein constituents are arranged in the form required by the Davson-Danielli model. This carbohydrate proposal is indeed highly favored by recent electrophoresis studies, as described in detail in Subsec. B below. Briefly it might be stated in advance that sialic acid (see chemical structure in Subsec. B) is responsible for a considerable portion of the surface charge of various intact cells at pH 7.4. The strongly acidic carboxyl group of this

molecule would account for the low isoelectric points found for intact cells. Carbohydrate at the surface might also account for the constancy of mobility in the intermediate pH range from 6.0 to 11.0, as discussed in Subsec. B.

B. Combined Electrophoretic and Biochemical Studies on Intact Cells (RBC, TA3 Ascites)

1. Experiments Involving Hydrolytic Enzymes

a. Introduction. Hydrolytic enzymes can be used to great advantage in studying the molecular structure responsible for the surface charge of intact cells. The usefulness of such enzymes stems from the fact that it is possible to know exactly what type of molecule, and usually what type of bond, is susceptible to attack by the enzyme. Consequently, it is possible to predict what sort of changes should be produced in the structure. Conversely—and this is the important part—when products of enzymatic degradation are observed together with changes in the surface structure after treatment, this can have important implications regarding the molecular structure of the cell surface.

In my experimental work reported below, changes in the surface charge, as determined by microelectrophoresis, have been the criterion used for detecting changes in the surface structure. Ponder[36] has quoted the experiments of Balantine and Parpart in which hemolysis and permeability were used as criteria of surface changes induced by the action of hydrolytic enzymes. Direct visualization of the surface structure by electron-microscope techniques promises to be another valuable approach when used in conjunction with the microelectrophoretic and enzymatic studies. As yet, no combined work of this nature has been reported.

The studies with the so-called receptor-destroying enzyme (RDE) have yielded by far the most valuable knowledge to date regarding the charge-determining structure on intact cells. The history of this subject begins with the observation that various influenza viruses and other related viruses will agglutinate human RBC.

After a short period of incubation the virus is eluted, and the cells may again be put into suspension. These viruses may be arranged according to a "receptor gradient"; i.e., according to whether or not virus "A" will agglutinate RBC that have already been agglutinated once by virus "B." It was found that RBC treated with an enzyme from Vibrio cholerae were no longer susceptible to agglutination by any of the viruses, hence the name "receptor-destroying enzyme."

In 1948 Hanig demonstrated that the electrophoretic mobility of virus-agglutinated, resuspended RBC was less than that of untreated RBC.[55] This was followed by the observation of Ada and Stone in 1950 that receptor-destroying enzyme produced a much greater reduction in the mobility than did any of the viruses.[42] This enzyme has since been characterized as a glycosidase specific for the O-glycosidic bond between terminal sialic acid (N-acylated neuraminic acid) and another sugar, often galactose or galactoseamine.[43] The structure of N-acetylneuraminic acid is given in Fig. 21. This enzyme is also referred to as neuraminidase or sialidase. In 1958 Klenk and Uhlenbruck demonstrated that crystalline N-acetylneuraminic acid (NANA) could be recovered from human RBC that had been treated with RDE.[56] In the same year Klenk suggested in a symposium discussion that the carboxyl group of sialic acid might be responsible for the surface-charge characteristics of human RBC.[57] This suggestion has only recently become widely known and appreciated.

The change in the mobility of influenza-virus-treated guinea pig RBC had been previously interpreted by Bateman et al. to mean that the removal of sialic acid resulted in the exposure of positively charged groups (such as amino groups).[58] At that time the enzyme had not yet been characterized as an O-glycosidase. Consequently there had been an erroneous interpretation made in the titration study of an RDE-treated sialomucoprotein,[59] upon which Batemen et al. had based their conclusions. The explanation given by them appears to be much less tenable in view of the specificity of the enzyme, for no charged groups are created by the hydrolysis of an O-glycosidic bond. One also wonders whether a molecule as small as sialic acid could effectively mask other charged groups.

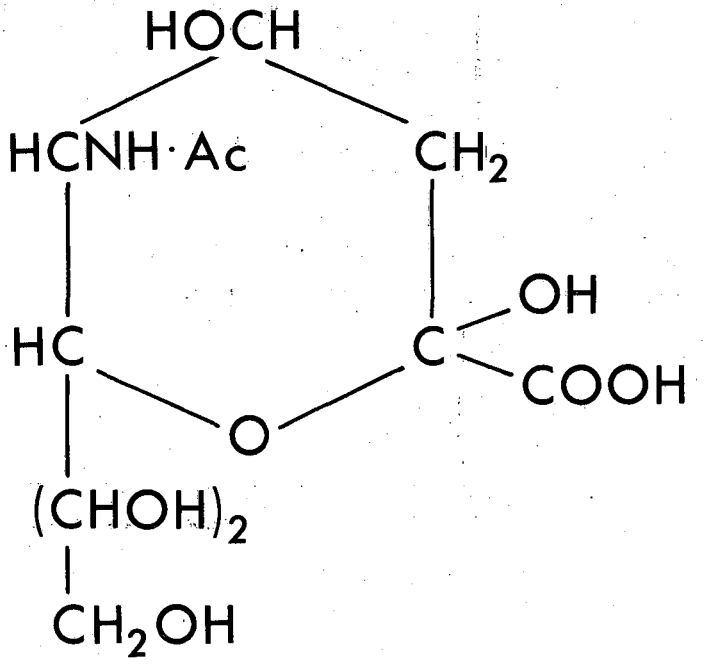

MU-31331

Fig. 21. The chemical structure of N-acetylneuraminic acid. The carboxyl group of this and other N-acylated neuraminic acids (sialic acids) is believed to be largely responsible for the negative charge of intact RBC.

The present interpretation, that the reduction in mobility results primarily from the removal of the negatively charged carboxyl group of sialic acid, has since received some rather convincing support. Eylar et al. showed that there was very nearly a one-to-one correspondence between the percentage decrease in the mobility of RBC at pH approximately 7.0 and the percentage of the total sialic acid (in the RBC ghost) removed from these cells by RDE.[44] This one-to-one correspondence appears to be valid for RBC of many species. The more recent work of Seaman and Uhlenbruck with RDE has continued to support the existence of this correspondence.[58]

Cook et al. had previously measured the amount of sialic acid released by RDE. They showed that this was approximately twice what one would expect if each sialic acid molecule removed were to correspond to a decrease in the surface charge by an amount equal to the value of a single elementary charge.[18] To make this comparison, they related charge reduction to mobility reduction by the equations of electrophoresis. This same discrepancy in the amounts of sialic acid has been reported by Eylar et al.[44] and by Seaman and Uhlenbruck.[58] Eylar et al. have also shown that the mobility of RBC of various species is proportional to the amount of sialic acid per unit area of the RBC. In this interspecies comparison there is a similar fourfold change in the amount of sialic acid for a twofold change in the mobility, which is twice the simplest theoretical expectation.

Similar experiments have been performed with other types of cells. Wallach and Eylar found a 72% reduction in the mobility of Ehrlich ascites cells at pH 6.4, ionic strength 0.072, associated with the removal of 73% of the sialic acid after incubation with RDE.[60] In this instance the amount of sialic acid released is nearly five times that which would be expected on the basis of mobility–surface-charge calculations. Similarly, Cook et al. reported a 33% decrease in the mobility of Ehrlich ascites tumor cells at pH 7.0, ionic strength 0.145, after incubation with RDE.[21] These authors did not present sufficiently reproducible results to allow an estimate of the ratio of experimental to theoretical sialic acid released. Treatment with RDE

has also been reported to reduce the mobility of rat (liver carcinoma) ascites cells by 60%, the mobility of normal leukocytes by 50%, and the mobility of bone marrow cells by 70%.[61] No estimates of the amount of sialic acid released after RDE treatment were reported in these latter studies. At the same time RDE treatment did not produce a decrease in the mobility of normal or rapidly proliferating rat liver cells.[61]

An explanation is called for as to why there is such a large discrepancy between the "theoretical" and experimentally observed amounts of sialic acid which are released after treatment with RDE. No one has as yet reported any experiments that might explain this discrepancy, although there are several possible explanations which might be investigated. Three classes of possibilities are discussed below.

(a) The first possibility is that the theory might inadequately describe the relationship between electrophoretic mobility and surface charge. In this connection it has been suggested that the "electrophoretic radius" might be much smaller than the true radius of the cell.[6] If so, Eq. (20) would have to be used instead of Eq. (22). In this way Eylar et al. found that use of an "electrophoretic radius" in the range 20 to 100 Å would increase the charge calculated from mobility by a factor of two. This would remove the discrepancy between theoretical and experimental amounts of sialic acid.[44] Unfortunately there does not presently appear to be any theoretical justification for the use of any radius other than the true radius of the particle in the equations of electrophoresis. Alternatively, it has been suggested that the surface of intact cells may be penetrable to counterions, in which case Haydon has proposed that theory would underestimate the amount of surface charge by a factor of $[1 + (1 - \alpha)^{1/2}]$, where α is the fraction of the total space within the surface not available to counterions.[62] It is unlikely that Haydon's proposal can account for the discrepancy, in view of certain criticisms of his

analysis* and in view of the improbability that it represents a large enough correction.[58] A third factor has already been discussed in Subsec. I.A. This is the question of how much of the counterion charge distribution lies within the surface of shear. It must be remembered that the mobility is related only to the net charge of the hydrodynamic unit (i.e., migrating species). The way in which this net charge is related to the number of dissociated (i.e., charged) groups depends upon the laws of the ionic double layer and upon the thickness of the "bound" water layer. For example, if half of the counterions were contained within the surface of shear, then the removal of two charged groups from the surface would be necessary to reduce the net charge by the value of one elementary charge. In a way, this third factor is an extension of the ideas contained in Haydon's analysis.

(b) The second possibility is that while the primary effect of RDE is the removal of sialic acid and its negatively charged carboxyl group, secondary changes in the surface structure might occur which alter the value of the cell's mobility. That is, the change in surface charge as calculated from the change in mobility might not agree with the change calculated on a one-to-one basis from the amount of sialic acid released. Seaman and Uhlenbruck[58] have given a comprehensive analysis of the factors that might be involved in such a secondary change. This matter will be discussed in greater detail later in this section. It does not seem likely that any of these secondary effects could account for the large ratios (from two to five) of "experimental" to "theoretical" sialic acid that have been found for

---

*The equations and figures given in Haydon's paper appear to have been based upon the assumption of planar geometry. The situation in intact cells much more closely approximates spherical geometry. Thus while Haydon's basic principles are sound (i.e., counterions will exist on both sides of a charged surface—even a closed surface—provided that there is space there in which they may exist), the proper equations corresponding to spherical symmetry would be required before exact calculations could be performed.

RBC and ascites tumor cells. On the other hand they may be largely responsible for the variations in this ratio from experiment to experiment and between laboratories.

(c) The third possibility is that some of the sialic acid molecules might be situated "deep" within the surface of the cell such that the dissociated carboxyl groups do not contribute net charge, yet such that the glycosidic bonds which link sialic acid to the cell membrane are susceptible to hydrolysis by the enzyme. This hypothesis would be attractive in the case of the RBC, if one imagined that one-half of the sialic acid were at the outer surface and the other half at the inner surface of the "shell" formed by the cell membrane. If this were true it would also explain the fact that the mobility of the RBC of various species is proportional to the amount of sialic acid per unit area, but that a fourfold increase in the sialic acid per unit area results in only a twofold increase in the mobility.[44] Extending this picture to other cells, one might expect that their various cytoplasmic membranes also contain sialic acid which would be released when the cell was exposed to RDE. In this case the total amount of sialic acid released would be much greater than just twice the amount of sialic acid at the cell surface, and one would expect to find a ratio of experimental to theoretical sialic acid greater than two. This explanation seems quite likely to be the correct one in the case of the Ehrlich ascites tumor cells studied by Wallach and Eylar,[60] for they showed that after the intact cells had been incubated with RDE, 98% of the sialic acid associated with the microsomal fraction is removed; and between 30 and 50% of the sialic acid associated with the nuclei, mitochondria, and soluble fractions is removed. In order to explain the susceptibility of the sialic acid on the cytoplasmic membranes of the intact cells to the action of RDE, these authors invoked the hypothesis that the cytoplasmic membranes were in constant exchange with the plasma membrane. They remarked, however, that this explanation was weakened by their inability to prevent such an exchange through inhibition of the cell's metabolism (with 10^{-4} M dinitrophenol or 10^{-3} M KCN). It seems likely to me that RDE penetrates the membrane

of both RBC and ascites tumor cells (although Wallach and Eylar claimed that this does not occur), after which it splits off sialic acid from the inner surface of the plasma membrane as well as from whatever cytoplasmic structures may contain this molecule.

Various studies on the action of numerous proteolytic enzymes have been performed. Thus far these results have been much more difficult to interpret than those obtained with RDE. Through the recent work of Seaman and Uhlenbruck, and others referred to in their paper,[58] it has been determined that the decrease in the mobility of RBC after incubation with proteolytic enzymes is accompanied by the release of a sialic-acid-containing mucoid or mucopeptide. Thus, the major contribution of these studies has been to show that in the RBC of most species sialic acid is associated with protein. It would be a matter of considerable interest if some of these muco-substances were to be purified and analyzed for their amino acid and sugar composition, but such work has not yet been reported.

The decreases in mobility (and occasional increases !) which occur after treatment with proteolytic enzymes are associated with much more complex changes than those accompanying the release of sialic acid after RDE treatment. The complexities probably involve the formation or exposure of new aniongenic groups at the surface of the cells subsequent to proteolysis, as described below.

Before moving on to a description of my own experiments it is perhaps wise to consider some of the possible pitfalls in interpretation that are associated with the combined enzymatic and electrophoretic experiments. Such experiments have their most clear-cut interpretation if it may be assumed that the surface structure (in particular the surface charge) after the enzyme action is equal to the original minus that of the split product. This possibility is most feasible when the split product is small. More often than not, however, it may be expected that removal of whole molecules and polymers (peptides, oligosaccharides, etc.) will result in the exposure of new charged groups. These may be groups that formerly lay beneath the split product (and thus were unable to dissociate) or groups that have

been exposed through structural rearrangements occurring subsequent to the enzymatic action. A second class of difficulties involves the possibility of other physical changes in the cell after enzyme treatment. The electrophoretic radius, the penetrability of the surface to counterions, or the conductivity of the particle as a whole may be altered. The conductivity can be determined by ac impedance measurements, although this is not commonly done. A third source of error arises from the possibility of adsorption of certain charged substances onto the surface of the cell. These may include the split product itself, substances leached out from the otherwise intact cell, impurities present in the enzyme preparation, and even the enzyme itself. The problem of undesirable adsorption can usually be controlled by adequate experimental care.

b. Methods and materials. The samples of RBC and ascites tumor cells used in these studies were prepared as described in earlier sections (see Subsecs. III. B and III. C). The buffer used throughout was 3×10^{-4} M $NaHCO_3$ in 0.145 M NaCl (Standard Buffer) as described previously. The pH was altered by the addition of 0.145 M HCl or 0.145 M NaOH when desired. Sprague-Dawley rats were used. There appears to be a significant difference in the mobility at pH 7.4 of these rat RBC (about -1.20) compared with the mobility of the RBC from Long-Evans rats (Sec. III, about -1.05), as may be seen by a comparison of Fig. 8 with the data in this section.

Table II contains a list of the enzymes used in this study, together with some of their biological, chemical, and physical properties. All enzymes were dissolved in Standard Buffer at the concentrations indicated in the following text, tables, and figures. Packed cells were added to the desired vol/vol concentration in the enzyme solution, and the resulting suspensions incubated in a 37°C water bath. At various time intervals an aliquot of the incubated cells was removed, the cells washed at least twice by centrifugation, and the final pellet resuspended in Standard Buffer for the electrophoresis experiments.

When chemical assays for enzymatically split products were desired, the cell suspensions were centrifuged after incubation for the

Table II. Name and characterization of enzymes used in this study.

	Receptor-destroying enzyme (RDE)	α-amylase	β-amylase	Hyaluronidase	Acid phosphatase	Basic phosphatase
Nature and specificity of enzyme action	The specific α-glycosidase cleaving the α-ketosidic linkage joining the potential keto group of a terminal N-acylatedneuraminic acid to an adjacent sugar residue in a disaccharide, trisaccharide, or polysaccharide; will cleave both a 2→3 and a 2→6 linkage	An α(1→4) - glycosidase which attacks glycosidic linkages in the interior of a polysaccharide chain, with the formation of oligosaccharides. Hydrolysis can occur on either side of a branching point; i.e., (1→6) glycosidic bonds	An α(1→4) - glycosidase which splits off disaccharides; action initiates at the nonreducing end of a polysaccharide chain, and action stops at branching point; i.e., at (1→6) glycosidic bonds	Specific for the hydrolysis of glycosidic bonds involving the reducing group of N-acetylglucosamine	Alcoholic and phenolic phosphomonoesters	Alcoholic and phenolic phosphomonoesters, p-nitrophenyl phosphate
Source of enzyme	Culture fluid, Vibrio cholerae	Bacterial	Sweet potato ?	Bovine testes	Wheat germ	Calf intestine
Purity	Unpurified	B grade	B grade	B grade	B grade	B grade
Enzymatic activity	Titer of 1:1600 is the end-point dilution, using influenza PR-8 in the virus hemagglutination test	2500 SKB units/g at 30° C	2000° Lintner (α-amylase free)	>300 U. S. P. units/mg	800 μg phosphorus liberated per mg per 30 min (disodium phenyl phosphate) 37° C, pH 5.0.	>2500 μg of phosphorus liberated per mg per 30 min (disodium phenyl phosphate) 37° C, pH 9.3.
Range of pH optimum		6.8 - 8.0	4 - 6	5.5 - 6.2	5.0 - 5.5	8.6 - 9.4
Isoelectric point			4.75			
Molecular weight	10 000 to 20 000	50 000 to 90 000	152 000			
Form available	Aqueous solution (frozen)	Dry powder	Dry powder	Dry powder	Dry powder	Dry powder
Manufacturer	Microbiological Associates	Calbiochem	Calbiochem	Calbiochem	Calbiochem	Calbiochem

desired time, the supernatant pipetted off, hemoglobin in the supernatant precipitated by heating for 3 min in boiling water, and a clear solution obtained by filtration through Whatman No. 42 filter paper.

Free sialic acid was determined by the method of Warren,[63] except that the final chromophore was extracted into 1.5 ml of cyclohexanone (rather than the 4.3 ml as recommended by him) to increase the sensitivity of the assay. Bound sialic acid was released in the free form after hydrolysis in 0.1 $\underline{M}$ H_2SO_4 at 80° C. Figure 22 shows the absorption spectrum of the chromophore produced by sialic acid in this assay. The spectrum reported by Warren is shown for comparison. The RDE solution contained a substance which also produced a chromophore that absorbed light in this wavelength region. Consequently it was necessary to correct for this interfering substance by subtracting the spectrum obtained with enzyme alone from the spectrum obtained with the supernatant from RDE-treated cells (both solutions having been previously heated as described above). Sialic acid was determined quantitatively as N-acetylneuraminic acid (NANA) by using the molecular extinction coefficient (at maximum absorption) of 57 000 reported by Warren. Cell counts were done in a hemocytometer.

Total carbohydrate was determined by the anthrone method; the procedure recommended by Mokrasch[64] was followed except that the optical density at 620 mμ minus the optical density at 700 mμ was used as the measure of carbohydrate. In this way, it was always possible to obtain a linear relation between the optical-density difference and the concentration of reducing sugar. In every experiment galactose and fucose were run at several known concentrations as standards.

c. Results and discussion: first phase. The first preliminary experiments performed with RDE were designed simply to see whether or not the enzyme preparation supplied by Microbiological Associates (Albany, California) would be effective in producing a reduction in the mobility of rat RBC and (mouse) TA3 ascites tumor cells. Figure 23 shows how the mobility of rat RBC (at pH 7.4, ionic strength 0.145) decreases with time of incubation with RDE.* A maximum reduction

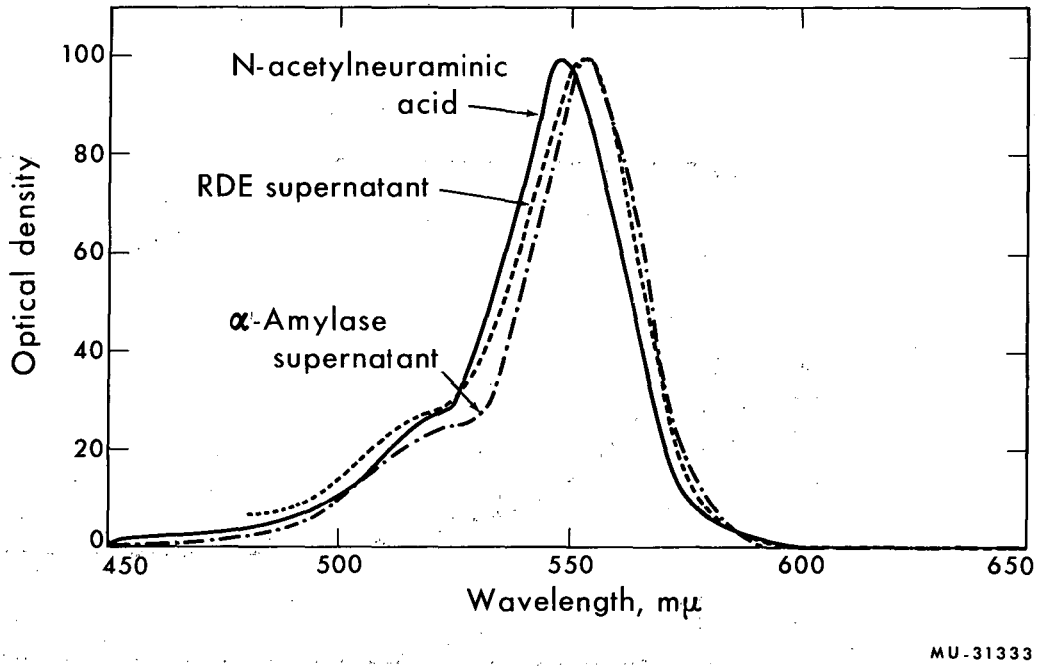

Fig. 22. Normalized absorption spectra of the chromophore produced in the thiobarbituric acid assay for free sialic acid. The spectrum for N-acetylneuraminic acid has been taken from the paper by Warren which describes this assay. Absorption curves obtained in this study, by using the supernatant from RDE and α-amylase-treated rat RBC, are shown for comparison. It is possible that the slight difference in the location of the absorption maximum reported by Warren (549 mμ) and that obtained in these studies (553 mμ) might be due to an error in the calibration of the wavelength scale (either his or ours). If the curves were to be shifted so that the absorption maxima coincided, they would be seen to be very nearly identical.

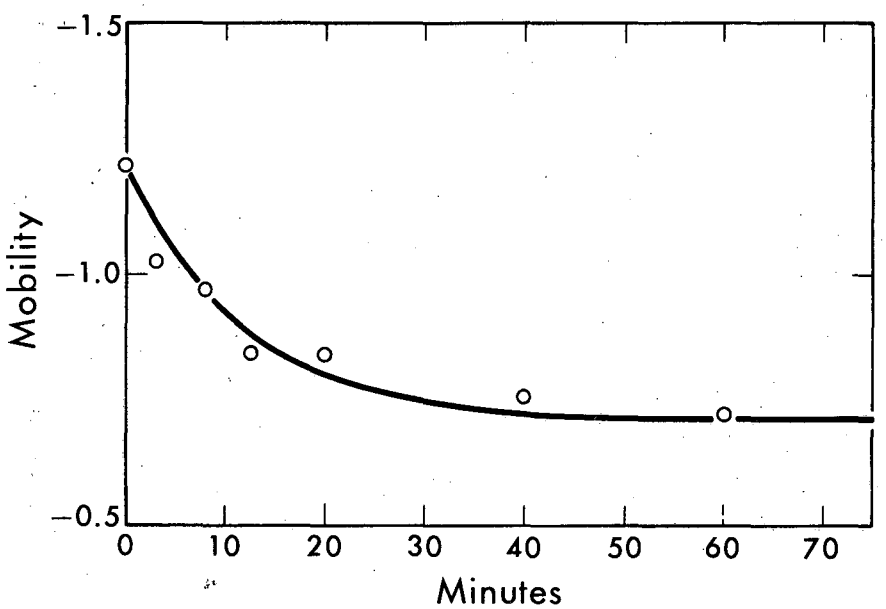

Fig. 23. Decrease in the (negative) mobility of rat RBC upon treatment with RDE. The commercial RDE solution was mixed with equal volumes of Standard Buffer. One volume of RBC was suspended in two volumes of enzyme solution and incubated at 37° C. The solid curve represents a function of the form $(A + Be^{-t/T})$, where t = time in minutes, and A, B, and T are constants.

of 42% was obtained in this experiment. The percent reductions that have been reported for the RBC of other species are shown in Table III. A large change is noted in the mobility of RDE-treated RBC after subsequent formaldehyde treatment. This is interpreted by Seaman and Uhlenbruck to mean that a large number of positively charged groups (such as amino groups) are exposed at the surface of these cells after RDE treatment.[58] They believe that formaldehyde complexes with these groups and prevents them from becoming positively charged. On the other hand Eylar et al. found no change in the mobility of their RDE-treated human RBC after formaldehyde treatment.[44] It would appear that their results are more indicative of action of pure RDE, for it is presumed that this enzyme would not expose positive groups. Figure 24 shows the results obtained when (mouse) TA3 ascites cells were incubated with RDE. These kinetic data are complicated by the fact that the untreated control cells show a reduction in the mobility, as discussed in Subsec. III. C. The final reduction is only 30% when compared to the final mobility of the control cells, but is more than 60% when compared to the initial mobility of the control cells. These values should be compared with the 72% reduction reported by Wallach and Eylar,[60] and the 33% reduction reported by Cook, et al.[21]

d. Results and discussion: second phase. The second phase of this study began with a search for hydrolytic enzymes, other than RDE and the proteolytic enzymes, that would have an effect upon the mobility of rat RBC. The polysaccharide-hydrolyzing enzymes α-amylase, β-amylase, and hyaluronidase were chosen because it was known from the studies with RDE that carbohydrate was present at the RBC surface. Acid and basic phosphatase were also tested on the chance that the phosphate groups of phospholipids might be involved in determining the charge, and that they could possibly be split off from the cell surface by these enzymes. It can be seen from Table IV that

---

* This curve represents fairly recent data. A similar experiment was done much earlier in this study, but the data appear to have been lost.

Table III. Maximum percentage decrease in the mobility of RBC from various species after treatment with RDE.[a]

	Human	Chimpanzee	Horse	Sheep	Calf	Chicken	Pig	Dog	Ox
Eylar et al.	94		20	74	84	72	67		
Seaman and Uhlenbruck	80	74	53	69		51	57	75	73
Formaldehyde-treated (Seaman and Uhlenbruck)	59	72	31	38			28	25	

[a] The measurements of Eylar et al.[44] were made at pH 6.8 and ionic strength 0.072. The measurements of Seaman and Uhlenbruck[58] were made at pH 7.4 and ionic strength 0.145. The latter authors have also reported corresponding values of the mobility reduction of the treated RBC after an additional treatment with formaldehyde.

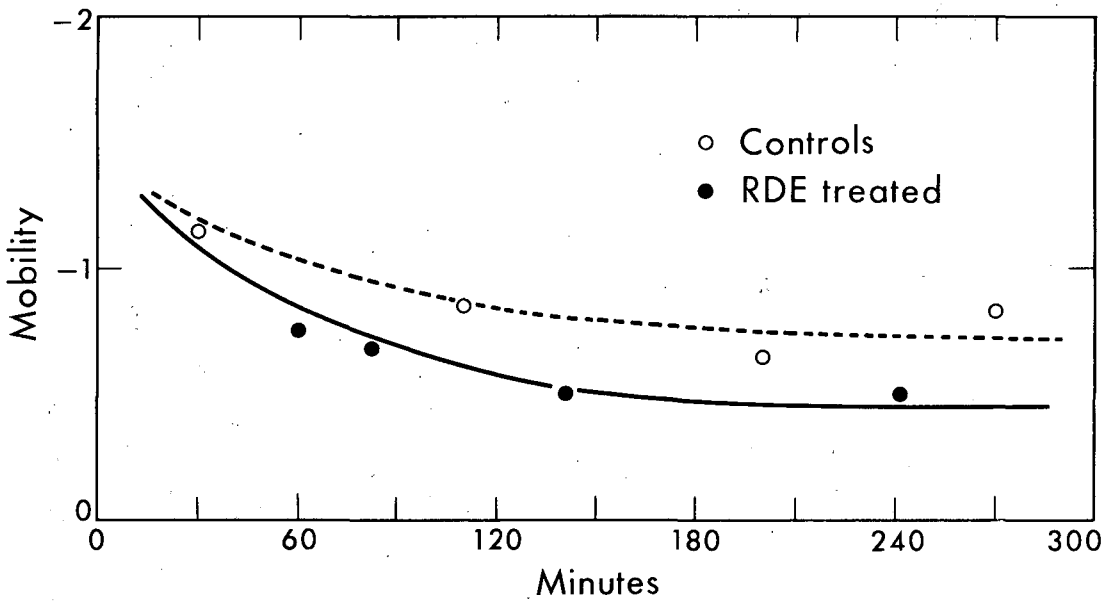

Fig. 24. Decrease in the (negative) mobility of (mouse) TA3 ascites tumor cells upon treatment with RDE. The commercial RDE solution was mixed with nine volumes of Standard Buffer. A 0.75% vol/vol cell suspension was made in this enzyme solution, and the cells were incubated at 37° C.

Table IV. Mobility of rat RBC at pH 7.4, ionic strength 0.145, after treatment with various enzymes.[a]

Date	Control mob.	RDE mob.	RDE % red.	α-amylase mob.	α-amylase % red.	β-amylase mob.	hyaluronidase mob.	acid phosphatase mob.	basic phosphatase mob.
11-23-62	-1.39 (t=0) -1.31 (180 min)			-0.89 (A), (i)	42[b]	-1.39 (120 min) (B), (i)	-1.39 (85 min) -1.17 (240 min) (A), (i)		
11-28-62	-1.25			-0.69[c] (C), (ii)	45				
1-2-63	-1.25			-0.64[c] (D), (ii)	49				
1-31-63	-1.15			-0.59 (65 min) (A), (i)	49			-1.14 (65 min) (A), (i)	-1.12 (65 min) (A), (i)
2-21-63	-1.17	-0.71 (60 min) (E), (iii)	39	-0.50 (60 min) (A), (iii)	56				
4-18-63	-1.22	-0.72[d] (E), (iii)	41	-0.55 (60 min) (A), (iii)	55				

[a]The following key denotes enzyme concentrations: (A) 1.0 mg/ml, (B) 1.6 mg/ml, (C) 0.5 mg/ml, (D) 0.01 mg/ml, (E) one volume of commercial enzyme solution and one volume of Standard Buffer. The RBC concentration during the incubation was as follows: (i) 2% vol/vol, (ii) 1% vol/vol, (iii) 33% vol/vol. The RBC were incubated at 37° C for the time indicated in the table; in some instances footnotes are given which refer to certain mobility-time curves. The percentage decrease in the mobility has also been tabulated for RDE and for α-amylase-treated RBC. Differences less than 0.05 are not significant.

[b]This percentage equals $\frac{(1.39 - 0.20) - (0.89 - 0.20)}{(1.39 - 0.20)} \times 100$. (See text for explanation.)

[c]See Fig. 26 for the mobility-time curve.

[d]See Fig. 23 for the mobility-time curve.

α-amylase is the only enzyme tested that has an obvious effect upon the mobility of rat RBC.

Sialic acid is removed from the RBC upon incubation with α-amylase, as will be described below. It is therefore probable that the mobility changes after α-amylase treatment are primarily ascribable to the removal of the negatively charged carboxyl group of sialic acid from the cell surface, as after RDE treatment.

In paired experiments, it appears as though the mobility reduction with α-amylase is significantly greater than that with RDE, as may be seen in Table IV. The experiment dated November 23, 1962 is somewhat irregular in that the mobility of the control cells as well as the α-amylase-treated cells is more negative, by about 0.20 mobility units, than that found in other experiments.

There are three observations which indicate that the surface of α-amylase-treated rat RBC is grossly different from that of the untreated RBC. First of all, the treated cells show a much stronger tendency to form aggregates, especially upon centrifugation, so that there is some difficulty in resuspending the pellet. Secondly, they have a much greater tendency to stick to the surface of a glass container. Thus they show evidence of both stickiness and adhesion as recently defined by Coman.[65] The untreated RBC, by comparison, show very little tendency to stick to one another or to adhere to the surface of their containers. Thirdly, the mobility-pH curve (after complete action of α-amylase on RBC) shown in Fig. 25 is noticeably different in shape as well as in magnitude from the curve for the untreated RBC. It would appear that after α-amylase treatment there are groups present at the RBC surface that have pK's in the approximate range pH 6.0 to 10.0, since the mobility-pH curve shows a gradual change throughout that region. The fact that the change in mobility results from the enzymatic action rather than from adsorption of the enzyme (protein) is demonstrated in the following way. The RBC were incubated with α-amylase at two enzyme concentrations: first 0.05% wt/vol and then 0.001% wt/vol. It is shown in Fig. 26 that in the two cases the kinetics differ but the end point is the same. This is to be

expected from the nature of enzymatic action alone. Furthermore it is unlikely that protein adsorption would take so long to reach completion as was found when the enzyme concentration was 0.001% wt/vol.

As mentioned previously, sialic acid is released into the supernatant when rat RBC* are incubated with α-amylase. Appropriate control experiments show that there is no sialic acid present when RBC are incubated without enzyme, nor is there any sialic acid present in the enzyme itself. The sialic acid is not released in the free form after α-amylase treatment of RBC, for none is at first detectable by the Warren method. The sialic acid is only detectable after acid hydrolysis of the supernatant. The rate at which the bound sialic acid is released (under the conditions employed) is illustrated by Fig. 27, where the optical density at 503 mμ (absorption maximum of the chromophore produced by sialic acid) is plotted vs the length of time for which hydrolysis was allowed to proceed. It is seen that approximately two hours is required for the complete release of sialic acid in the free form. The control experiment, in which the supernatant from RDE-treated RBC was subjected to the same acid hydrolysis, shows that free sialic acid itself is gradually destroyed under these conditions. A similar observation has already been reported by Gibbons.[66]

Four experiments were performed in order to make a quantitative comparison of the amount of sialic acid released by the two enzymes, α-amylase and RDE. The washed and packed RBC were suspended in two volumes of enzyme solution and incubated for at least 1 h at 37°C. The α-amylase solution used was 1 mg/ml of enzyme in Standard Buffer, whereas the RDE solution was one volume of the commercial preparation diluted with one volume of Standard Buffer. The results of this study are given in Table V.

---

*The RBC from a polycythemic individual were also incubated with α-amylase in an attempt to purify milligram quantities of the hydrolysis product. This product behaved similarly to the one obtained from rat RBC. The purification of the split product was, however, abandoned because of the length of time required for such a project.

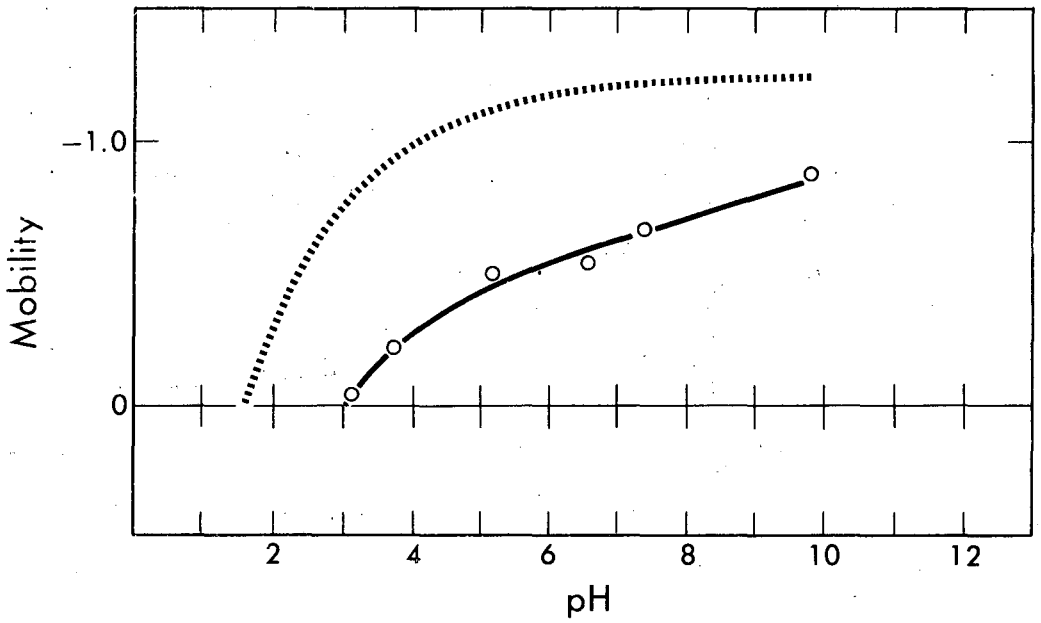

Fig. 25. Mobility-pH curve obtained for α-amylase-treated rat RBC. The dashed curve is a portion of the mobility-pH curve for untreated rat RBC taken from Fig. 28a.

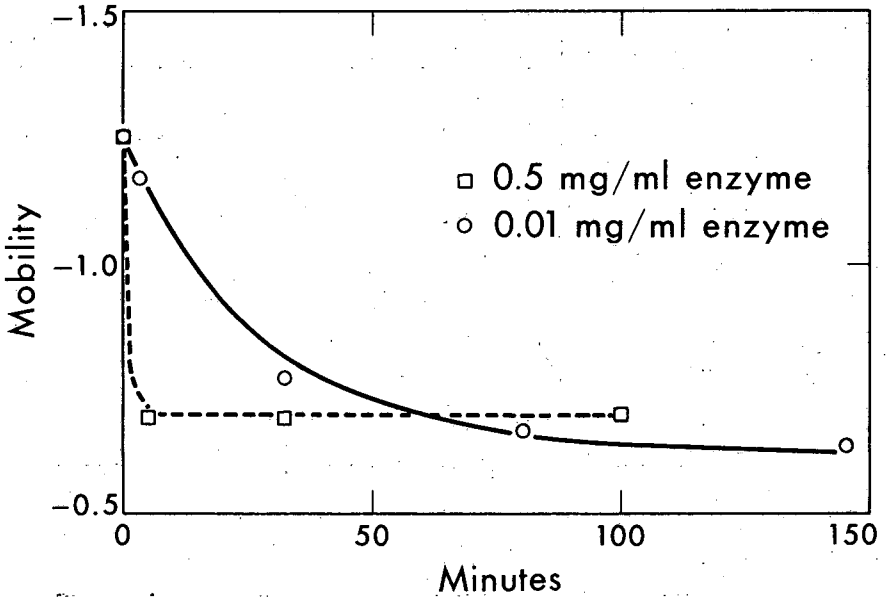

Fig. 26. Different kinetic curves found for the decrease in (negative) mobility of rat RBC incubated with α-amylase at 37° C under different conditions. The concentration of RBC was about 1% vol/vol. The enzyme concentration was 0.5 mg/ml in one case and 0.01 mg/ml in the other. The solid curve represents a function of the form $(Ae^{-t/T} + B)$, where t = time in minutes, and A, B, and T are constants.

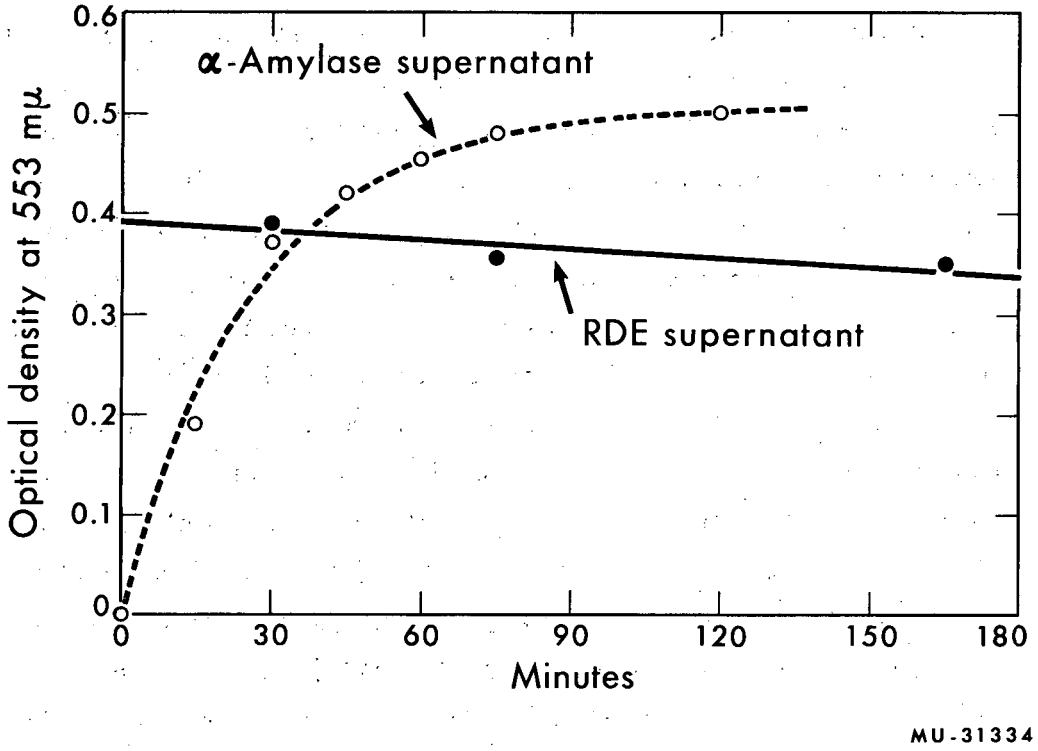

Fig. 27. Maximum optical density developed in the thiobarbituric acid assay (for free sialic acid) after hydrolysis in 0.1 M H_2SO_4 at 80° C. The curve obtained with the supernatant from α-amylase-treated rat RBC shows that the sialic acid released by this enzyme is initially in the bound form. The dotted curve represents a function of the form $A(1 - e^{-t/T})$, where t = time in minutes, and A and T are constants. The curve obtained with the supernatant from RDE-treated rat RBC shows that free sialic acid, present at the beginning, is slowly destroyed under this condition of hydrolysis.

Table V. Micromoles of sialic acid (as NANA) released per 10^{10} RBC after enzyme treatment.

Date	1-26-63	4-9-63	4-18-63	5-10-63
α-amylase	0.22	0.25	0.27	0.32
RDE	0.22	0.18	0.27	0.19

The value reported after α-amylase treatment in the experiment of 5-10-63 is anomalously large, indicating that some mistake probably was made. Excluding the results of that last experiment, it appears that the amount of sialic acid released by the two enzymes is very nearly the same. The somewhat higher amounts found in the later experiments probably reflect the fact that the cells were incubated with enzyme for longer periods than in the first experiments.

It may be assumed that the maximum amount of sialic acid that can be removed from the intact rat RBC is of the order of 0.27 micromoles per 10^{10} cells. This corresponds to the removal of 1.6×10^{7} molecules per cell. This number may be compared with the net charge of 1.2×10^{7} electrons on these rat RBC [calculated according to Eq. (29)], corresponding to a mobility of -1.20 (micron)(sec^{-1})(volt^{-1})(cm) at ionic strength 0.145. Similarly, the number of charges removed from these RBC, corresponding to an approximate reduction of 0.50 mobility units, calculates out to be 0.51×10^{7} electrons. Thus, the ratio of amounts of "experimental" to "theoretical" sialic acid released was of the order of three in these experiments. It is seen that these results do not agree very well with the previous suggestions that (a) sialic acid is completely responsible for the mobility of intact RBC, and (b) one-half of the sialic acid is buried deep in the surface of the RBC (see Subsec. V. B. 1. a). On the other hand it is not unlikely that the commercial RDE preparation used in this study contained enzymatic impurities that caused the exposure of new charged groups at the surface of the RBC. This was also the explanation ascribed to the results of Seaman and Uhlenbruck.[58] In such a situation one need no longer expect that removal of 100% of the sialic acid would correspond to a 100% reduction in the mobility. Nor would one any longer expect the

ratio of amounts of "experimental" to "theoretical" sialic acid to be exactly equal to two. Further enzymatic purification in such studies is obviously called for to clarify this question.

My experiments designed to measure total carbohydrate (using galactose as the color standard) were generally unsatisfactory for two reasons. First of all, it was often found that carbohydrate was released from RBC incubated at 37°C without enzyme, in fact often a greater amount than that released by RBC incubated with RDE. Some hemoglobin was also released upon incubation, usually less in the presence of RDE. These experiments suggested that the larger amounts of carbohydrate in the control supernatant were released by RBC which had hemolyzed. Secondly the molecular ratio of total carbohydrate (expressed as galactose equivalents) to sialic acid (as NANA) varied considerably from experiment to experiment. The values obtained were 3.9, 8.2, and 3.8 after α-amylase treatment and (in the same three experiments) 1.2, 0.8, and 3.9 after RDE treatment. It seems apparent, therefore, that a certain (variable) amount of soluble carbohydrate is being leached from the treated RBC as well as from the control RBC during incubation. It is my guess that this carbohydrate is in fact intracellular sugar which would ordinarily be used in the glycolytic metabolism of the RBC. Because of this possible leakage, it is not possible to say how much of the total carbohydrate assayed in the supernatant of α-amylase-treated RBC is actually associated with sialic acid. It is possible, however, to say that there cannot be more than 3 moles of simple sugar in the α-amylase-split product, because ratios of total sugar to sialic acid of approximately four were obtained on two occasions. Before completely accurate information of this sort can be obtained, it will be necessary to purify somehow the compound released after α-amylase treatment. In that way one would be able to determine precisely the total (other) carbohydrate associated with sialic acid.

A certain amount of useful information regarding the carbohydrate structure at the cell surface can be obtained from arguments based solely upon the known specificity of the various enzymes that

will remove sialic acid. First of all, it is known from the specificity of RDE that sialic acid occupies the terminal position of an oligosaccharide. From the fact that α-amylase releases sialic acid in the bound form and from the known specificity of α-amylase for α(1 → 4)-glycosidic bonds, it follows that there is at least one simple sugar associated with sialic acid and at least one sugar associated with the RBC after α-amylase treatment. Thus there exists, at the outer surface of the cell membrane, an oligosaccharide composed of at least three monomer sugar units, of which one is sialic acid. This oligosaccharide is in most cases associated through a primary bond with the protein component of the cell surface, as determined through the use of proteolytic enzymes. In the case of the horse RBC, however, a considerable amount of the sialic acid is also associated with the lipid component.[67]

2. Experiments Involving OsO_4-Fixed and $KMnO_4$-Fixed Rat RBC

a. Introduction. In the work discussed up to this point, microelectrophoresis has been the physical technique used to study the surface properties of intact cells. The cells have been exposed to low pH, low ionic strength, and to various hydrolytic enzymes. In some instances irreversible alteration of the mobility of these cells has been observed. A certain amount of information regarding the surface structure of the cell membrane can be inferred from such observations, especially when a highly specific agent is used to produce the irreversible alteration.

In the course of the previous experiments, it was suggested[68] that electron microscopy would be a valuable additional technique for studying the properties of the cell surface. While electrophoresis primarily gives information regarding the nature of chemical groups at the cell surface, electron microscopy might potentially show something about the physical make-up—i.e., the ultra-architecture—of the cell surface. In addition it could add to our present knowledge regarding the sequence of events responsible for the irreversible alteration of the mobility of an intact cell under various conditions.

Preparation of samples for electron microscopy usually starts with fixation of the specimen. It is entirely possible that the method of fixation itself produces irreversible changes in the surface structure which ought to be reflected as changes in the mobility. If this were true, electron microscopy of such fixed specimens might tell very little about the initial structure of the cell surface. Therefore the first step in the parallel microelectrophoretic and electron-microscope study has been to compare the surfaces of OsO_4-fixed, $KMnO_4$-fixed, and unfixed normal rat RBC according to electrophoretic criteria.

Some previous work has already been reported on the effects of fixation upon the electrophoretic mobility of RBC. Heard and Seaman have reported a method of treatment with formaldehyde and acetaldehyde that stabilizes human RBC against the usual irreversible mobility changes which occur in solutions of low pH or low ionic strength.[41] Their method requires a period of approximately three weeks for completion, in contrast with the very rapid fixation afforded by OsO_4 and $KMnO_4$. For this reason it was thought that OsO_4 or $KMnO_4$ would be more suitable fixatives for electron microscopy, provided that they caused no changes in the cell surface, as judged by electrophoresis. The results and possible implications of the electrophoretic study on OsO_4-fixed rat RBC are described in the paragraphs below.

b. Methods. The RBC were obtained from ether-anesthetized rats as previously described. Solutions of the desired pH/ionic strength were obtained as described in Subsec. III. B. All cells (fixed as well as unfixed) were stored at room temperature as 10% vol/vol cell suspensions, for the duration of the experiment. This generally lasted 4 to 5 h, never more than 12 h.

For OsO_4 fixation the following stock solutions were used: (a) 0.143 M sodium barbital in 0.143 M sodium acetate, (b) 0.10 M HCl, (c) 2% wt/vol OsO_4 in Standard Buffer. One volume of the 10% cell suspension was added to a solution of two volumes (a), two volumes (b), and five volumes (c). After 1 min the cells were centrifuged

(at room temperature) for 2 min at approximately 500 g. The supernatant was discarded, the fixed cells washed twice in 100 volumes of Standard Buffer, and the final pellet resuspended in 10 volumes of Standard Buffer. Because of the volatility and extreme toxicity of OsO_4 all work was carried out in a ventilated hood.

For permanganate fixation the following additional stock solution was used: (d) 1.2% wt/vol $KMnO_4$ in Standard Buffer. One to two volumes of the 10% cell suspension were added (in an ice bath) to a solution of 2.5 volumes (a), 2.5 volumes (b), and 5.0 volumes (d). After 2 min the fixed cells were centrifuged, washed, and resuspended as in the paragraph above.

In certain experiments (as indicated in the Figures) the fixed cells were dehydrated in a manner similar to that employed with fixed tissues prepared for electron microscopy: 1 min in chilled 25% ethanol, 1 min in chilled 50% ethanol, 1 min in chilled 75% ethanol, 1 min in 95% ethanol at room temperature, and finally 15 min in 100% ethanol at room temperature. Between each step the cells were centrifuged, the supernatant discarded, and the cells resuspended in the new solvent solution. After the exposure to absolute ethanol the cells were again washed with Standard Buffer and made into a 10% vol/vol cell suspension.

c. Results. At ionic strength 0.145 the mobility-pH curve for OsO_4-fixed rat RBC is identical to the curve for normal unfixed rat RBC in the region where data can be obtained for the latter.* Figure 28(a) shows the combined results of four experiments with the OsO_4-fixed cells and two experiments with the unfixed cells. This curve is qualitatively identical to that first found by Furchgott and Ponder[17] for human RBC over the portion of the pH range from about 1.6 to 11.0. Figure 28(b) shows that the mobility-pH dependence of $KMnO_4$-fixed

*A slight shift in the magnitude, but not the shape, of the curve was found if the 2% OsO_4 solution was made with distilled water rather than with Standard Buffer.

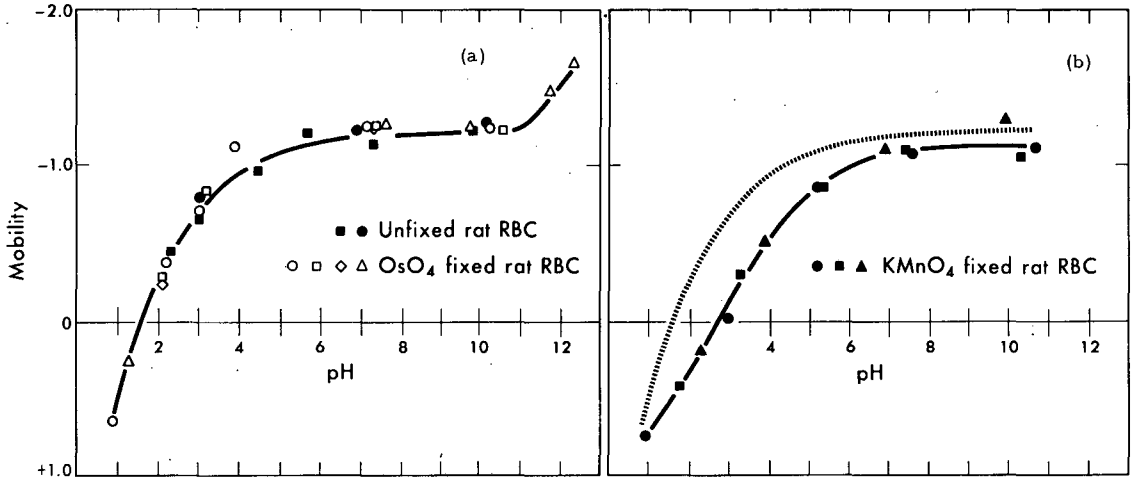

Fig. 28. Comparison of the mobility-pH curves for unfixed, OsO_4-fixed, and $KMnO_4$-fixed rat RBC. The dotted curve in Fig. 28 (b) is a portion of the curve shown in Fig. 28 (a). The data indicated by the clear squares in Fig. 28 (a) and by the dark squares in Fig. 28 (b) were obtained with fixed cells which had been dehydrated in ethanol.

RBC is qualitatively different from that of OsO_4-fixed (or unfixed) RBC. The difference between the two types of fixed cells is greatest below pH 7.0.

The dependence of mobility upon ionic strength is shown in Fig. 29 where the mobility of fixed and unfixed RBC, at pH 7.3 ± 0.2, is plotted as a function of the reciprocal of the Debye-Huckel constant, κ. At 25°C, $\kappa = 0.327 \times 10^8 \ (\Gamma/2)^{1/2} cm^{-1}$, where $\Gamma/2$ is the ionic strength. This method of displaying the ionic strength data was used by Furchgott and Ponder,[17] and has been further discussed by Brinton and Lauffer.[6] While the data obtained with both types of fixed RBC appear to fall on the same curve, there is a marked difference between this curve and that found for the unfixed RBC. Data have not been included for the unfixed RBC at the lowest ionic strengths ($1/\kappa > 30 \times 10^{-8}$ cm), because it was not possible to obtain reproducible values for the mobility from experiment to experiment. It was observed that for unfixed rat RBC the value of the mobility at these low ionic strengths was extremely sensitive to small variations in the initial pH, among other factors.

A remarkable feature of the fixed RBC, noted in the course of these experiments, was their great stability at the low pH's and low ionic strengths. No change in the mobility was exhibited throughout the period of observation (which was as long as 20 min), even at the extreme pH's of 0.9 or 12.3 or in ionic strengths as low as 0.00725 ($1/\kappa = 36.0$). In addition, Table VI shows that the mobility of OsO_4-fixed cells appears to be restored to normal (within experimental error) when the cells are returned to Standard Buffer after a 5-min exposure to low pH or to low ionic strength. This reversibility experiment could not be performed with the OsO_4-fixed cells after exposure to pH 12.3 because of lysis at that pH (see below). Similar experiments were not attempted with the $KMnO_4$-fixed RBC as the majority of our interest has been centered about the characterization of the OsO_4-fixed RBC.

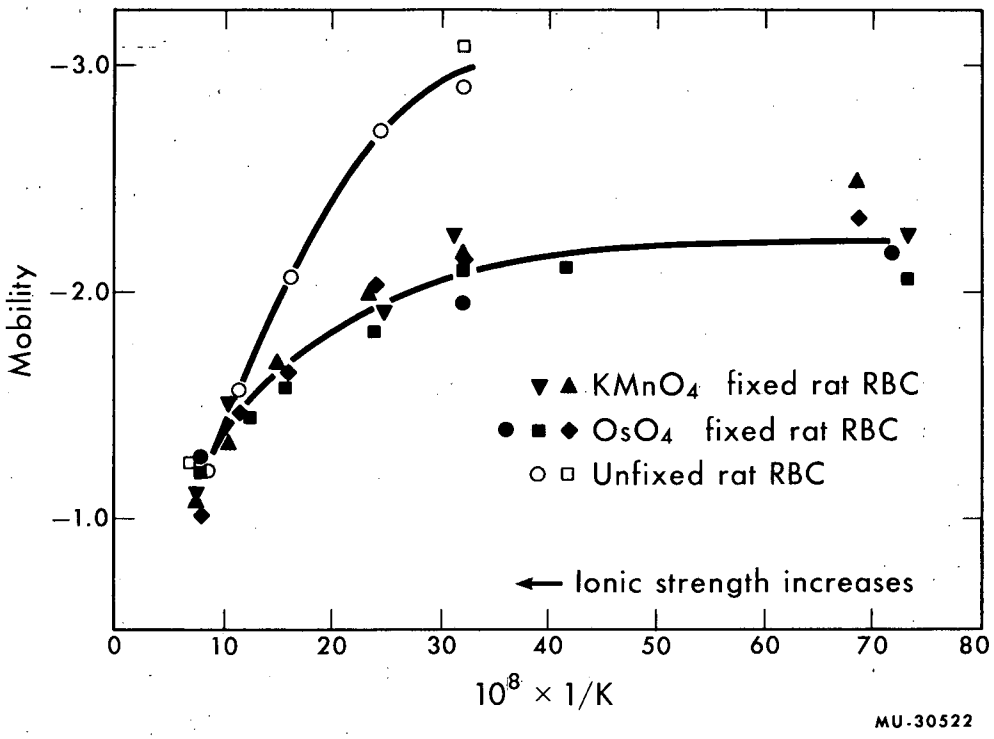

Fig. 29. Mobility of fixed and unfixed rat RBC at pH 7.3 ± 0.2 as a function of the inverse of the Debye-Hückel constant. The Debye-Hückel constant, κ, is defined in Eq. (27); at 25 °C, $\kappa = 0.327 \times 10^8 (\Gamma/2)^{1/2}\ cm^{-1}$, where $\Gamma/2$ = ionic strength. All mobility values have been corrected to the viscosity of water.

Table VI. Mobility of OsO_4-fixed rat RBC measured in Standard Buffer following a five-minute exposure to the indicated solution conditions.

pH 0.90 ionic strength 0.145	pH 7.0 ionic strength 0.00725	Standard Buffer
-1.24	-1.20	-1.28

In contrast with the great stability of the fixed cells at low pH it has long been known that the unfixed cells show rapid changes in acid solutions. For example, Furchgott and Ponder[17] noted that unfixed RBC undergo rapid hemolysis below pH 2.0, at which time the ghosts instantly acquire a positive mobility. At pH's above 2.0 but below 4.0 to 4.5 they observed (as have various authors since that time) that the mobility of unfixed RBC also becomes more positive with time. Such changes occur more slowly, the higher the pH. Examples of the time dependence of the mobility at pH 3.1 ± 0.1 have been shown for unfixed rat RBC in Figs. 18 and 19. In addition I have observed that the unfixed RBC are rapidly and completely dissolved at pH's above 11.0. The stability of guinea pig RBC[69] and human RBC[24] at low ionic strengths has been rather carefully examined by other authors. Heard and Seaman have presented a complete map of the pH-ionic-strength regions of stability for human RBC.[24] No work of this nature has been attempted with the unfixed rat RBC in this study.

A word should be said about the morphological appearance of the fixed compared with the unfixed cells. Immediately after OsO_4 fixation, the cells appeared to be either sphered or to have an oval shape. Only a small percent were in the form of an ideal biconcave disk. If the OsO_4-fixed cells were stored at room temperature in the 0.145 M NaCl solution for several days, they gradually reassumed the form of a biconcave disk. At pH 11.8 and 12.3 the freshly fixed cells were swollen and greatly elongated by the time observations commenced. The fixed cells are also considerably more resistant to alkali than are the unfixed. Lysis occurs only slowly at pH 11.8; it is complete in 2 to 3 min at pH 12.3, though intact ghosts still remain. The mobility of the ghosts appeared

identical to that of the intact cells. Neither swelling nor lysis occurred in the OsO_4-fixed cells at pH's below 11.8.

The $KMnO_4$-fixed RBC appear, at a magnification of 200×, to be smooth spheres about 4 to 5 μ in diameter. At higher magnification, however, it is seen that they are uniformly crenated spheres. The $KMnO_4$-fixed cells undergo a reversible swelling accompanied by a loss of crenation when placed in ethanol or in aqueous solutions of pH 8.0 or greater. The tonicity and the ionic strength do not appear to affect the shape of these objects. These observations on the various morphological changes have, as yet, no explanation.

d. Discussion: Mobility-pH data with OsO_4-fixed cells. The OsO_4-fixed rat RBC have been found to be very stable at low pH, even down to pH 0.9. Furthermore the mobility of these fixed cells is identical to that of the unfixed cells throughout the entire range of pH over which a comparison can be made. Thus the surface structures, at least the charge-determining ones, are not altered by this "drastic" treatment. The remarkable stability of the fixed cells has made it possible for the first time to obtain measurements of the reversible mobility of RBC below their isoelectric point at pH 1.6 (ionic strength 0.145) and at a pH as high as 12.3. In this way it has been possible to demonstrate two new features of the mobility-pH curve for RBC at ionic strength 0.145. First of all it is shown that these cells (reversibly) acquire a positive mobility below their isoelectric point with no indication of an inflection point in the mobility-pH curve, down to pH 0.9. Secondly it is found that the mobility increases in absolute value above pH 11.0. It is believed that these new features represent "real" properties of the cell surface; i.e., properties which are present at a physiological pH in the unfixed cells. The identity between the mobility of fixed and unfixed RBC, and the reversibility of the mobility of the fixed RBC are the basis of this belief. In particular, the positive mobility found below pH 1.6 cannot be ascribed to positively charged products of hydrolysis at that pH, as the mobility at pH 7.4 is not affected by exposing the fixed cells to pH 0.9 for 5 min.

The stability in the mobility of the OsO_4-fixed RBC at low pH is accompanied by other equally remarkable features. The fixed cells do not appear to be morphologically altered upon suspension in distilled water, upon dehydration in absolute ethanol, or upon air-drying (from distilled water) on a glass slide. Similarly it has been observed that the fixed cells will not stain appreciably with eosin, even after being boiled for 5 min directly in the flame of a bunsen burner. Unfixed RBC by comparison take on an intense pink color in the eosin solution after incubation in hot (not boiling) water for less than a minute; if boiled they disintegrate completely. In view of the apparent impermeability (to a small dye molecule) and stability under the stresses of low pH, low osmotic pressure, dehydration, and extreme heat, it is perhaps not too far from the truth to say that the OsO_4 has in some way "cemented" together the membrane of the RBC.

The ability of OsO_4-fixed (human) RBC to bind specific antibody has been studied by Bessis et al.[70] They found that the ability to bind specific antibody was unaffected by OsO_4 fixation although agglutination was considerably reduced. This latter fact they ascribed to the rigidity of the fixed cells. The unaltered binding of specific antibody is a very sensitive indication that the structures on the surface of the RBC (at least the binding sites) have not been altered by the OsO_4 treatment. A similar conclusion has already been drawn from the electrophoretic identity of the fixed and unfixed cells.

It is instructive at this point to consider what is known about the chemistry of OsO_4 with biological materials. Unsaturated lipids react quite rapidly with OsO_4 whereas saturated lipids do not.[71] Proteins also react with OsO_4, although often at a considerably slower rate compared with lipids.[72] Carbohydrates do not react at all.[71] The bulk of the chemical evidence suggests that OsO_4 fixes biological materials by reacting with carbon-carbon double bonds to form an addition compound, possibly as a crosslink between molecules. If so, this would help explain why the structure of the RBC is so greatly stabilized by OsO_4 fixation. Similarly the fact that both the antibody-binding structures and the charge-determining structures are

unaffected by OsO_4 fixation is explainable on the basis of the above-quoted chemistry. The blood group antigens are thought to be carbohydrate in character.[73] In addition the evidence is that an acidic carbohydrate (sialic acid) is responsible for a large portion of the net charge on RBC (Subsec. V. B. 1). This last point is discussed in further detail in the paragraphs below.

Upon first consideration Fig. 28(a) looks like the mobility-pH curve of an amphoteric substance that is characterized by both strongly acidic and strongly basic groups. The carboxyl group of sialic acid seems to compose a substantial fraction of the strongly acidic groups. Sialic acid itself apparently accounts for no more than 100% of the net charge at pH 7.4. The net charge will, however, be less than the total charge from all strongly acidic groups, because of the presumed basic component of the cell surface. Thus, referring to Fig. 28(a), there must be a comparable number of strongly acidic groups, A_sH, of a different type. These would be responsible for the continued loss of negative charge as they become neutralized at the extremely low pH's.

The net positive charge that results below pH 1.6 is to be ascribed to the presence of strongly basic groups, B_s, at the outer surface of the RBC. Similarly the greater negative charge (i.e., mobility) above pH 11.0 is to be ascribed to the neutralization of these strongly basic groups. This model is summarized in a schematic fashion in Fig. 30(a).

The above would seem to be the likely interpretation to be drawn from the mobility-pH data had not Heard and Seaman already concluded that the RBC surface was strictly anionic in nature at pH 7.4.[16, 24, 41] Their conclusion implies that this particular interpretation of the mobility-pH curve is incorrect. An alternative interpretation which is in agreement with the anionic hypothesis can be constructed as follows. The positive mobility at very low pH is ascribed to the presence of a very weak base, B_w, at the outer surface. The reaction at low pH would then be

$$B_w + H^+ \rightleftharpoons B_wH^+.$$

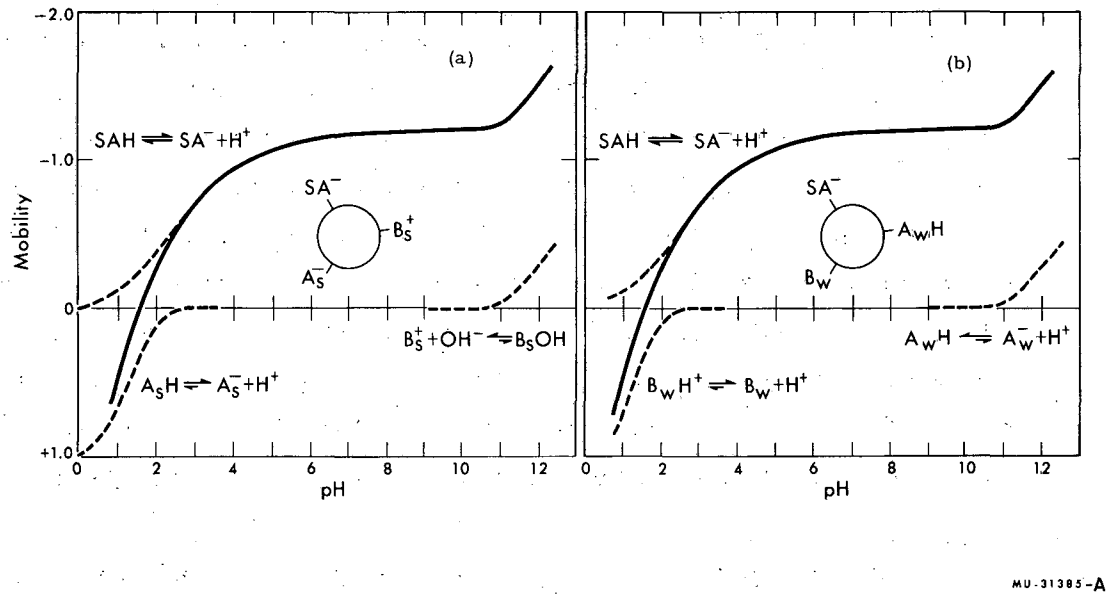

Fig. 30. Schematic representation of the acid-base characteristics of the rat RBC surface. The complete mobility-pH curve is shown as the solid curve, and the dissociation of the various acids and bases is indicated by the dashed curves. Figure (a) indicates the dissociation of sialic acid (SAH), a second strong acid (A_SH), and a strong base (B_S). Figure (b) indicates the dissociation of sialic acid (SAH), a weak base (B_W), and a weak acid (A_WH). The charged state of the groups at pH 7.4 is indicated by the schematic RBC surface in the center of each figure.

Simiarly the larger negative mobility above pH 11.0 would be ascribed to the presence of a very weak acid, A_wH. The reaction at high pH would then be

$$A_wH \rightleftharpoons A_w^- + H^+.$$

This model is summarized in a schematic fashion in Fig. 30(b).

This second interpretation becomes all the more attractive when the structure of sialic acid is taken into careful consideration. In addition to the carboxyl group there is an amide group which is expected to behave as a weak base (Noller, p. 196).[74] Furthermore, any of the hydroxyl groups of this sugar could behave as a weak acid. Glucose, for example, has a pK at 12.0.[75] Therefore sialic acid itself has all the qualitative features necessary to explain the entire mobility-pH curve from pH 0.9 to 12.3. This immediately suggests the possibility that sialic acid alone is responsible for the surface charge of (rat) RBC throughout this entire pH range. It is, however, only a possibility and must not be considered proven as yet. Furthermore, it is not safe to speak of "the RBC" as if RBC of every species were the same. According to the work thus far published[44, 58] there is a considerable species variation with regard to the types of sialic acid present in RBC, and the degree to which the mobility of RBC can be decreased after removal of the sialic acid through incubation with the receptor-destroying enzyme, (RDE). It is not yet clear whether the residual negative mobility after RDE treatment can be ascribed to (a) sialic acid that was not susceptible to the action of the enzyme (b) other anionic groups that were originally present in addition to sialic acid, or (c) anionic groups that are exposed upon the removal of sialic acid.

e. Discussion: Mobility-pH data with $KMnO_4$-fixed cells. It has been shown in Fig. 28(b) that the mobility-pH curve of the $KMnO_4$-fixed rat RBC is quite different from the curve for OsO_4-fixed (and unfixed) RBC. While the two curves are very nearly the same above pH 7.0, the general shapes of the two curves below this point are quite different, and the isoelectric point of the $KMnO_4$-fixed cells is one pH unit higher than that of the OsO_4-fixed cells. It is therefore

concluded that the mobility-pH curve of $KMnO_4$-fixed rat RBC reflects a change in the pK of the anionic groups rather than an increase in the number of cationic groups (at pH 7.4). A suggestion can be made as to what chemical reaction lies behind this apparent change in pK. The $KMnO_4$ reacts with carbohydrate according to the equation (Noller, p. 121)[74]

$$\begin{matrix} RCH-CHR' \\ | \quad | \\ OH \quad OH \end{matrix} + 6\,KMnO_4 \rightarrow 3\,RCOOK + 3\,KOOCR' + 6\,MnO_2 + 6\,H_2O.$$

It is possible that $KMnO_4$ reacts with the carbohydrate at the cell surface in such a way that the carboxyl group of sialic acid is split off, and a second carboxyl group is created to take its place. It must be pointed out, however, that $KMnO_4$ could just as well be reacting with the proteins or the lipids of the cell membrane to accomplish the same result. At this time there is no experimental evidence that might tell us more precisely what the true reaction might be.

f. Discussion: Ionic-strength data. The fact that the mobility-pH curve at ionic strength 0.145 is identical for the unfixed RBC and for the OsO_4-fixed RBC has been interpreted to mean that the two objects are identical with respect to their surface charge. Consequently it may seem surprising to find that the mobilities of the fixed and the unfixed cells vary in a radically different manner with changing ionic strength. On the other hand the mobility–ionic-strength curve for the $KMnO_4$-fixed cells appears to be identical to that of the OsO_4-fixed cells. Since all three types of objects have very nearly the same mobility at ionic strength 0.145 (and pH 7.4) it might be expected that all three would have the same mobility at other ionic strengths (and pH 7.4), the mobility being governed by the equation [derived from Eq. (29)]

$$\mu\eta = \sigma_Q (1/\kappa + a_i), \tag{32}$$

where σ_Q = charge per unit surface area,

η = viscosity,

a_i = radius of the counterion.

Some possible explanations of the difference in the ionic-strength curves (unfixed vs fixed) are as follows.

(a) The unfixed RBC surface may be changing at the lower ionic strengths. This suggestion gains some support from the fact that the isoelectric point of the unfixed RBC increases considerably as the ionic strength decreases. The alternative possibility, that the fixed RBC surface is changing at the lower ionic strengths seems unlikely in view of the stability of these cells and in view of the fact that the RBC fixed by two different methods show the same ionic-strength behavior.

(b) The fixed cells may have a different "electrophoretic" radius than the unfixed RBC, as discussed in some length by Brinton and Lauffer.[6] This would seem to make a convenient explanation. Unfortunately, as previously pointed out, there seems to be no theoretical justification for the use of any radius in the equations of electrophoresis other than the gross radius of the whole particle.

(c) There could be a difference in the penetrability to counterions, as discussed by Haydon.[62] This seems unlikely to be a satisfactory answer as the two curves should be different from each other by a similar factor throughout the entire range of ionic strength.

(d) The conductivity of the fixed cells might be increased to the point where it becomes comparable to that of the surrounding medium at the lower ionic strengths. The more complete Eq. (21), rather than Eq. (22), is necessary to describe the mobility as a function of ionic strength. Using the same relationship between the zeta potential and surface charge as in Eq. (29), one obtains from Eq. (21)

$$\mu\eta = \sigma_Q \left(1/\kappa + a_i\right) \frac{2\sigma}{2\sigma + \sigma'} \tag{33}$$

where

σ = conductivity of the medium, a function of the ionic strength

σ' = conductivity of the particle.

According to this explanation the conductivity of the unfixed RBC is always much less than that of the surrounding medium; therefore, the mobility of the unfixed RBC would always be greater than or equal to the mobility of the fixed RBC. This fourth explanation could be tested by suitable measurements of the high-frequency electrical impedance of these cells.*

g. The emerging picture of the charge-determining structure of the RBC. Furchgott and Ponder[17] were the first to measure what probably corresponds to the true isoelectric point of intact human RBC. The value of 1.7 reported by them was considerably lower than what they found for either the extracted lipid or the extracted protein fractions of the RBC ghost. Low values of the isoelectric point of other mammalian cells have also been reported.[19, 20, 22] The Ehrlich ascites cells studied by Cook, et al.[21] and the liver cells studied by Bangham and Pethica[22] are the only mammalian cells reported to have an isoelectric point above 3.0. As mentioned above, the studies of Heard and Seaman with various monovalent anions[24, 16] and on the effects of aldehyde treatment[41] imply that there are no cationic groups contributing to the net charge of human RBC at pH 7.4.

If the charged groups of either the lipid or the protein are to be responsible for the charge on the surface of RBC, these groups must be ordered in a very special way so that the isoelectric point of the whole is less than that of any of its components taken separately. In addition Heard and Seaman's experiments and the approximate constancy of the mobility between pH 6.0 and 11.0 argue that groups which

---

*It should also be pointed out that the extreme low ionic strengths could have a different effect on mobility. After a period of time this stress may cause the unfixed RBC membrane to become somewhat more permeable. The conductivity of the cell would correspondingly increase and as a result the mobility would decrease. This may in fact be the proper explanation of the irreversible decrease in the mobility with time at low ionic strengths which has been reported for guinea pig RBC[69] and human RBC.[24]

would be positively charged at pH 7.4 and groups with pK' s in the range 6.0 to 11.0 must be effectively prevented from dissociating; i. e., they must be "folded" away in the surface structure.

The alternative explanation is that the lipid and protein of the cell membrane structure play a relatively minor role in the determination of net charge. In this picture they are sufficiently far back from the surface of shear that their counterions move with the cell as a whole and thus are effectively undissociated. The charge on the surface of the RBC must then be dominated by other substances whose dissociable groups have only extremely low and extremely high pK values. The importance of sialic acid in determining the surface charge of human RBC[44, 18] has been discussed in great detail. The suggestion to be made from the present study is that sialic acid may be completely responsible for the normal charge on the surface of RBC. This substance has no cationic groups at pH 7.4, and it has all the acid-base characteristics necessary to explain the entire mobility-pH curve from pH 0.9 to 12.3.

3. Calculations Involving the Electrokinetic Charge, the Surface Area, the Amount of Sialic Acid, and the Total Carbohydrate

The chief purpose of the calculations carried out below is to further test the plausibility of the hypothesis that carbohydrate effectively coats the outermost surface of the RBC (Subsec. V. A. 3), and that the acid-base characteristics of sialic acid are responsible for most of the mobility-pH curve at ionic strength 0.145 (Subsec. V. B. 2). These calculations will be carried out for the particular case of human RBC rather than for rat RBC, for there is no estimate of total sialic acid available for the latter. Furthermore, an estimate of total carbohydrate is available for human RBC ghosts, and this is necessary for these calculations. (A comparison, for the rat RBC, between surface charge density and the amount of sialic acid released by enzymes has been made in Subsec. V. B. 1.)

To begin with, we might consider the surface charge density as calculated by Eq. (29), using the parameters tabulated in Eq. (30). Such a calculation yields

$$\frac{\text{charge}}{\text{area}} = \sigma_Q = \frac{\mu\eta}{(a_i + \frac{1}{\kappa})} = 1.1\times10^{-2}\ \frac{\text{coulomb}}{m^2} = 0.69\times10^{17}\ \frac{\text{charges}}{m^2}, \tag{34}$$

which is equivalent to one elementary charge per 1450 $Å^2$. If we imagine the charges to be arranged in a square lattice, this figure would put them a distance of 38 Å apart.

By comparison Eylar et al. have reported that there are 2.4×10^7 molecules of sialic acid per (human) RBC. For a surface area of 1.6×10^{-10} m^2 (used by them) this amounts to 1.5×10^{17} sialic acid molecules/m^2, which is equivalent to one sialic acid molecule per 670 $Å^2$. Whether this figure, or one half as big, is to be compared with the charge density calculated from the electrophoretic mobility depends upon whether all the sialic acid or only half is distributed over the outer surface of the RBC membrane, (see Subsec. V. B. 1). Alternatively, the electrokinetic equation (34) might give too low a value for the surface charge density (as discussed by Eylar et al.[44]) so that the calculated charge per unit area might really correspond to all the sialic acid molecules being on the outer surface. If this were the case there would be one charge (i. e., one sialic acid molecule) per 670 $Å^2$, thus putting the charges at a distance of 26 Å from one another.

Keeping in mind the figures for the area associated with each charge and/or sialic acid molecule, it is instructive to consider the maximum surface area of sialic acid and its associated sugars. Figure 31 is a photograph of a molecular model of N-acetylneuraminic acid (the most typical sialic acid). The chemical structure of this molecule has been shown in Fig. 21. The pyranose ring backbone of a second sugar molecule is shown attached to the sialic acid by an O-glycosidic bond. Sialic acid itself can assume a shape resembling an equilateral triangle roughly 10 Å on edge, so the maximum area that can be assigned to this molecule is less than 60 $Å^2$. As may be judged from Fig. 31, any associated simple sugars will have somewhat less of a surface area, probably no more than 40 $Å^2$ per sugar molecule.

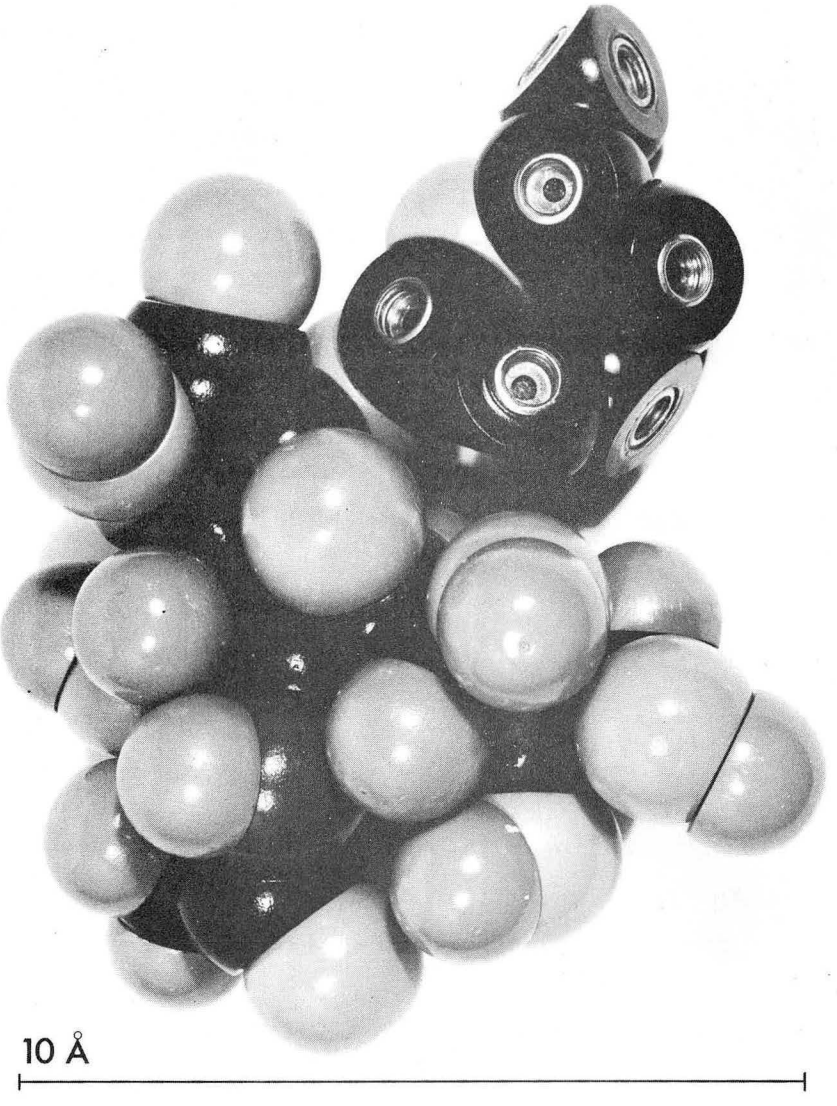

ZN-3869

Fig. 31. A molecular model of N-acetylneuraminic acid. The pyranose ring backbone of a second sugar molecule is shown in the upper right of the photograph.

The maximum possible area covered by the oligosaccharide, of which sialic acid is the terminal sugar, depends upon the total number of sugar molecules involved. From the work with RDE and α-amylase it is known that there are no less than two simple sugars associated with each sialic acid (Subsec. V. B. 1). An upper limit can be established on the basis of the total carbohydrate determinations reported by Ludewig.[76] He found that human RBC stroma (ghosts) were 4.4% by weight carbohydrate, of which about one-fourth by weight was sialic acid. Assuming molecular weights of 309 for sialic acid (NANA) and 180 for the other sugars (e.g., galactose), one obtains the maximum number of simple sugars per molecule of sailic acid from the equation

$$0.25 = \frac{309}{309 + n180} \quad . \tag{35}$$

This calculation gives the result that there cannot be more than five molecules of simple sugar per molecule of sialic acid.

Assigning maximum surface areas of 60 $Å^2$ to sialic acid and 40 $Å^2$ to each remaining simple sugar, one would estimate that the maximum total area covered by the sialic-acid-containing oligosaccharide is between 140 and 260 $Å^2$. These figures are based upon the estimated composition of the oligosaccharide given in the previous paragraph. It should be recalled that division of the total RBC surface area by the total number of sialic acid molecules leads to one such molecule per 670 $Å^2$. Of the total available outer surface area, therefore, at most one-half (actually a little less than one-half) can be covered by the sialic-acid-associated oligosaccharide. If the sialic acid is distributed equally over the inner and the outer surfaces, the ratio of area covered by carbohydrate to total area will be at most one to four. The situation is indicated schematically for a hypothetical segment of the RBC surface in Fig. 32. The figure is meant to indicate one oligosaccharide per 670 $Å^2$; the oligosaccharide (one shaded area) covers roughly one-half of this area. If half of the sialic acid is on the inner surface of the membrane, then there would be one oligosaccharide (stippled area) per 1340 $Å^2$. This latter figure

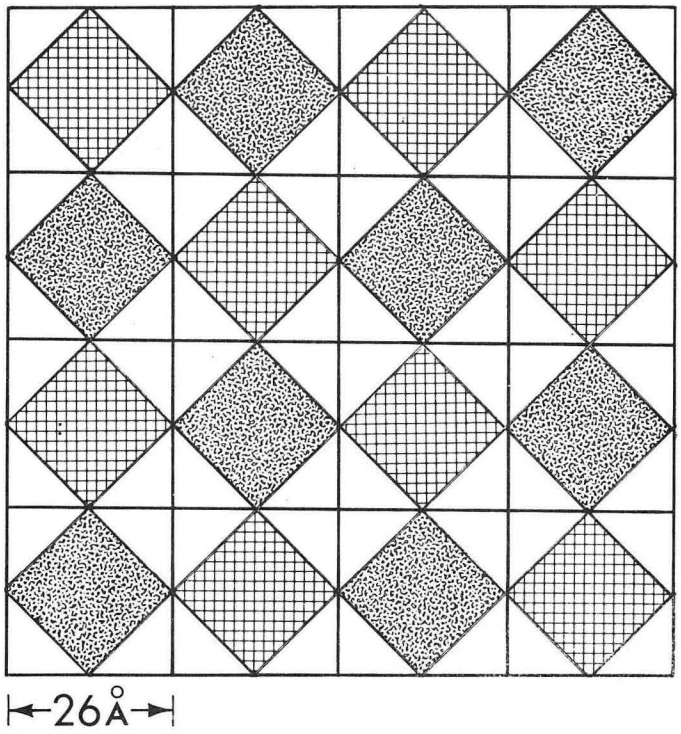

Fig. 32. A schematic representation of the maximum area occupied by carbohydrate compared with the total area of the RBC surface. The shaded areas represent carbohydrate. If the carbohydrate is equally distributed over the inner and the outer surfaces of the RBC membrane, then only the stippled areas are to represent carbohydrate at the outer surface.

corresponds more closely to the number of charges per unit area calculated from the electrokinetic equations.

It is evident from these calculations that even by the most generous estimates it is not possible to say that carbohydrate forms a physical layer or film over the entire surface of the RBC.* Carbohydrate covers at most only half of the surface, and quite possibly only one-fourth of the surface. Nevertheless there appear to be very few functional groups, other than those associated with carbohydrate, that can contribute to the net charge of the RBC. Therefore, from an electrokinetic point of view, carbohydrate does indeed form a complete layer over the RBC surface.

An explanation is called for as to why functional groups other than carbohydrate should not form a part of the electrophoretic surface. One possibility is that the carbohydrate is not flattened out to the maximum extent, as has been assumed, but rather is in (the beginning of) a helical configuration, as in starch. This would have the effect of raising the sialic acid molecule (and its dissociable groups) away from the protein and lipid components. In this way it would be possible for sialic acid to be close to the surface of shear such that most of its counterions would move independently of the cell as a whole. The dissociable groups of the protein and lipid could have their counterions lying within the surface of shear and therefore moving with the cell. While this may all be possible, there is absolutely no direct evidence in support of it.

The calculations carried out in the previous paragraphs have pertained specifically to human RBC. The general nature of the conclusions obtained probably applies to most mammalian cells for

---

*These estimates are of course based upon present experimental data. There is always the possibility that future experiments will show a greater amount of carbohydrate in RBC ghosts so that it could become more feasible to imagine a complete physical layer of carbohydrate over the whole surface.

reasons given below. Unfortunately our inability to obtain pure plasma membranes from tissue cells prevents direct measurements and calculations of the kind that have been made for RBC. Several lines of evidence suggest that the outermost surface of the tissue cells might be rather similar to that of the RBC. First of all, many of them have very low isoelectric points, as do the RBC, and their mobilities generally show no change in the region pH 6.0 to 11.0. Secondly, the mobility of most mammalian cells can be drastically reduced by the removal of sialic acid; i.e., by treatment with RDE. These two factors have been discussed in greater detail in Subsec. V.B.1. Finally, cytochemical and histochemical studies with the light microscope have shown that the cell membrane (plasma membrane) of various tissue cells contains appreciable amounts of carbohydrate.[77,78,79] Therefore it may be said that the available information for most tissue cells is at least consistent with the belief that the outermost surface might be similar to the surface of (human) RBC, with respect to carbohydrate composition.

C. Electron Microscope Study of the Surface Ultrastructure (RBC)

a. Introduction. In the experiments described below, the electron microscope has been used to examine very small structures at the cell surface. Before discussing these experiments it seems appropriate to go into some of the limitations on how small a structure can be seen by this method. The microscope used in this study was a Hitachi HU-11, which has a practical limit of resolution of less than 8 Å. In order to resolve structures having dimensions this small, however, it is necessary that the specimen have sufficient contrast (i.e., difference in electron density). Unfortunately biological structures are not very "contrasty," and so methods must be used to enhance their contrast. The usual method in examining surface structure is to evaporate metal (in a vacuum) at an angle to the surface, and thus to achieve a shadowing of the surface structure. This technique limits the achievable resolution to approximately 20 Å, because the

evaporated metal condenses in grains of about this size. A final limitation on the size of the structures that can be seen stems from the probability that the significance of any structure whose largest dimension is less than 50 Å is usually questionable, unless the structure occurs in something like a repeating lattice.

A relatively small amount of work has already been reported, in which the electron microscope has been used to investigate surface structures with dimensions on the order of 100 Å. In 1953 Hillier and Hoffman described a technique in which RBC ghosts were prepared by osmotic shock, exposed to 0.1% phosphotungstic acid for about 3 min, washed in distilled water, air-dried on a collodion film, and shadow-cast with chromium.[80] Hoffman has subsequently discussed degree of variability in the resulting pictures. This seems to be as great for fresh blood taken from the same individual on different days as it is for blood taken from different individuals on the same day.[81] The surface of human RBC ghosts prepared in this way was found to have a "pebbly" or granular structure, the diameter of the granules being most commonly on the order of 100 to 200 Å, but occasionally running up to 500 Å. Similar structures were seen on the surface of ghosts prepared from mouse, pig, and camel blood. Hillier and Hoffman interpreted this granular structure in terms of "plaques," which they assumed were lying at the surface of the cell. They also reported seeing in unshadowed specimens an underlying tangential network of fibers 20 Å in diameter and 200 Å in length. I have never been able to see this feature in the published reproductions of their photographs.

The granular or pebbly nature of the RBC surface has been observed by a second method in which the surface of an intact RBC is shadow-cast with metal, the film so formed is stabilized with a second film of carbon evaporated uniformly over the surface, and the metal-carbon replica so formed is separated from the cell by mechanical stripping or by NaOH digestion of the organic material.[82,83] This method appears superior to that of Hillier and Hoffman for two reasons. First of all, the replica technique demonstrates true surface contours, whereas the structures seen in metal-shadowed ghosts could

be (a) surface contours, (b) variations in the electron density throughout the entire thickness of the ghost, or (c) a combination of both. The heavier the metal-shadowing, of course, the more the surface contours will dominate. It seems likely to me that much of the variability that was seen by Hoffman[81] can be ascribed to variations in the thickness of the metal-shadowing. A second disadvantage of Hillier and Hoffman's method is that one cannot be certain that the structure of the ghost is identical to that of the intact RBC, as has been thoroughly discussed by Ponder.[84] Furthermore, Finean has reported evidence to suggest that the lipid and protein components may undergo some rearrangement if the ghost is air-dried after no fixation, or after fixation with phosphotungstic acid.

The replica technique described in the paragraph above has been used by Coman and Anderson on OsO_4-fixed, air-dried mouse RBC[82] (although most of their work has been with tissue cells). They have shown a picture of the surface of a RBC which bears a striking resemblance to that seen by Hillier and Hoffman.[80] Haggis has also used the replica technique to show a similar surface structure ("cobblestones"). He believes this represents the structure of human RBC that had been rapidly frozen in 20% glycerol solutions.[83]

b. Methods and Results. I have employed two techniques for specimen preparation. In the first technique ghosts were made from (rat) RBC by hypotonic shock and washed twice in distilled water. A suspension of these ghosts in distilled water was then aspirated onto formvar* films (mounted on electron-microscope specimen grids) that were kept at the temperature of dry ice. The glass slides upon which these grids were mounted were then placed upon a metal heat sink (also chilled to dry-ice temperature) inside a small lyophilization apparatus, and the specimen was fixed by freeze-drying. The specimen was finally shadow-cast with chromium. It was not exposed to phosphotungstic acid nor was it air-dried, so that some criticisms mentioned previously do not apply in this case.

The most typical result obtained is shown in Fig. 33(a). The frozen dried ghosts retain their spherical shape and cast a long

*Shawinigan Resins Corp., Springfield 1, Mass.

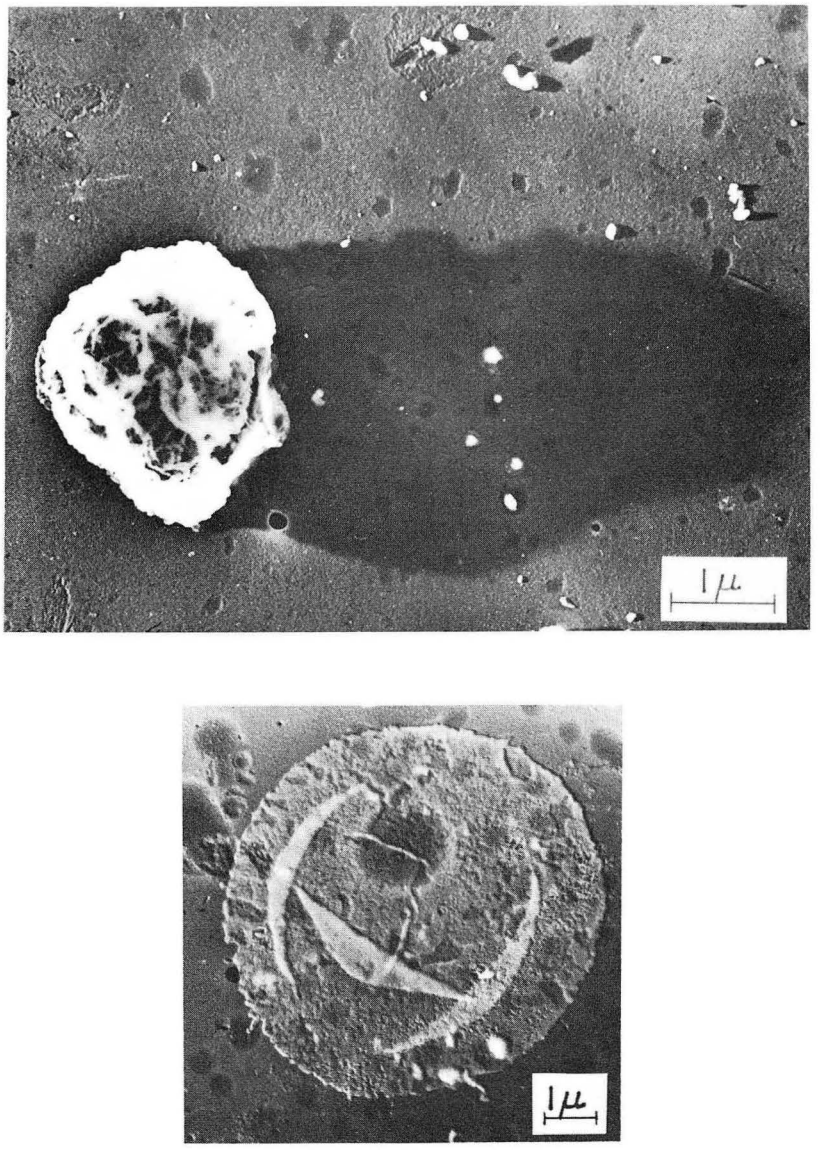

ZN-3872

Fig. 33. Electron micrographs of rat RBC ghosts prepared by hemolysis of RBC in distilled water. Figure (a) shows a typical ghost after freeze-drying while Fig. (b) shows a typical ghost after air-drying. Chromium shadowed.

shadow after chromium has been evaporated obliquely to the surface. An example is also shown in Fig. 33(b) of air-dried and shadowed ghosts. This demonstrates that the freeze-drying procedure has preserved the original three-dimensional character to a far greater extent than has the air-drying—a fact which has long been known to electron microscopists. In most instances it was not possible to observe any surface structures in the frozen-dried ghosts because of the curvature of the surface. In some instances, however, the RBC ghost was torn, and upon lyophylization this "single membrane" would lie flat on the formvar film. An extreme instance in which this occurred is shown in Fig. 34. Once again it is shown that the surface has a very pebbly or granular structure. In this case the diameter of the bumps is on the order of 400 Å. Both the species of animal used and the method of specimen preparation may account for the discrepancy, in the observed granule size, between this result and that of others mentioned above. The electron-dense spots in this picture can be seen from their corresponding long shadows to be regions in which the material of this single membrane is standing on edge, perhaps due to folds that were made in the free-floating membrane.*

Although this surface structure of frozen-dried ghosts was in good qualitative agreement with the structures seen by others, this method of sample preparation did not seem suitable for use in correlative microelectrophoresis studies. The primary reason for this judgment was the fact that the very low ionic strengths required for this sample preparation are known to produce irreversible alterations in the electrophoretic mobility—and so presumably in the surface structure. Consequently it seemed desirable to use a technique of sample preparation that involved chemical fixation prior to exposure of the specimen to low ionic strength. It was shown in Subsec. V. B. 2 that the OsO_4-fixed rat RBC is electrokinetically identical to the

---

*All pictures are printed so that the lightest regions represent highest electron density.

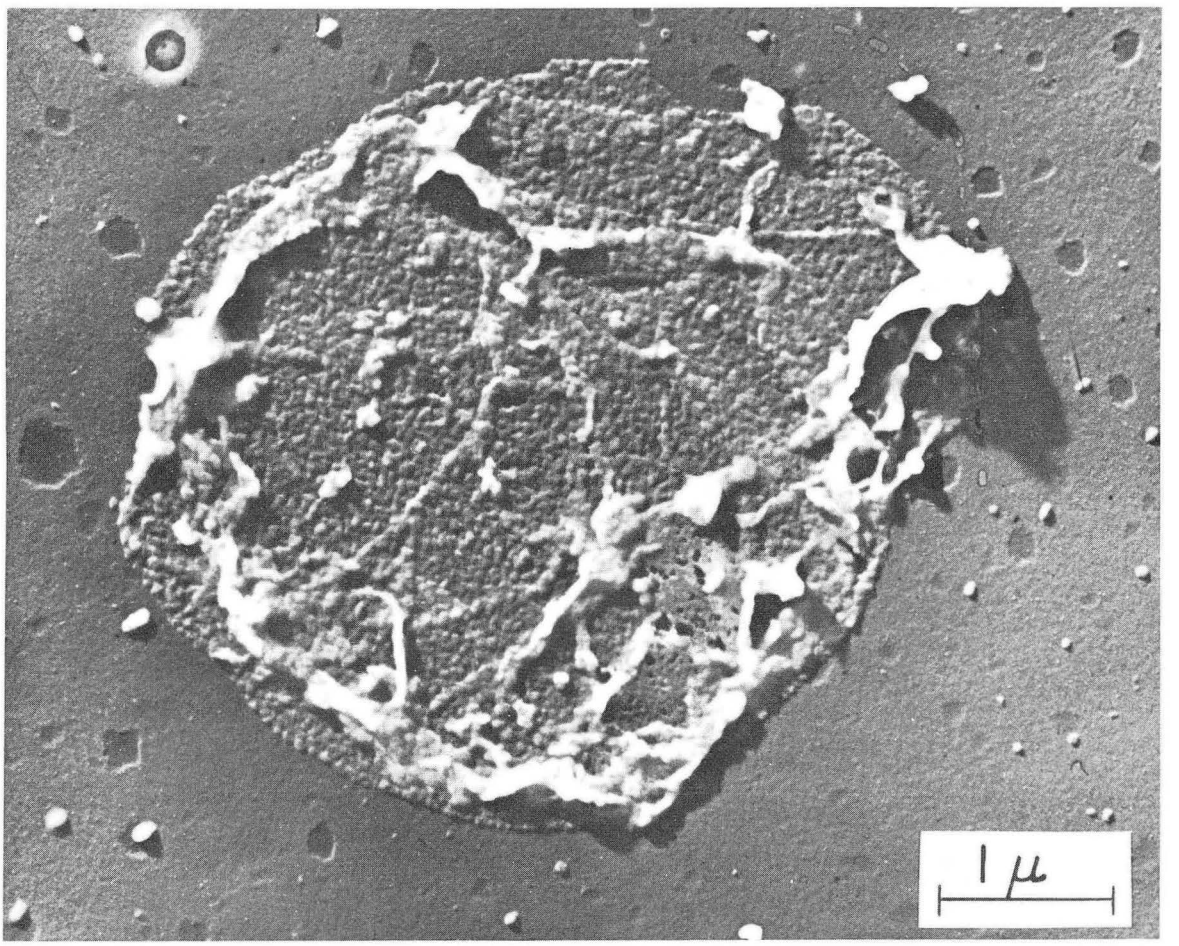

ZN-3873

Fig. 34. An extreme example of the pebbly or granular structure that may be seen in freeze-dried RBC ghosts when a single membrane lies fairly flat on the formvar film. Chromium shadowed.

unfixed RBC at ionic strength 0.145, and that exposure of the fixed cell either to distilled water or to ethanol does not affect its mobility. So it seemed likely that the surface structure of the OsO_4-fixed RBC would be the same as that of the unfixed cell. In addition it probably would not be altered by the methods used to prepare samples for electron microscopy.

A replica technique must be used to examine the surface structure of the OsO_4-fixed RBC, as it is not possible to make ghosts from these objects by osmotic shock. The procedure used was as follows. The rat RBC were fixed as described in Subsec. V. B. 2, and the fixed cells were washed twice in 100 volumes of distilled water. The fixed cells were suspended in distilled water at concentrations varying between 0.1 to 1.0% vol/vol. The suspension was aspirated onto prechilled glass slides, and the specimen was frozen-dried as described above. Carbon was then evaporated at an angle of 90 deg to the surface of the slide in order to deposit a uniform film over the surface.* This carbon film was floated off the glass slide onto 0.145 M NaOH and the organic material was digested for various lengths of time at room temperature. The carbon film was then picked up from underneath with a glass slide; the excess NaOH wiped off the glass slide with a tissue paper; and the carbon film floated off, onto the surface of distilled water, so that the NaOH would be removed (by dilution). Small segments of the carbon film were then picked up from underneath with a stainless steel electron-microscope specimen grid.

When these specimens were examined without metal-shadowing it became obvious that, in general, not all of the organic material was removed by the NaOH hydrolysis. Apparently the layer of OsO_4-fixed material adjacent to the carbon film is very resistant to the relatively mild alkaline hydrolysis used in these experiments. Stonger alkali

---

*The surface was not preshadowed with chromium. Instead, the plan was to develop contrast in the replica itself either by negative staining with phosphotungstic acid or by metal-shadowing.

solutions were not used as it became very difficult to float the carbon film off the glass onto these solutions.

In some instances, especially when hydrolysis had been allowed to proceed for only a few hours, two very interesting structures were seen in the residual organic material. The first of these was a pebbly structure strongly resembling that described above. In addition, the appearance of a number of "pebbles" suggested the form of looped ends of yarn or rope. This pebbly structure is shown in Fig. 35. The diameter of the bumps is on the order of 400 Å. The second type of structure had the appearance of a tangled mass of "yarn" or "rope." An example is shown in Fig. 36. In this figure a few bumps also remain, and in some instances the rope can be seen to be looped, as if partially forming such a bump. The diameter of the rope is about 200 Å, and appears to be remarkably constant in these pictures. Figure 37 is another example in which both the pebbly structure and the tangled-rope structure can be seen.

It would be attractive to think that the bumps seen in some photographs correspond to the rope seen in others, in that the bumps are made up of looped-over rope. It is imagined that the more ordered "looped" structure is the original one, and that the "rope" untangles upon prolonged exposure to the 0.145 M NaOH. It would also be attractive to think that the bumps attached to the carbon film correspond to the bumps seen in the frozen-dried ghosts and in the work of others mentioned previously. It must of course be remembered that the organic material attached to the carbon film has been exposed to some very traumatic solution conditions and might very well bear no relationship whatever to the original surface structure of the intact RBC.

D. A New Model for the Cell Membrane: Lipoprotein "Yarn" with Carbohydrate "Caps"

Let us now put together the various results and conclusions obtained in this study of surface charge and other surface properties. If we mix these with a judicious amount of speculation it is possible to come up with a model of the structure of the cell membrane. The

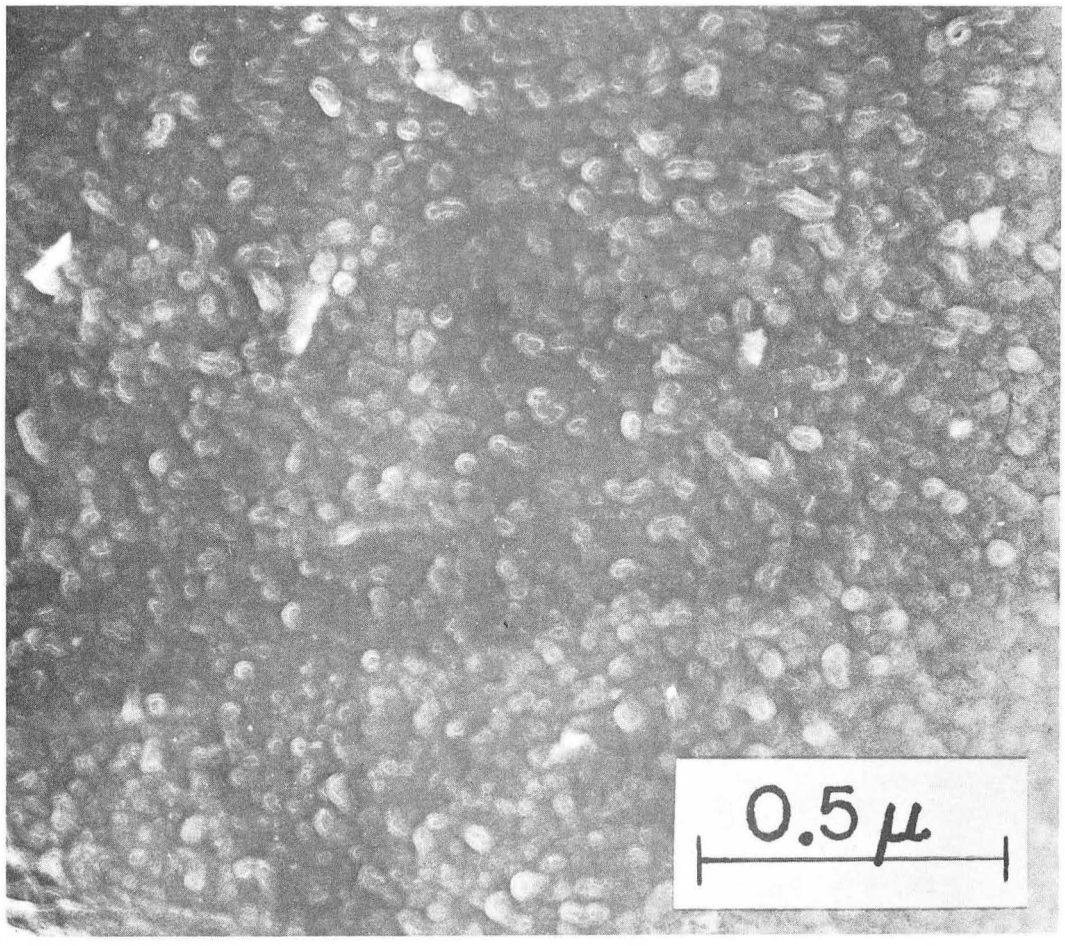

ZN-3874

Fig. 35. An electron micrograph of a carbon replica of the OsO_4-fixed, frozen-dried rat RBC surface showing undigested material. In this case the material is in the "looped" configuration. Unshadowed.

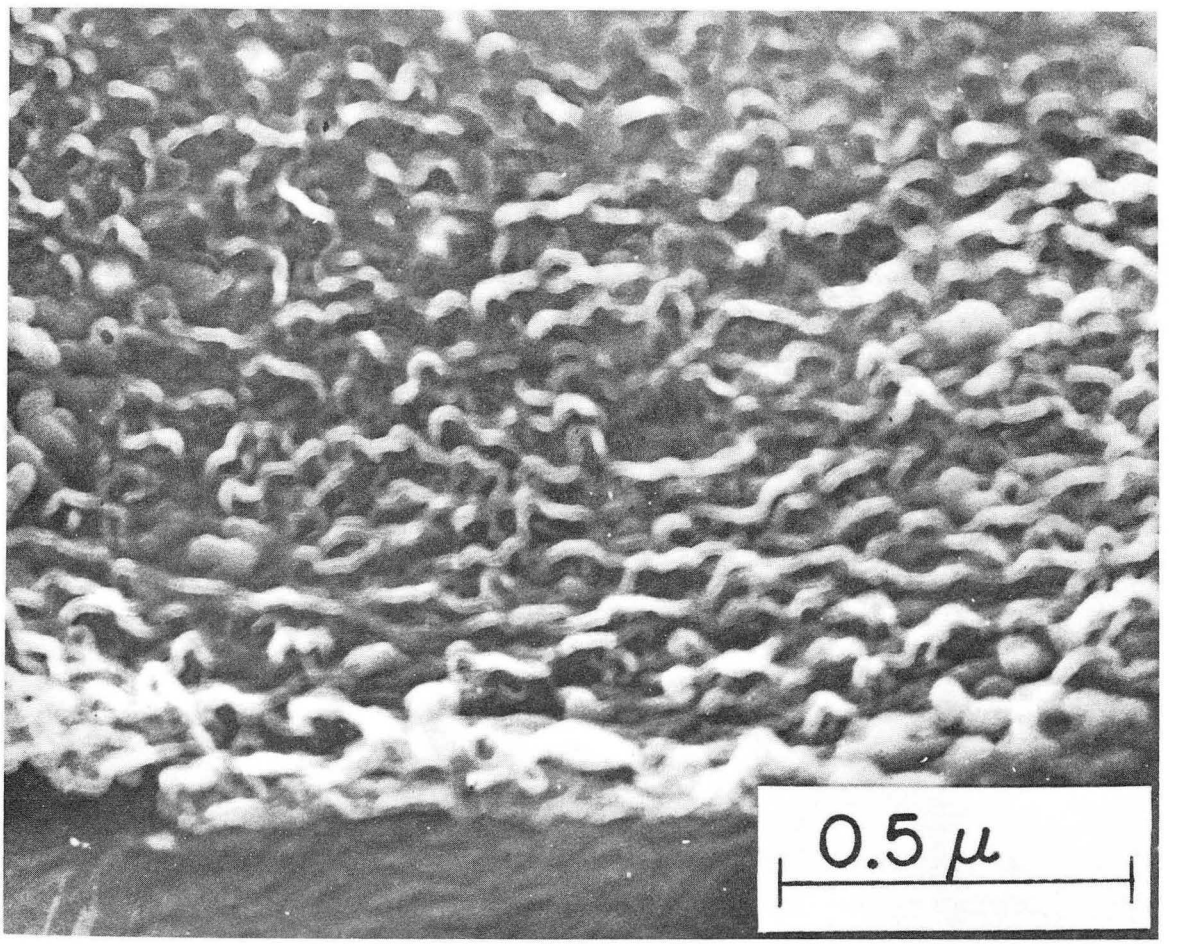

ZN-3875

Fig. 36. An electron micrograph of a carbon replica of the OsO_4-fixed, frozen-dried rat RBC surface showing undigested organic material. In this case the material is mostly in the "tangled" configuration. Unshadowed.

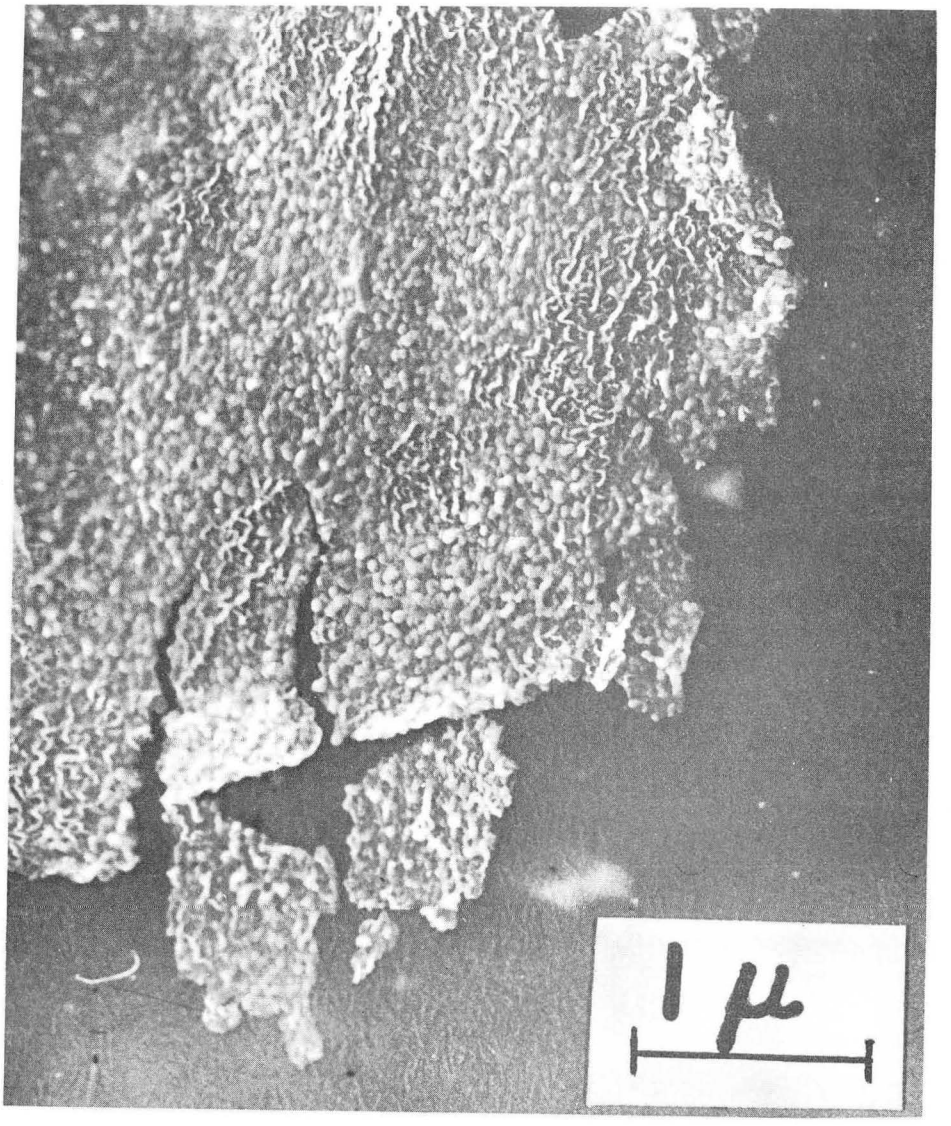

ZN-3876

Fig. 37. An electron micrograph of a carbon replica of the OsO_4-fixed, frozen-dried rat RBC surface showing undigested material. In this case the material is about equally in the "looped" and in the "tangled" configuration. Unshadowed.

concoction so obtained hardly contains enough substance to be dished up as the main course; rather, coming at the end of this paper, it is something of a dessert.

This model must only be considered as a picture consistent with the various results obtained in this study. In some instances the interpretations and conclusions presented below are preliminary in nature. (This is particularly true with regard to the results obtained in the electron microscope studies.) The eventual piecing together of a well-documented knowledge of the structure of the cell membrane is still a task for the future. Bearing this in mind, the model described below is intended both to summarize the results thus far obtained and to define certain interesting possibilities for future research.

The proposed model of the cell membrane has two major features. First the lipid and the protein components of the membrane are imagined to be combined in the form of very long strands, thus forming the "yarn" or "rope" as shown in Figs. 35, 36, and 37. This yarn is imagined to be looped back and forth like the nap of a hooked rug. For this reason the surface of the cell membrane should have a pebbly or bumpy appearance in its natural state.

The second feature of the model is that carbohydrate is deposited at the surface of the membrane structure in a manner described below. It may exist exclusively on the outermost portion of the cell membrane, or it may be distributed approximately equally on both the inner and the outer surfaces. (I prefer the latter hypothesis as it offers a simple explanation (a) for the factor of two in the ratio of "experimental" to "theoretical" amounts of sialic acid released after RDE treatment and (b) for the slope of two in the straight-line relationship between mobility and amount of sialic acid per unit area of the surface.) It is further imagined that the outer carbohydrate takes the form of a "cap" at the very top of the loop in the lipoprotein yarn. In this way it would be nearest to the surface of shear, and would be most effective in dominating the electrophoretic behavior of the intact cell.

A rather simple mechanism for elaborating new membrane is suggested by this model. The first step in the production of new

membrane material becomes the manufacture of more lipoprotein yarn.[68] The yarn could easily be constructed so that it would naturally assume the looped configuration as it was incorporated into the membrane. This means that something would have to be built into the yarn at periodic intervals (corresponding to the thickness of the membrane) that would cause the yarn to loop over.

Conceivably this is the role played by the sialic-acid-associated oligosaccharide in cell physiology. It is indeed a well-established fact that carbohydrate stabilizes the structure of proteins, for the mucoproteins generally are not heat-precipitable, and carbohydrates can prevent the surface denaturation of proteins.[85] So too it may be that carbohydrate serves to stabilize the lipoprotein yarn in the looped configuration. In this connection it is interesting to point out that the area of a circle 400 Å in diameter (the typical diameter of a loop) is 1260×10^2 Å^2. Since there would be one oligosaccharide per 1340 Å^2 (i.e., sialic acid distributed equally over both surfaces of the membrane), one would conclude that there are about 90 to 95 oligosaccharide "molecules" per loop-top.

A few comments may be made about the permeability properties of this proposed surface structure. Transport across the membrane would proceed between neighboring strands of the looped yarn. The surface of these strands should have both a lipid and a protein character. This would serve to explain the relationship between permeability and lipid solubility (see Scheer, page 118).[11] Regarding "facilitated transport"[86] (i.e., enzymatically catalized transport) one would imagine that the various enzymes (permeases) or carriers would be located along the surface of, or as an integral part of, the strands. In this connection the many carrier models ("rotators," "shuttle buses," etc.) become much simpler to visualize than in the case of the Davson-Danielli model of the cell membrane. Finally, this model offers a mechanism, other than phagocytosis, by which large molecules could be transported across the cell membrane. The alternative suggested by this model is that the flexible yarn could twist and give way[68] as the large molecule either diffused through, or was actively "passed" through via a carrier-type mechanism.

These last few comments on mechanisms for elaborating new surface and on the permeability properties do not, of course, support the model proposed above. They merely show that the model could be consistent with a few "biological" requirements. And that is the best that can be done at this time.

ACKNOWLEDGMENTS

I wish to express my deepest thanks to the members of my thesis committee, Professor Howard Mel, Professor Cornelius Tobias, and Professor Daniel Mazia, for the helpful suggestions, advice, and encouragement given to me. Their assistance has greatly enhanced the development of the research reported in this paper.

Thanks are also due: to Professor Thomas Hayes both for instruction in the use of the electron microscope and for valuable discussions regarding the results obtained in that phase of the work, to Mr. Paul Todd for supplying HeLa cells used in part of this study, to Mr. David Allen Zelman for valuable technical assistance with the chemical assays, and to many others too numerous to mention for instruction in various techniques used in this study.

This research was performed under the auspices of the Atomic Energy Commission; the use of facilities provided in Donner Laboratory is gratefully acknowledged.

NOTATION

Greek Symbols

$\Gamma/2$ = ionic strength

ζ = electrokinetic or zeta potential

η = coefficient of viscosity

κ = Debye-Huckel constant

$\lambda = \frac{\sigma - \sigma'}{2\sigma + \sigma'}$; see below for definition of σ and σ'

μ = mobility = velocity per unit field strength

$\xi = \frac{\partial \Psi}{\partial r} + \lambda a^3 r \int_{\infty}^{r} \frac{1}{r^4} \vec{\nabla} \cdot \vec{\nabla} \Psi \, dr$;
a is the radius of the colloidal particle; see below for the definition of Ψ

ρ = volume charge density

σ' = bulk electrical conductivity of a colloidal particle

σ = bulk electrical conductivity of the medium in which the particle is suspended

σ_Q = charge per unit area of a colloidal particle

Φ = electric potential associated with an applied electric field

Ψ = electric potential associated with the charge on a particle

Other Symbols

$\underline{1}$ = unit tensor

a = radius of a colloidal particle

$b = \frac{g}{K} \frac{dK}{dg}$; see below for definition of g and K

E_0 = magnitude of the applied field

$\vec{F}_{direct}$ = direct force exerted on a charged particle by the applied electric field

$\vec{E}_{in}, \vec{E}_{out}$ = the applied electric field inside and outside a sphere of radius "a"

$\vec{E}_Q$ = the electric field associated with a charge, Q, on a sphere

$\vec{F}, \vec{G}$ = symbols used to denote force per unit volume

g = mass per unit volume

$\vec{j}$ = electric current per unit area

K = dielectric constant

$m\mu$ = millimicrons

$\hat{n}$ = unit vector normal to the surface of the colloidal particle

$\underset{\sim}{P}$ = the portion of the mechanical stress tensor (see below) associated with the velocity gradients in the fluid flow

p = hydrostatic pressure

Q = net charge on the colloidal particle

$\underset{\sim}{T}_{mech}$ = mechanical (i.e., hydrodynamic) stress tensor

$\underset{\sim}{T}_{elec}$ = (electrical) Maxwell stress tensor

Abbreviations

NANA = N-acetylneuraminic acid

O.D. = optical density

RBC = red blood cells (erythrocytes)

RDE = receptor-destroying enzyme

Unusual Words

oligosaccharide = a complex (polymerized) carbohydrate consisting of two or more monomer units (simple sugars)

sialic acid = an acidic amino sugar; see structure in Fig. 21

Standard Buffer = 3×10^{-4} M $NaHCO_3$ in 0.145 M NaCl

Miscellaneous

$\vec{}$ denotes a vector, $\hat{}$ denotes a unit vector, and $\underset{\sim}{}$ denotes a tensor

APPENDICES

A. The CGS System of Units

The cgs system of units has been employed throughout Sec. I of this thesis. A comparison of the electrostatic equations in the cgs system and in the MKS system may be found in Joos, p. 267.[4] The fundamental equations used in this report were

$$\left.\begin{aligned} \oint \vec{E} \cdot d\vec{S} &= \frac{4\pi}{K} Q, \\ \vec{\nabla} \cdot \vec{E} &= \frac{4\pi}{K} \rho, \end{aligned}\right\} \quad \text{(A-1)}$$

which apply only to the cgs system.

Coulomb's law states that the mutual force exerted by two charges Q_1 and Q_2 separated a distance r in a medium with dielectric constant K is given by

$$|\vec{F}| = \gamma \frac{Q_1 Q_2}{4\pi K r^2}. \quad \text{(A-2)}$$

In the cgs system, $\gamma = 4\pi$. The charge is measured in electrostatic units (esu), the distance in centimeters, the force in dynes, and the dielectric constant is dimensionless. In the MKS system (used in Sec. II of this report), $\gamma = 1/\epsilon_0$, where ϵ_0 is called the <u>permittivity of free space</u>. Here the charge is measured in coulombs (i.e., ampere-sec), the distance in meters, the force in newtons, $\epsilon_0 = 8.86 \times 10^{-12}$ amp-sec/meter-volt, and K is again dimensionless.

It sometimes happens that the permittivity of free space is suppressed when Coulomb's law is written in the MKS system of units. The equation is then written as

$$|\vec{F}| = \frac{Q_1 Q_2}{4\pi K r^2}. \quad \text{(A-3)}$$

When this occurs it must be remembered that the dielectric constant differs from that used in the cgs system by a factor 8.86×10^{-12} and has units amp-sec/meter-volt. For this reason it is probably best to carry along the factor ϵ_0 in the MKS equation. If the factor ϵ_0 is <u>not</u> suppressed, the dielectric constant will be identical in both systems of units.

B. The Solution of Laplace's Equation in Henry's Electrophoresis Problem

The purpose of this appendix is to derive what the electric field will be everywhere in and around a spherical particle of conductivity σ', which is immersed in an infinite medium of conductivity σ, when a homogeneous electric field is applied to the system. In the steady state, it must be true that the current normal to the surface of the sphere is the same inside as out, for the surface of the sphere cannot act as a source or sink of electric charge. On the other hand, if $\sigma' \neq \sigma$ the component of the electric field normal to the surface must be different inside than it is outside. This says that charges have initially accumulated at the surface; the amount of this surface charge is given by (Joos, p. 267)[4]

$$\hat{n} \cdot (\vec{E}_{out} - \vec{E}_{in}) = \frac{4\pi}{K} \sigma_Q , \qquad \text{(B-1)}$$

where

$\hat{n}$ = unit vector normal to the surface,

σ_Q = surface-charge density.

This surface charge will produce a distortion of the electric field near the spherical particle. In order to determine what the electric field will be everywhere, it is necessary to solve Laplace's equation

$$\nabla^2 \Phi = 0 \qquad \text{(B-2)}$$

for the potential, Φ, associated with the applied electric field. Given the potential, it is possible to calculate the electric field from the equation

$$\vec{E} = -\vec{\nabla}\Phi. \tag{B-3}$$

In this problem, it is most convenient to solve Laplace's equation in spherical coordinates. This coordinate system is illustrated in Fig. 38. From Panofsky and Phillips (p. 76 ff),[5] the general solution of Laplace's equation inside and outside the sphere is given by

$$\left.\begin{aligned} \Phi_{inside} &= \sum_{n=0}^{\infty} A_n r^n P_n(\cos\theta), \\ \Phi_{outside} &= \sum_{n=0}^{\infty} B_n r^{-n-1} P_n(\cos\theta) - E_0 r P_1(\cos\theta), \end{aligned}\right\} \tag{B-4}$$

where

r, θ, ϕ = spherical coordinates of a point in space,
E_0 = magnitude of the applied field, infinitely far away,
$P_n(\cos\theta)$ = the Legendre polynomial of order n,
A_n, B_n = constants to be determined from the boundary conditions,

provided that the solution has no ϕ dependence. This condition will be satisfied if the coordinate system is so oriented that the electric field infinitely far away satisfies the equation $\vec{E} = E_0 \hat{z}$, as may be seen from symmetry arguments.

The value of the constants A_n and B_n can be determined from two sets of boundary conditions: for $r = \infty$, $\nabla\Phi = E_0 \hat{z}$; for $r = a$ (radius of sphere),

$$\sigma \left| \hat{n} \cdot \vec{E}_{out} \right| = \sigma' \left| \hat{n} \cdot \vec{E}_{in} \right| \tag{B-5a}$$

$$\text{(i.e., } \left| \hat{n} \cdot \vec{j}_{out} \right| = \left| \hat{n} \cdot \vec{j}_{in} \right| \text{)},$$

$$\Phi_{out} = \Phi_{in}. \tag{B-5b}$$

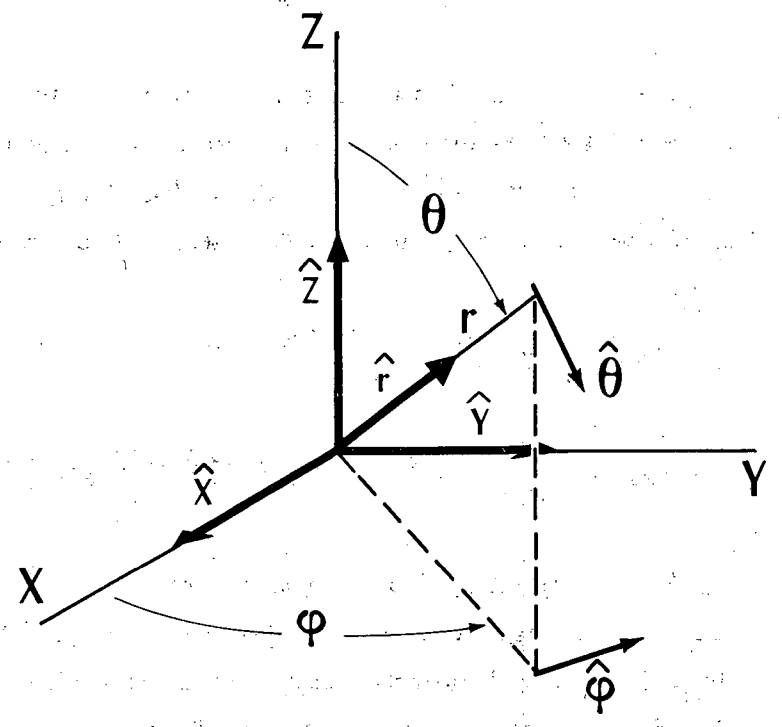

Fig. 38. Relation of spherical to cartesian coordinates. A caret over a coordinate letter indicates a unit vector.

Since the boundary conditions must hold for all values of the angle θ, the coefficients of P_n must be equal for all n. It follows from this that

$$A_n = B_n = 0, \tag{B-6}$$

for $n \neq 1$, while for $n = 1$,

$$A_1 = -2\, a^{-3} B_1 \sigma \quad - E_0 \sigma, \tag{B-7a}$$

$$A_1 a = B_1 a^{-2} \quad - E_0 a. \tag{B-7b}$$

Equations (B-7) can be solved for A_1 and B_1 to give

$$\left.\begin{aligned} A_1 &= -(1+\lambda) E_0, \\ B_1 &= -\lambda E_0 a^3, \\ \lambda &= \frac{\sigma - \sigma'}{2\sigma + \sigma'}. \end{aligned}\right\} \tag{B-8}$$

From the result obtained in Eqs. (B-4) and (B-8), it follows that the potential everywhere is given by

$$\left.\begin{aligned} \Phi_{\text{inside}} &= -E_0(1+\lambda)\, r \cos\theta, \\ \Phi_{\text{outside}} &= -E_0\left(r + \lambda \frac{a^3}{r^2}\right) \cos\theta. \end{aligned}\right\} \tag{B-9}$$

The electric field everywhere is obtained from Eq. (B-3) and is given by

$$\left.\begin{aligned} E_{\text{inside}} &= \hat{r}\, E_0(1+\lambda) \cos\theta - \hat{\theta} E_0(1+\lambda) \sin\theta, \\ E_{\text{outside}} &= \hat{r}\, E_0\left(1 - 2\lambda \frac{a^3}{r^3}\right) \cos\theta - \hat{\theta} E_0\left(1 + \lambda \frac{a^3}{r^3}\right) \sin\theta. \end{aligned}\right\} \tag{B-10}$$

C. Calculation of the Mechanical (Hydrodynamic) Force in Henry's Electrophoresis Problem

The purpose of this appendix is to calculate the integral

$$\vec{F}_{mech} = \oint_{\substack{\text{sphere of} \\ \text{radius a}}} \underset{\sim}{T}_{mech} \cdot d\vec{S}, \tag{C-1}$$

where the mechanical stress tensor is defined by

$$\begin{aligned} \underset{\sim}{T}_{mech} &= \underset{\sim}{P} - \underset{\sim}{1}\, p \\ P_{ij} &= \eta(\nabla_i v_j + \nabla_j v_i) \end{aligned} \tag{C-2}$$

when the pressure p and the velocity $\vec{v}$ are as given according to Eq. (7) in Sec. I. It may be seen that

$$\left.\begin{aligned} \nabla_r v_r\Big|_a &= \cos\theta \,\frac{KE_0}{6\pi\eta}\left(\frac{\partial}{\partial r}\int_{\infty}^{r} \xi\, dr\Big|_a - \frac{1}{a^3}\frac{\partial}{\partial r}\int_a^r r^3 \xi\, dr\Big|_a\right), \\ \nabla_r v_\theta\Big|_a &= \sin\theta\left[\frac{3U}{2a} - \frac{KE_0}{4\pi\eta a}\int_{\infty}^{a}\xi\, dr - \frac{KE_0}{6\pi\eta}\left(\frac{\partial}{\partial r}\int_{\infty}^{r}\xi\, dr\Big|_a\right.\right. \\ &\qquad \left.\left. + \frac{1}{2a^3}\frac{\partial}{\partial r}\int_a^r r^3\xi\, dr\Big|_a\right)\right], \\ \nabla_r v_\phi\Big|_a &= 0, \\ \nabla_\theta v_r\Big|_a &= \nabla_\theta v_\theta\Big|_a = \nabla_\theta v_\phi\Big|_a = 0, \\ \nabla_\phi v_r\Big|_a &= \nabla_\phi v_\theta\Big|_a = \nabla_\phi v_\phi\Big|_a = 0. \end{aligned}\right\} \tag{C-3}$$

Then if the substitutions

$$\left.\begin{aligned} &\frac{\partial}{\partial r}\int_{\infty}^{r}\xi\,dr\Big|_{a} = \xi(a) \\ \text{and}\quad &\frac{1}{a^3}\frac{\partial}{\partial r}\int_{a}^{r} r^3\,\xi\,dr\Big|_{a} = \xi(a) \end{aligned}\right\} \quad (C\text{-}4)$$

are made in Eq. (C-3), one obtains the following equation for the mechanical (hydrodynamic) stress tensor:

$$\left.\begin{aligned} \underset{\sim}{T}_{mech}\Big|_{a} &= \eta \sum_{i=r,\theta,\phi}\ \sum_{j=r,\theta,\phi} \hat{i}\hat{j}\,(\nabla_i v_j + \nabla_j v_i)\Big|_{a} - \underset{\sim}{1}\,p\Big|_{a} \\ &= \eta(\hat{r}\hat{\theta}+\hat{\theta}\hat{r})\sin\theta\left[\frac{3U}{2a} - \frac{KE_0}{4\pi a\eta}\int_{\infty}^{a}\xi\,dr\right. \\ &\left. - \frac{KE_0}{4\pi\eta}\,\xi(a)\right] - \underset{\sim}{1}\left\{\int_{\infty}^{a} -\frac{K}{4\pi}\nabla^2\Psi\,\frac{\partial\Psi}{\partial r}\,dr\right. \\ &\left. + \cos\theta\left[\frac{3\eta}{2a}\,U - \frac{1}{a}\,\frac{KE_0}{4\pi}\int_{\infty}^{a}\xi\,dr - \frac{KE_0}{4\pi}\left(3\frac{\partial\Psi}{\partial r} - 2\xi\right)\right]\right\}. \end{aligned}\right\} \quad (C\text{-}5)$$

When the following identities are employed,

$$\left.\begin{aligned} &\underset{\sim}{T}_{mech}\cdot\vec{dS} = \underset{\sim}{T}_{mech}\cdot\hat{r}\;dS, \\ &(\hat{r}\hat{\theta}+\hat{\theta}\hat{r})\cdot\vec{dS} = \hat{\theta}\;dS, \\ &\underset{\sim}{1}\cdot\vec{dS} = \hat{r}\;dS, \end{aligned}\right\} \quad (C\text{-}6)$$

one obtains the expression for the mechanical (hydrodynamic) force

$$\vec{F}_{mech} = \eta \left[\frac{3}{2} \frac{U}{a} - \frac{KE_0}{4\pi\eta a} \int_{\infty}^{a} \xi \, dr - \frac{KE_0}{4\pi\eta} \xi(a) \right] \oint \hat{\theta} \sin\theta \, dS$$

$$+ \int_{\infty}^{a} \frac{K \nabla^2 \Psi}{4\pi} \frac{\partial \Psi}{\partial r} \, dr \oint \hat{r} \, dS \qquad \text{(C-7)}$$

$$- \left[\frac{3\eta}{2a} U - \frac{KE_0}{4\pi a} \int_{\infty}^{a} \xi \, dr - \frac{KE_0}{4\pi} \left(3 \frac{\partial \Psi}{\partial r} - 2\xi \right) \right] \oint \hat{r} \cos\theta \, dS,$$

which is reduced by the following equations,

$$\oint \hat{\theta} \sin\theta \, dS = - \hat{z} \frac{8\pi}{3} a^2,$$

$$\oint \hat{r} \, dS = 0 , \qquad \text{(C-8)}$$

$$\oint \hat{r} \cos\theta \, dS = \hat{z} \frac{4\pi}{3} a^2 ,$$

to the form

$$\vec{F}_{mech} = \hat{z} \left(- 6\pi\eta a U + KE_0 \, a \int_{\infty}^{a} \xi \, dr + KE_0 \, a^2 \left. \frac{\partial \Psi}{\partial r} \right|_a \right). \qquad \text{(C-9)}$$

This is the result quoted in Eq. 10 of Sec. I.

D. Calculation of the Electrical Force (Direct Force) in Henry's Electrophoresis Problem

The purpose of this appendix is to calculate the integral

$$\vec{F}_{direct} = \oint_{\substack{\text{sphere of} \\ \text{radius a}}} \underset{\sim}{T}_{elec} \cdot d\vec{S}, \qquad \text{(D-1)}$$

where the electrical stress tensor (Maxwell stress tensor) is defined by

$$\underset{\sim}{T}_{elec} = \frac{K}{4\pi} \left[\vec{E} \vec{E} - \underset{\sim}{1} \frac{(1-b)}{2} \vec{E} \cdot \vec{E} \right], \qquad \text{(D-2)}$$

where

$$b = \frac{g}{K}\frac{dK}{dg},$$

g = mass density,

K = dielectric constant.

The electric field in Eq. (D-2) is the vector sum

$$\vec{E}(a) = \vec{E}_{applied}(a) + \vec{E}_Q(a), \tag{D-3}$$

where the applied field at the surface of the sphere is as given in Eq. (B-10) of Appendix B as

$$\vec{E}_{applied}(a) = \hat{r}\, E_0(1-2\lambda)\cos\theta - \hat{\theta}\, E_0(1+\lambda)\sin\theta \tag{D-4}$$

and the electric field associated with the charge on the particle is given by

$$\vec{E}_Q(a) = \frac{Q}{Ka^2}\,\hat{r}\,. \tag{D-5}$$

Making these substitutions, one obtains the result that

$$\begin{aligned}
\frac{4\pi}{K}\underset{\sim}{T}_{elec} &= \vec{E}_{applied}\vec{E}_{applied} + \vec{E}_{applied}\vec{E}_Q + \vec{E}_Q\vec{E}_{applied} + \vec{E}_Q\vec{E}_Q \\
&\quad - \underset{\sim}{1}\frac{(1-b)}{2}\left(|\vec{E}_{applied}|^2 + 2\vec{E}_{applied}\cdot\vec{E}_Q + |E_Q|^2\right) \\
&= \hat{r}\hat{r}\left[(1-2\lambda)^2 E_0^2\cos^2\theta + 2(1-2\lambda)\frac{QE_0}{Ka^2}\cos\theta + \frac{Q^2}{K^2a^4}\right] \\
&\quad - \hat{r}\hat{\theta}\left[(1-2\lambda)(1+\lambda)E_0^2\cos\theta\sin\theta + \frac{QE_0}{Ka^2}(1+\lambda)\sin\theta\right] \\
&\quad - \hat{\theta}\hat{r}\left[(1-2\lambda)(1+\lambda)E_0^2\cos\theta\sin\theta + (1+\lambda)\frac{QE_0}{Ka^2}\sin\theta\right] \\
&\quad + \hat{\theta}\hat{\theta}(1+\lambda)^2 E_0^2\sin^2\theta \\
&\quad - \underset{\sim}{1}\frac{(1-b)}{2}\left[(1-2\lambda)^2 E_0^2\cos^2\theta + (1+\lambda)^2 E_0^2\sin^2\theta \right. \\
&\quad \left. + 2(1-2\lambda)\frac{QE_0}{Ka^2}\cos\theta + \frac{Q^2}{K^2a^4}\right].
\end{aligned} \tag{D-6}$$

Keeping in mind the following equations,

$$\left.\begin{aligned} \hat{r}\,\hat{r} \cdot \vec{dS} &= \hat{r}\,dS, \\ \hat{r}\,\hat{\theta} \cdot \vec{dS} &= 0, \\ \hat{\theta}\,\hat{r} \cdot \vec{dS} &= \hat{\theta}\,dS, \\ \hat{\theta}\hat{\theta} \cdot \vec{dS} &= 0, \\ \underset{\sim}{1} \cdot \vec{dS} &= \hat{r}\,dS, \end{aligned}\right\} \quad (D\text{-}7)$$

and that

$$\left.\begin{aligned} \oint \hat{r}\,dS &= \oint \cos^2\theta\,\hat{r}\,dS = \oint \cos\theta \sin\theta\,\hat{\theta}\,dS \\ &= \oint \sin^2\theta\,\hat{r}\,dS = 0, \end{aligned}\right\} \quad (D\text{-}8)$$

one finds the following result for the direct force exerted on the charged sphere by the applied field:

$$\left.\begin{aligned} \vec{F}_{direct} = \oint \underset{\sim}{T}_{elec} \cdot \vec{dS} = \frac{K}{4\pi} \Bigg\{ &- (1+\lambda)\,\frac{QE_0}{Ka^2} \oint \hat{\theta} \sin\theta\,dS \\ &+ \left[2(1-2\lambda)\,\frac{QE_0}{Ka^2} - (1-b)(1-2\lambda)\,\frac{QE_0}{Ka^2} \right] \oint \hat{r} \cos\theta\,dS \Bigg\}. \end{aligned}\right\} \quad (D\text{-}9)$$

When one substitutes

$$\left.\begin{aligned} \oint \hat{\theta} \sin\theta\,dS &= -\hat{z}\,\frac{8\pi}{3}\,a^2, \\ \text{and} \quad \oint \hat{r} \cos\theta\,dS &= \hat{z}\,\frac{4\pi}{3}\,a^2. \end{aligned}\right\} \quad (D\text{-}10)$$

in Eq. (D-9), this result is simplified into the form

$$\vec{F}_{direct} = \left[QE_0 + b\,\frac{(1-2\lambda)}{3}\,QE_0 \right] \hat{z}\,. \quad (D\text{-}11)$$

Finally if the electrostriction term, $[b(1-2\lambda)/3]\,QE_0$, is dropped, one obtains the result quoted in Eq. (18) of Sec. I.

REFERENCES

1. D. C. Henry, Proc. Roy. Soc. (London) A 133, 106 (1931).
2. J. Lyklema and J. Th. G. Overbeek, J. Colloid Sci. 16, 501 (1961).
3. F. Booth, Proc. Roy. Soc. (London) A 203, 514 (1950).
4. Georg Joos and Ira M. Freeman, Theoretical Physics (Blackie and Son, Limited, London, 1959), 3rd Edition.
5. W. K. H. Panofsky and Melba Phillips, Classical Electricity and Magnetism (Addison-Wesley Publishing Co., Inc., Reading, Mass., 1956).
6. Charles C. Brinton and Max A. Lauffer, The Electrophoresis of Viruses, Bacteria, and Cells, and the Microscopic Method of Electrophoresis, in Electrophoresis, Milan Bier, ed. (Academic Press, Inc., New York, 1959).
7. J. T. Davies and E. K. Rideal, Interfacial Phenomena (Academic Press, Inc., New York, 1961), pp. 56 ff.
8. L. V. Heilbrunn, An Outline of General Physiology (W. B. Saunders Co., Philadelphia, 1953), 3rd Edition.
9. J. St. L. Philpot and J. E. Stanier, Nature 174, 651 (1954).
10. M. S. Bingley and C. M. Thompson, J. Theoret. Biol. 2, 16 (1962).
11. Bradley T. Scheer, General Physiology (John Wiley & Sons, Inc., New York, 1953).
12. J. M. Tobais, D. P. Agin, and R. Pawlowski, Circulation 26, 1145 (1962); also P. Mueller, D. O. Rudin, H. Ti Tien, and W. C. Wescott, Circulation, 26, 1167 (1962).
13. Various authors in Electrochemistry in Biology and Medicine (John Wiley & Sons, New York, 1955).
14. Hermann P. Schwan, in Biological and Medical Physics (Academic Press, Inc., New York, 1957), Vol. 5.
15. Eric Ponder, in Medical Physics (Year Book Publishers, Chicago, 1944), Vol. I, p. 1203.
16. G. V. F. Seaman and D. H. Heard, J. Gen. Physiol. 44, 251 (1960).

17. R. F. Furchgott and E. Ponder, J. Gen. Physiol. 24, 447 (1941).

17a. A. L. Loeb, J. Th. G. Overbeek, and P. H. Wiersema, The Electrical Double Layer Around a Spherical Particle (M.I.T. Press, Cambridge, Massachusetts, 1961).

18. G. M. W. Cook, D. H. Heard, and G. V. F. Seaman, Nature 191, 44 (1961).

19. A. D. Bangham, B. A. Pethica, and G. V. F. Seaman, Biochem. J. 69, 12 (1958).

20. D. J. Wilkins, H. Ottewill, and A. D. Bangham, J. Theoret. Biol. 2, 165 (1962).

21. G. M. W. Cook, D. H. Heard, and G. V. F. Seaman, Exp. Cell Res. 28, 27 (1962).

22. A. D. Bangham and B. A. Pethica, Proc. Roy. Phys. Soc. Edinburgh 28, 43 (1960).

23. A. R. Gilby and A. V. Few, Biochim. Biophys. Acta 30, 421 (1958).

24. D. H. Heard and G. V. F. Seaman, J. Gen. Physiol. 43, 635 (1960).

25. Arne Tiselius and Harry Svensson, Trans. Faraday Soc. 36, 16 (1940).

26. Lewis B. Barnett and Henry B. Bull, Arch. Biochem. Biophys. 89, 167 (1960).

27. Koichiro Aoki and Joseph F. Foster, J. Am. Chem. Soc. 79, 3385 (1957).

28. V. Bolingbroke and M. Maizels, J. Physiol. (London) 149, 563 (1959).

29. A. C. Nevo, I. Michaeli, and H. Schindler, Exp. Cell Res. 23, 69 (1961).

30. J. Masaki and E. F. Hartree, Biochem. J. 84, 347 (1962).

31. H. A. Abramson, J. Gen. Physiol. 12, 711 (1929).

32. Eric Ponder, Blood 6, 350 (1951).

33. Professor Herschel Roman (Department of Genetics, University of Washington, Seattle, Washington), private communication.

34. A. A. Eddy and A. D. Rudin, Proc. Roy. Soc. (London) B 148, 419 (1958).

35. J. Amez, L. N. M. Duysens, and D. C. Brandt, J. Theoret. Biol. 1, 59 (1961).

36. Eric Ponder, Hemolysis and Related Phenomena (Grune and Stratton, Inc., New York, 1948).

37. T. A. J. Prankerd, The Red Cell (Charles C. Thomas, Publisher, Springfield, Illinois, 1961).

38. J. S. Fruton and S. Simmonds, General Biochemistry (John Wiley & Sons, Inc., New York, 1958), 2nd Edition.

39. Eric Ponder and Ruth V. Ponder, J. Exp. Biol. 32, 175 (1955).

40. Torsten Teorell, J. Gen. Physiol. 35, 669 (1952).

41. D. H. Heard and G. V. F. Seaman, Biochim. Biophys. Acta 53, 366 (1961).

42. G. L. Ada and Joyce D. Stone, Nature 165, 189 (1950).

43. Alfred Gottschalk, The Chemistry and Biology of Sialic Acids and Related Substances (Cambridge University Press, London, 1960).

44. E. H. Eylar, M. A. Madoff, O. V. Brody, and J. L. Oncley, J. Biol. Chem. 237, 1992 (1962).

45. Hugh Davson, Circulation 26, 1022 (1962).

46. E. Gorter and F. Grendel, J. Exp. Med. 41, 439 (1925).

47. J. F. Danielli, Cold Spring Harbor Symp. Quant. Biol. 6, 190 (1938); also E. N. Harvey and J. F. Danielli, Biol. Rev. Cambridge Phil. Soc. 13, 319 (1938).

48. A. K. Parpart and A. J. Dziemian, Cold Spring Harbor Symp. Quant. Biol. 8, 17 (1940); also A. K. Parpart and R. Ballentine, in Modern Trends in Physiology and Biochemistry (Academic Press, Inc., New York, 1952), p. 135.

49. J. Lee Kavanau, Nature 198, 525 (1963).

50. R. R. Dourmashkin, R. M. Dougherty, and R. J. C. Harris, Nature 194, 1116 (1962).

51. A. D. Bangham and R. W. Horne, Nature 196, 952 (1962); also A. M. Glauert, J. T. Dingle, and J. A. Lacy, Nature 196, 953 (1962).

52. F. Husson and V. Luzzati, Nature 197, 822 (1963).

53. J. B. Finean and M. G. Rumsby, Nature 197, 1326 (1963).
54. L. G. Bell, J. Theoret. Biol. 3, 132 (1962).
55. M. Hanig, Proc. Soc. Exp. Biol. Med. 68, 385 (1948).
56. E. Klenk and G. Uhlenbruck, Z. Physiol. Chem. 311, 227 (1958).
57. E. Klenk, discussion in Chemistry and Biology of Mucopolysaccharides (Ciba Foundation Symposium, J. and A. Churchill, Ltd., 1958), p. 311.
57a. J. B. Bateman, A. Zellner, M. S. Davis, and P. A. Mc Caffrey, Arch. Biochem. Biophys., 60, 384 (1956).
58. G. V. F. Seaman and G. Uhlenbruck, Arch. Biochem. Biophys. 100, 493 (1963).
59. C. C. Curtain, Australian J. Exptl. Biol. Med. Sci. 31, 623 (1953).
60. D. Wallach and E. H. Eylar, Biochim. Biophys. Acta 52, 594 (1961).
61. G. Ruhenstroth-Bauer, G. F. Fuhrmann, E. Granzer, W. Kübler, and F. Rueff, Naturwiss. 16, 363 (1962).
62. D. A. Haydon, Biochim. Biophys. Acta 50, 450 (1961).
63. L. Warren, J. Biol. Chem. 234, 1971 (1959).
64. L. C. Mokrasch, J. Biol. Chem. 208, 55 (1954).
65. D. R. Coman, Cancer Res. 21, 1436 (1961).
66. R. A. Gibbons, Biochem. J. 82, 32P, (1962).
67. I. Yamakawa, R. Irie, and M. Inanaga, J. Biochem. (Tokyo) 48, 490 (1960).
68. C. A. Tobias (Division of Medical Physics, University of California, Berkeley, California), private communication.
69. J. B. Bateman and Arnold Zellner, Arch. Biochem. Biophys. 60, 44 (1956).
70. M. Bessis, M. Bricka, and J. Breton-Gorius, Compt. Rend. Soc. Biol. 147, 369 (1953).
71. G. F. Bahr, Exp. Cell Res. 7, 457 (1954).
72. T. L. Hayes, F. T. Lindgren, J. W. Gofman, S. W. Spaulding, and J. P. World, Donner Laboratory Semiannual Report, Lawrence Radiation Laboratory Report UCRL-10683, Fall 1962 (unpublished).

73. W. T. J. Morgan, Proc. Roy. Soc. (London) B151, 308 (1960).
74. Carl R. Noller, Textbook of Organic Chemistry (W. B. Sounders Co., Philadelphia, 1951).
75. E. S. West and W. R. Todd, Textbook of Biochemistry (The Macmillan Company, New York, 1957), p. 57.
76. S. Ludewig, Proc. Soc. Exp. Biol. Med. 104, 250 (1960).
77. G. Gasic and T. Gasic, Nature 196, 170 (1962).
78. Albert Dorfman, J. Histochem. Cytochem. 11, 2 (1963).
79. Holde Puchtler and C. P. Leblond, Am. J. Anat. 102, 1 (1958).
80. J. Hillier and J. F. Hoffman, J. Cellular Comp. Physiol. 42, 203 (1953).
81. J. F. Hoffman, J. Cellular Comp. Physiol. 47, 261 (1956).
82. D. R. Coman and T. F. Anderson, Cancer Res. 15, 541 (1955).
83. G. H. Haggis, Proc. Roy. Phys. Soc. Edinburgh, 28, 115 (1960).
84. Eric Ponder, The Cell Membrane and Its Properties, in The Cell (Academic Press, Inc., New York, 1961), Vol. II.
85. E. Gorter and L. Nanninga, Discussions Faraday Soc. 13, 205 (1953).
86. J. F. Danielli, Circulation 26, 1163 (1962).